10 cys
10/28/64

~~CONFIDENTIAL~~

UNCLASSIFIED

MASTER

SNAP-21 PROGRAM, PHASE II

DEEP SEA RADIOISOTOPE-FUELED THERMOELECTRIC GENERATOR POWER SUPPLY SYSTEM

QUARTERLY REPORT NO. 1

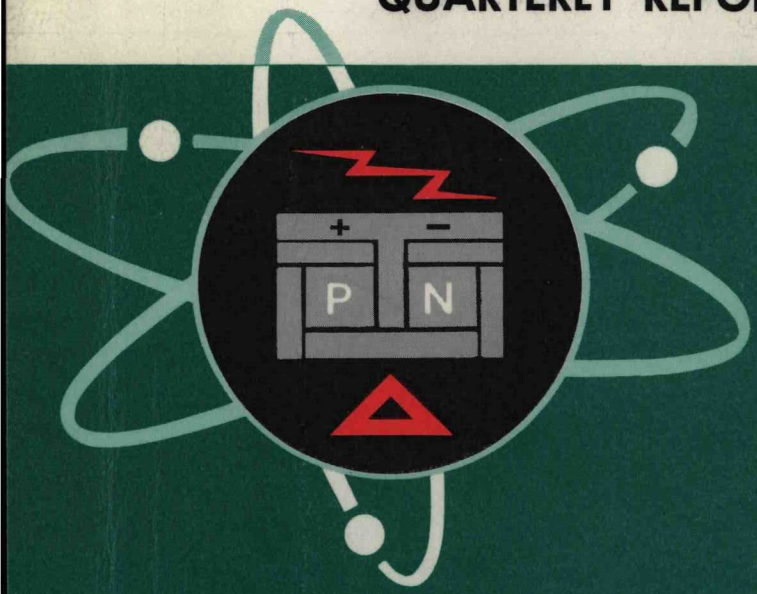

3M Electrical Products Division
MINNESOTA MINING & MANUFACTURING CO.
ISOTOPE POWER LABORATORY, BLDG. TCA-547, PH 646-7985
2501 HUDSON ROAD, ST. PAUL, MINN. 55119

1 8120

phl

~~CONFIDENTIAL~~

UNCLASSIFIED

DISCLAIMER

LEGAL NOTICE

This report was prepared as an account of Government sponsored work. Neither the United States, nor the Commission, nor any person acting on behalf of the Commission:

A. Makes any warranty or representation, expressed or implied, with respect to the accuracy, completeness, or usefulness of the information contained in this report, or that the use of any information, apparatus, method, or process disclosed in this report may not infringe privately owned rights; or

B. Assumes any liabilities with respect to the use of, or for damages resulting from the use of any information, apparatus, method, or process disclosed in this report.

As used in the above, "person acting on behalf of the Commission" includes any employee or contractor of the commission, or employee of such contractor, to the extent that such employee or contractor of the Commission, or employee of such contractor prepares, disseminates, or provides access to, any information pursuant to his employment or contract with the Commission, or his employment with such contractor.

~~THIS DOCUMENT~~ FOR OFFICIAL USE ONLY PENDING PATENT CLEARANCE

DISTRIBUTION

Distribution of this document is in accordance with M 3679 (44th Edition) category C-92a.

TABLE OF CONTENTS

TABLE OF CONTENTS (Continued)

LIST OF FIGURES

LIST OF FIGURES (Continued)

LIST OF TABLES

1.0 SUMMARY

Progress during the first quarter of the SNAP-21 Phase II Development Program is summarized as follows:

- Over-all program planning was completed and a program plan prepared.
- A subcontract for design, development and fabrication of the thermal insulation system was initiated. To date, work on this subcontract consists of planning, ordering long lead time materials, and design and analysis of major components, especially the neck tube, a structural support member for the biological shield.
- Liaison was conducted with other thermal insulation vendors and one potential backup source located.
- Design effort was initiated on the over-all 10-watt system and on the following 10-watt components: thermal insulation inner liner, biological shield, and shield-to-liner bolts. Conceptual design of the 20-watt system was also initiated.
- Long lead time materials were ordered and a residual Phase I biological shield was refurbished for use during this phase. A copper flame spray process was developed for the inner liner.
- Documentation and reports during this quarter were submitted in accordance with the program plan schedule.

2.0 INTRODUCTION

This is the first quarterly report on Contract AT(30-1)3691 for Phase II of the SNAP-21 Development Program. The period of performance for the contract is June 20, 1966 to October 1969. Phase I of the SNAP-21B Program was concluded in June 1965. Details of this effort have been presented in the Final Summary Report, No. MMM 3391-19. Phase II has been divided into three major tasks:

- Task I - Develop and deliver a series of 10-watt radioisotope-fueled thermoelectric power supply systems for deep sea applications.
- Task IIA - Design, develop, and demonstrate a 20-watt thermoelectric power supply system for deep sea applications.
- Task IIB - Develop and deliver, for deep sea applications, a series of 20-watt radioisotope-fueled thermoelectric power supply systems that were designed during Task IIA.

In addition to the Phase II effort outlined above, some testing initiated during the Phase I development effort is still continuing and will be reported in the Phase II Progress Reports.

This report will present all details of program effort from June 20, 1966 through September 30, 1966.

3.0 PROGRAM PROGRESS

3.1 PROGRAM MANAGEMENT

3.1.1 PLANNING

Program planning during this report period was primarily concerned with the preparation of the first draft of the program plan. This planning consisted of preparing program master schedules for Tasks I and IIA and a preliminary schedule for Task IIB. These master schedules identify subtasks within each major task and provide the time phasing, sequence and due dates for completion of the subtasks. Detailed planning and schedules for the various subtasks has been initiated and will be developed, to provide day-to-day working documents.

3.1.2 CONTROL

Several program control procedures have been initiated in both technical and administrative areas.

For administrative control of costs, a series of cost accounting code numbers have been established for Task I. Specific numbers have been assigned to various labor and material elements of Task I so that an accurate accrual of costs for each of these elements can be made. In addition, a procedure has been established which identifies persons authorized to initiate and approve program expenditures and their specific responsibilities in this regard.

To provide control of the flow of technical information, preliminary procedures have been established for the review and approval of drawings, specifications, reports, and other documents.

3.1.3 PROGRAM STATUS

Figure 3-1 has been prepared to provide a graphic presentation of program progress compared with planned effort. This figure is a reproduction of the Task I Master Schedule as presented in the Program Plan and has estimated actual progress superimposed on the planned effort.

As shown in Figure 3-1, effort has commenced on all scheduled subtask efforts except power conditioner, fuel capsule, tooling and test station design.

Estimated progress on those subtask elements that have been initiated is shown in Figure 3-1 by the dashed line superimposed on the solid scheduled line.

The thermoelectric generator and fuel capsule are pacing items in the design area at this time, and the insulation system and biological shield are pacing items in the procurement and fabrication area.

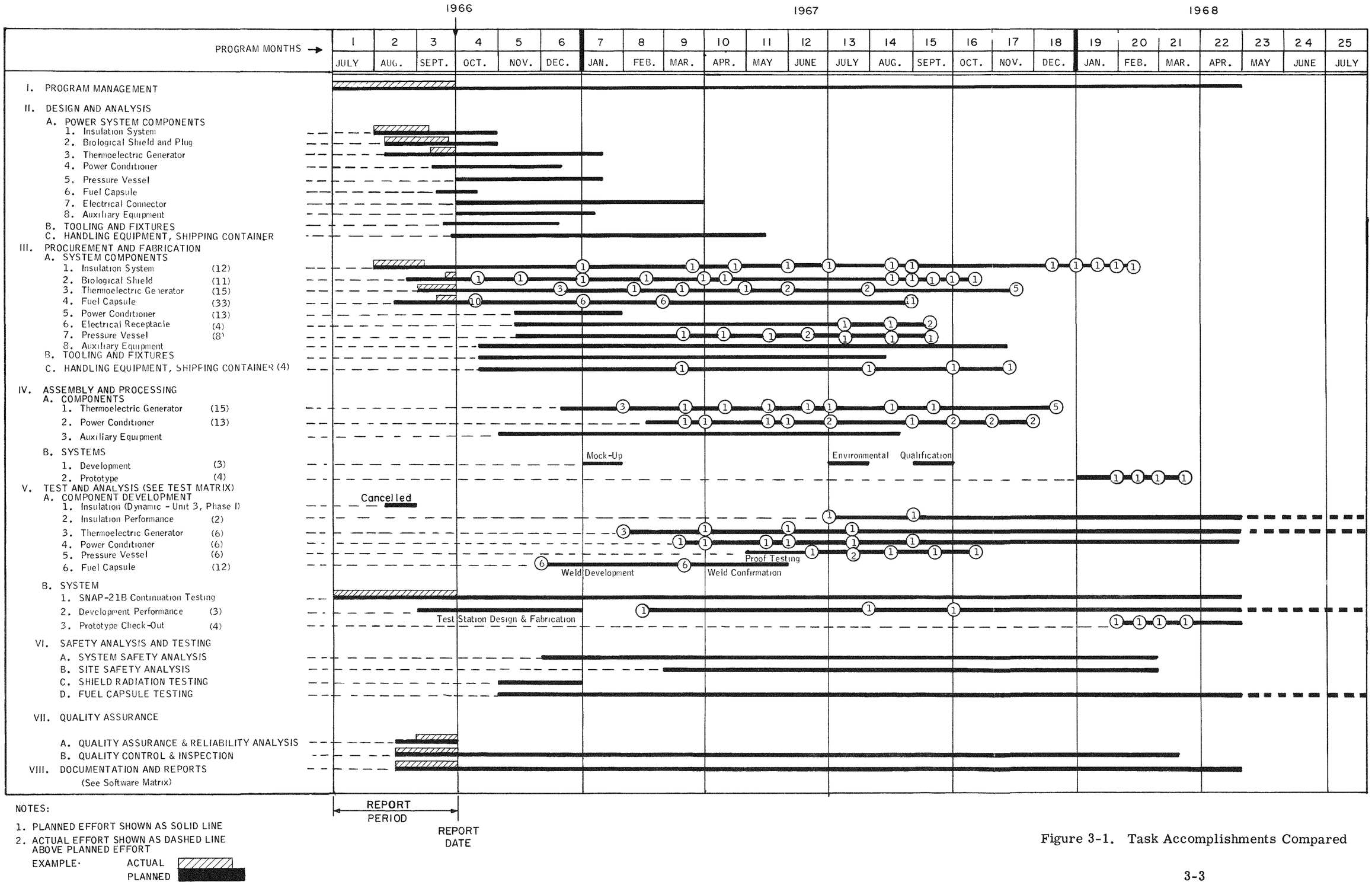

NOTES:

1. PLANNED EFFORT SHOWN AS SOLID LINE
2. ACTUAL EFFORT SHOWN AS DASHED LINE ABOVE PLANNED EFFORT

EXAMPLE: ACTUAL / PLANNED

Figure 3-1. Task Accomplishments Compared

3.2 TECHNICAL MANAGEMENT AND CONTROL

3.2.1 CONFIGURATION CONTROL

Effort was initiated during this report period to establish a configuration control plan specifically tailored to the SNAP-21 Program needs. Meetings were held with appropriate groups within 3M to identify the specific control points within each participating group.

As a result of these meetings, an interface chart was drawn up that graphically presents what specific functions are involved in configuration control as it will be practiced on the SNAP-21 Program. This is shown in Figure 3-2.

During the next report period a configuration control plan will be drawn up and formalized. This plan will identify areas of responsibilities and individuals or functions responsible for them.

3.2.2 LINDE SUBCONTRACT PROGRESS

The effort in the early portion of the report period was directed toward establishing a definitive subcontract. Negotiations were held which resulted in a letter subcontract, AT(30-1)3691-5511 executed on 16 September for the period 1 August through 30 September. This letter subcontract was extended to 31 October.

3.2.2.1 Program Planning

In accordance with the subcontract requirements, a preliminary program plan was completed and submitted to 3M for approval. The program plan contains a description of all tasks and subtasks into which the subcontract is divided in order to accomplish the work objectives. Criteria for the demonstration of performance is outlined to permit visible control of progress.

a) Quality Control Plan

A preliminary Quality Control Plan was 90 percent completed during this report period. The Linde Quality Control Coordinator, in cooperation with the Linde Project team, is preparing the plan. The plan will meet the requirements of MIL-Q-9858A. This plan specifies the responsibilities of various personnel concerned with the quality assurance task, and specifies in detail the responsibilities and execution of the quality assurance functions in each area. As work progresses, the preliminary Quality Assurance Plan

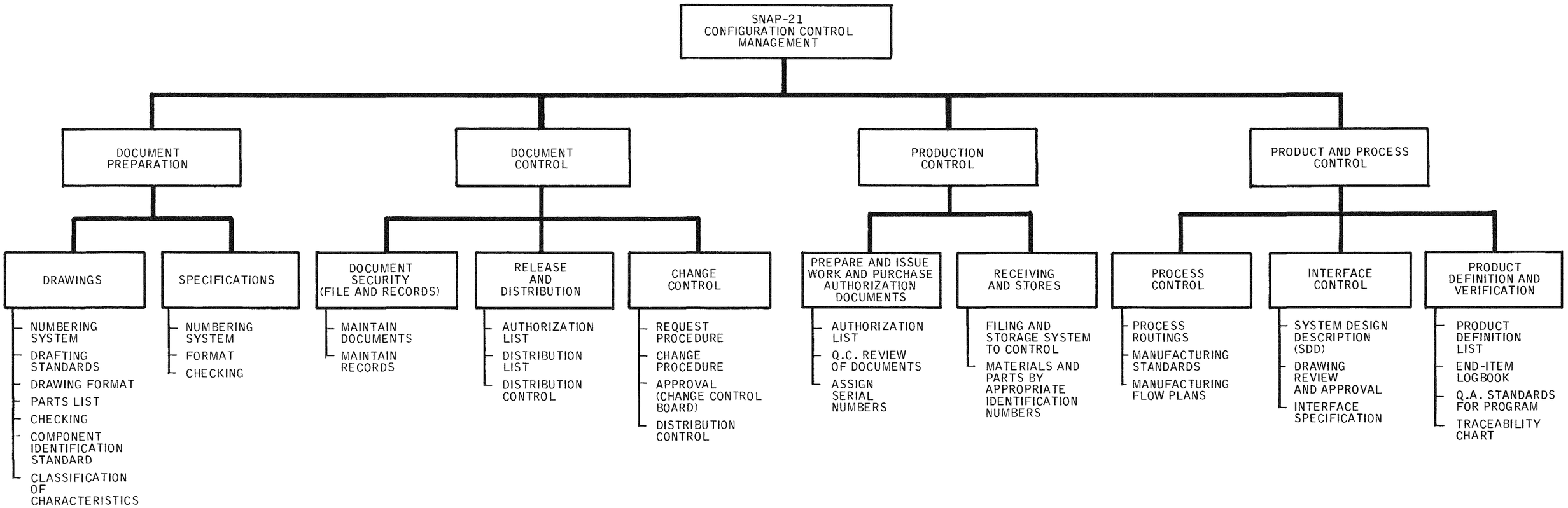

Figure 3-2. Configuration Control Interface Chart

will be revised and modified, in keeping with the development nature of the program, to form the formal Quality Control Plan which will be used during the fabrication of the delivery HTVIS units. The formal Quality Control Plan (written to MIL-Q-9858A), the Manufacturing Flow Plan, and the Acceptance Test Plan will be submitted as separate documents at the final design review for Task I.

b) Development Test Plan

The majority of the Development Test Plan was completed during this report period. The Development Test Plan completely specifies the development test work to be accomplished. This plan is comprehensive and includes detailed test procedures, estimated number of tests tests to be conducted, test objectives, methods of data gathering and reduction to obtain desired information, instrumentation to be used during the testing, drawings of test set-ups, sample calculations, and the anticipated methods of presenting results. The Development Test Plan will be submitted to the 3M Company for approval at the preliminary design review scheduled for early October.

3.2.2.2 Preliminary Design and Analysis of Model "A" HTVIS (10 watt)

The HTVIS (High-Temperature Vacuum Insulation System) is a multifoil type insulation having an extremely low thermal conductivity. The insulation system has the characteristic of being an excellent high temperature thermal insulator. Metallic foils provide high thermal resistance to radiant heat flow. Convective and conductive heat flow is reduced to a minimum by evacuating the system to less than ten microns of pressure and by separating the metallic foils with fibrous insulation.

The insulation system concept is shown in Figure 3-3. A key component of the system is the neck tube which serves as the structural support member for the fuel source and biological shield. This neck tube is the major conductive heat leak path for the system, consequently it must be optimized from a structural versus heat leak standpoint. The following paragraphs discuss the design and analysis effort on this component.

a) Neck Tube Material Selection (see Figure 3-3 for schematic of neck tube)

An initial survey of high temperature alloys revealed approximately 25 alloys whose properties merited further investigation. This investigation resulted in narrowing the selection to three alloys. Based on yield strength, stress rupture life, oxidation

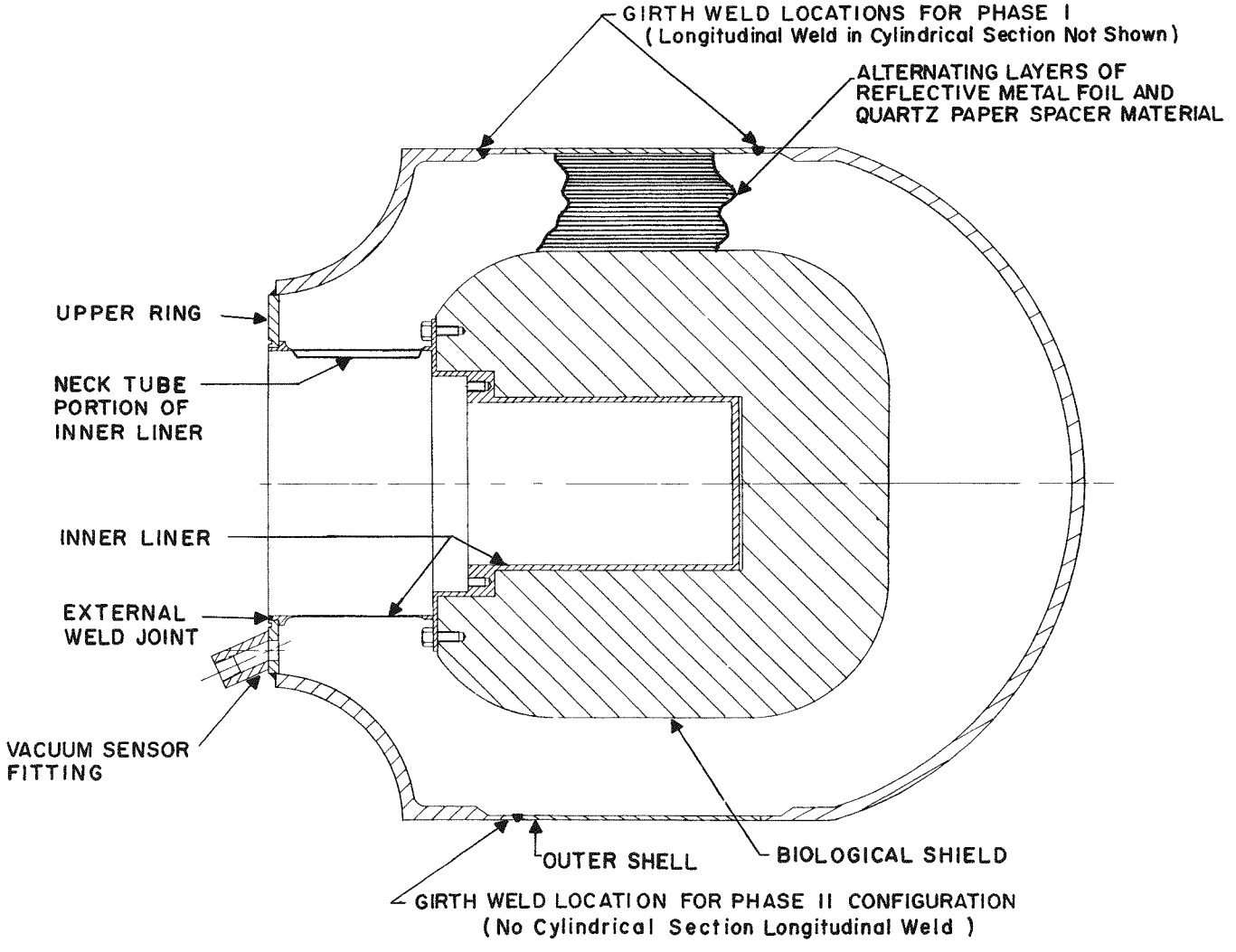

Figure 3-3. 10-Watt High Temperature Vacuum Insulation System (HTVIS)

resistance, weldability, and thermal conductivity, neck tube materials are recommended in the following order:

1) Inconel-625
2) Hastelloy-X
3) Inconel-600

Inconel-625 exhibits a typical yield strength of 44,500 psi at 1350° F. The stress rupture at 1340° F and 50,000 hours is 16,000 psi. This material has better oxidation resistance than Inconel-600 or Inconel-X-750. It is, however, very new. It is currently in an experimental status with little or no proven long term data. Also, welding rod for this alloy would be made on a lab sample basis.

Hastelloy-X exhibits a typical yield strength of 38,200 psi at 1340° F. The rupture stress at 1340° F and 50,000 hours is 10,000 psi. This material has better oxidation resistance than Inconel-600.

Inconel-600 exhibits a typical yield strength of 19,500 psi at 1350° F. The rupture stress at 1350° F and 50,000 hours is 5000 psi. The material is considered one of the most stable superalloys for long-term use.

Although Inconel X-750 was used for the neck tube during Phase I, it is not recommended at this time because it is a precipitation hardening alloy and this property may cause brittleness or a change in properties with long-term high-temperature use.

All the above-mentioned materials are weldable, and all exhibit thermal conductivities within approximately 10 percent of each other. Subsequent to selecting the above three candidate materials, an availability survey was conducted. During this survey it was found that Inconel-625 was relatively non-available as a stock item, and that long-term waiting periods up to 30 weeks would be required after ordering components. In view of the availability problem and the lack of historical data on Inconel-625, Hastelloy-X has been selected as the material to be used in the Model A neck tubes. Hastelloy-X properties are being used in the design analyses.

b) Neck Tube Structural Analysis

Three independent stress analyses were conducted on the neck tube (the thin, cylindrical support section of the inner liner) during this report period. These independent analyses, using different techniques, were felt to be necessary to correlate results since the failure mode, inelastic buckling, has been historically difficult to analyze. The results of these analyses are tabulated below:

Analytical Method	Hot End Thickness	Cold End Thickness
1	0.0115	0.0155
2	0.014	0.015
3	0.0115	0.016
Phase I	0.011	0.011

Each of these analyses showed that the 0.011-inch thick Phase I neck tube design was marginal under dynamic conditions. In fact, for the worst case (horizontal position 3g shock) the factor of safety was 1.02 compared to the 1.5 safety factor established during Phase II as an over-all system design goal. Further analyses indicated that highest stresses occur at the cold end, decreasing to a minimum value, determined by shear and bending, at the hot end.

Analytical Method 1 has been selected for current design calculations, since it is based on a combination of empirical data and theoretical calculations, however, further analysis is being conducted to verify these results.

Based on this analysis, a neck tube tapering from 0.0155 at the cold end to 0.0115 at the hot end will provide a factor of safety of 1.5. For a factor of safety of 1.75, these thicknesses taper from 0.0175 to 0.0135 at the cold and hot ends, respectively. The calculated total insulation system heat loss for the optimum (1.5 F.S.) design is 36 watts, and for the "heavy wall" (1.75 F.S.) 40 watts. These analyses are based on the following publications:

1) NACA Technical Note 3783: Buckling of Curved Plates and Shells.

2) Kein Bertran: Information on Buckling of Unstiffened Thin-Walled Circular Cylindrical Shells.

3) Harris, R. A. et al: The Bending Stability of Thin-Walled Unstiffened Circular Cylinders including the Effects of Internal Pressure, Journal of Aeronautical Sciences, Vol. 25, May, 1958.

The neck tube analyses are included in appendixes to this report.

The stress-rupture strength analysis of the neck tube under 1g loading conditions in combined bending and tension showed that the design is adequate for a five-year life. The calculations showed a design factor of safety of 1.16 based on extrapolated (1000 hours) rupture strength of Hastelloy-X at 1325° F. This estimate is conservative in that it assumes a constant temperature of 1325° F and does not consider radioisotope decay with time. Further investigations to establish more accurate data for the expected life are in progress.

c) Outer Vacuum Enclosure

An evaluation of materials for the outer shell resulted in the selection of Type 304 stainless steel. This material was selected on the basis of its weldability to itself and Hastelloy-X, yield strength (35,000 psi at 100° F) and vast background of experience available for its fabrication and use.

A visit was made to Hydroforming Company of America to investigate the possibility of extending the straight cylindrical portion of the outer shell heads to enable closing the unit with only one weld. It was determined that the present design, which uses four parts, could be made from two formed parts. The top head will be made to include the upper ring flange, which is presently welded in place. To perform this operation, new dies and more liberal inside radii will be required. In addition, a thicker blank would be required. The bottom head and cylindrical skirt can be made in one piece. The closing weld of the unit would be located where the upper weld of the present units is now located. By using a two-piece design it would be possible to eliminate two welds, which should markedly improve the ability to fabricate a unit within dimensional tolerance and reduce the potential of a weld leak (see Figure 3-3). Further discussions are to be held with Hydroforming Company of America when the outer shell configuration is complete and required thicknesses are determined.

d) Insulation Materials

The insulation materials have been selected for the Model A 10-watt power system units. For the insulation temperature range of 1350° F to 1270° F, 0.5 mil nickel foil radiation shields will be used. In the temperature range of 1270° F to 800° F, copper radiation shields will be used, and in the temperature range of 800° F to ambient, aluminum radiation shields will be used. There will be 60 nickel shields, 69 copper shields, and 43 aluminum shields. The above temperature ranges were selected using information from the Linde AEC Contract AT(30-1)3632 concerning material vaporization rates while maintained at high temperatures. Calculations revealed that if copper were to be used in the temperature range 1340° F to 1270° F, a maximum of 4.0 pounds of copper would be vaporized and redeposited during the five-year operating life. If, however, the copper is subjected to a maximum temperature of 1270° F, vaporization would be limited to be a maximum of 0.35 pounds.

The radiation shield spacer material used between the nickel and the copper radiation shields will be either quartz paper or quartz cloth, depending on the particular unit involved. Dexter 106 glass paper will be used to separate the aluminum foils. Using the above insulation materials, the insulation heat leak has been calculated to be 8.9 watts.

All insulation materials are on order or on hand as residuals from the Phase I effort.

e) SNAP-21B Prototype Unit

In order to establish system thermal and electrical characteristics early in Phase II, a complete system will be assembled using residual Phase I components. The only new component that is required is an insulation system.

To meet schedule requirements, it is planned to use existing outer shells for this unit (available from previous subcontract). Because the seal-off and getter activation device has not been developed at this time, the unit will be evacuated through a valve mounted on the upper flange. The getter pod will also be mounted on the top flange and will be located within the space envelope allotted by 3M Company. Plans call for activating the getter by a conventional pinch method.

3.2.2.3 Planned Activities for the Next Period

The following items are scheduled for the next report period:

- A definitive subcontract will be submitted to the Commission for approval.
- The Preliminary Design Review will be held at 3M on October 5 and 6.
- The Development Test Plan will be submitted at the Preliminary Design Review.
- The Preliminary Quality Assurance Plan will be submitted at the Preliminary Design Review.
- Outgassing investigations will be initiated.
- Getter testing will be initiated and completed.
- The vacuum seal-off will be developed and tested.
- Weld development testing will be initiated.
- The SNAP-21B prototype unit will be assembled, tested, and delivered.
- Development Unit 1 will be assembled and insulated.
- Development Unit 2 assembly will be initiated.

3.3 LIAISON

3.3.1 SEA ENVIRONMENTAL TESTING - NRDL

On May 26, 1966, representatives of 3M and the Naval Radiological Defense Laboratory (NRDL) met and discussed, in generalities, sea environment testing of SNAP-21. It was learned that NRDL was preparing a broad support program for the AEC concerning the safety of Sr-90 fueled SNAP devices in ocean environments. A subsequent meeting was held to work out a definitive program for SNAP-21. The following basic elements of a test program were worked out:

a) Sea Environment Testing

- Test site to be San Clemente Island off the coast of Long Beach, California (ocean depth 150 ft.).
- Four electrically-heated fuel capsules to be deployed at 75 ft., 10 ft., on the bottom, and under 12 inches of bottom.
- Two electrically-heated system mock-up test specimens to be implanted at 75 ft., and on the bottom.
- Possibly an electrically-heated subsystem incorporating a fuel capsule, shield and insulation envelope will be implanted.
- One Sr-90-fueled capsule to be exposed in a deep ocean site (Hawaii-Pacific Missile Range).
- Test details to be similar to those of the SNAP-19 Program.

b) Laboratory Studies

- Parametric studies of coupled and uncoupled materials to be conducted for evaluating the effects of:
  1) Temperature on material degradation
  2) Quenching on corrosion

3) Ionizing radiation on the corrosive environment

4) Radiation damage to encapsulating materials

5) Erosion on encapsulation material

- Heat transfer studies to evaluate the effects of:

1) Complete or partial burial

2) Marine organisms on heat transfer characteristics

A tentative program implementation schedule was prepared and submitted to NRDL for review. It was considered desirable to initiate laboratory studies as early as possible to provide maximum time exposure to test specimens. This would also provide valuable input for the sea site tests (two system mock-ups are scheduled to commence laboratory testing four months in advance of actual sea testing).

NRDL's broad proposal to the AEC was presented about June 20, 1966. A review of and commentary on the preliminary draft of the proposal was requested from 3M by the AEC. While maintaining an active interest in using NRDL capabilities for sea environment testing, 3M has awaited AEC action on the proposal before pursuing further in this area.

3.3.2 REVISED ICC SHIPPING REGULATIONS - NYOO-AEC

The Operations Safety Branch was contacted with regard to revision of ICC shipping regulations. Changes have been proposed which would allow radiation levels of:

200 mr at surface of vehicle

10 mr at 2 meters from vehicle

2 mr to the driver or other personnel in vehicle

1 Rad at 1 meter from surface of radiation package

These proposed, but not approved, relaxations apply to exclusive use vehicle only and are expected to be adopted in the near future. Such changes, if acceptable to the contracting officer, would allow for a smaller, thereby lighter, shield which would significantly change the insulation system design.

3.3.3 TITANIUM ALLOY DEVELOPMENT

3.3.3.1 David Taylor Model Basin

In the interim period since selection of 721-titanium alloy for use in the pressure vessel, additional performance data and new alloy compositions have been developed. An inquiry was made to the structural Mechanics Laboratory of David Taylor Model Basin concerning this latest knowledge and technology as applied to deep submergence pressure vessels. They stated that the stress corrosion cracking problem encountered with 721-Ti alloy had been overcome by a 621-Ti alloy incorporating 0.8 percent molybdenum. This modification provides nearly the same strength as 721-Ti and similar working and fabrication properties. Stress corrosion studies of these and other titanium alloys are being conducted at the Metallurgical Division of the Naval Research Laboratory, the Marine Engineering Laboratory, and the Naval Applied Science Laboratory. Liaison with these groups will be continued so that advantage can be taken of the most recent data.

3.3.3.2 Reactive Metals Company

Representatives of Reactive Metals Company visited 3M and briefed 3M personnel on the modified titanium alloy mentioned in the previous paragraph. Several heats of this material have been poured. Ingots up to 10,000 lbs. have been produced, as well as 4-inch plates. Present procurement lead times are six weeks for ingots and three to four weeks additional for billets.

3.3.4 INSULATION SYSTEM DEVELOPMENTS

Since the insulation system is such a vital part of the over-all SNAP-21 power supply, it is highly desirable to have alternate approaches to support the Linde effort. Accordingly, joint 3M Company — AEC meetings were held with the following organizations which are engaged in related development work.

3.3.4.1 Numec

A meeting was held with Nuclear Materials & Equipment Corporation representatives who described the insulation system used in a 5-watt isotope-fueled thermoelectric generator which they have developed. This effort was reviewed in the light of its applicability to the SNAP-21 Program. Any further action on this concept is pending receipt of additional information.

3.3.4.2 Battelle Memorial Institute

Battelle devised an insulation system while under contract to NASA. This effort consisted of two parts: Phase I - Study and Analysis; and Phase II - Hardware Development. The system consists of a web and foil concept in a vacuum enclosure capable of providing structural support. Three-inch diameter discs have been prepared and tested to verify design calculations. Using foil with an emissivity of 0.3, an approximate conductivity factor of 1/20 of that for solid metal of the same material was obtained. The system is made by assembling the webs with a filler which is etched out after the webs and foils are pressure-diffusion welded together. A refinement in the etching technique appears feasible, which could result in a reduction in emissivity to 0.1. Prior to etching, the system can be machined to any shape desired. The heat loss compares favorably with other systems on a total heat loss basis, including structural support. Battelle has offered to perform preliminary calculations on the SNAP-21 system to predict heat losses if their system were employed.

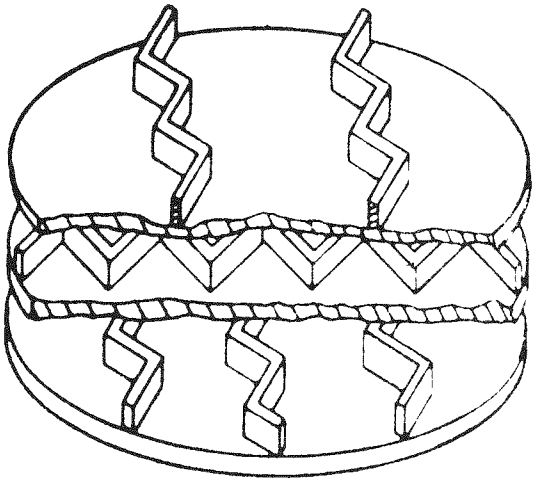

Schematic of Insulation Internal Geometry

3.3.4.3 Linde

An opportunity to review the progress being made by Linde under Contract AT(30-1)3632 was obtained at the AEC Program Review of September 13, 1966. The purpose of this program is to develop insulation systems for operation to 1800° F. Seven areas of endeavor and progress were outlined:

1) Material processing
2) Off-gas studies

3) Material compatibility

4) Physical stability

5) Thermal conductivity

6) Vacuum enclosure

7) Vibration effects

Much of this effort will be directly applicable to the SNAP-21 insulation envelope.

3.3.5 FEEDTHROUGH CONNECTOR - AMERICAN LAVA COMPANY

Past experience on SNAP programs has shown that the feed-through connectors for power leads and instrumentation has been a problem. Generally, the connectors have developed leaks during the processing into final assemblies and during assembly testing.

A visit to American Lava Co. was arranged to discuss connector problems and possible solutions. American Lava proposes to produce connector blocks of alumina, Al_2O_3, which could then have feedthrough wires brazed or soft-soldered into place, depending on the application. The alumina block would be brazed or soft-soldered into a connector base which then could be brazed or soft-soldered into the final assembly. Of utmost importance in this type of connector is that the connector base design incorporate flexibility and minimum mass to allow brazing or welding into the final assembly without excessively stressing the part and causing cracking of the hard ceramic or glass connector block.

3.4 DESIGN AND ANALYSIS

3.4.1 TASK I, 10-WATT SYSTEM

The design and analysis effort on the over-all system and major components of the 10-watt system are presented below. A schematic of the 10-watt system calling out major components is shown in Figure 3-4.

3.4.1.1 Over-all System

A complete layout of the 10-watt system was done and a dimensional study of the interfacing components made to determine if there would be any assembly problem in integrating the residual parts to be used for the first development system, No. 10 D-1, shown in Figure 3-4. A thermal expansion study was also conducted to ensure that there will not be any interference of parts or components under the intended operating temperatures and pressures.

3.4.1.2 Insulation for Development System No. 10 D-1

The prototype insulation to be used in System 10 D-1 will be fabricated from residual Phase I parts. From the dimensional study of the layout, an envelope boundary was determined allowing Linde, who is fabricating the insulation system, to place the getter outside the insulation envelope. The getter capsule container will be of a partial torroid shape and will fit around the thermoelectric generator cold frame. This will allow removal of the generator without disturbing any components of the insulation system. In order to facilitate assembly of this first unit, it is necessary that the generator mounting plate and segmented ring be placed on the insulation envelope upper head before installing and welding the getter capsule and vacuum gage tubes in place. A positive cold-weld seal is provided for the getter and evacuation tube to prevent leakage after final evacuation and processing of the system.

A study was conducted of dimensional tolerances for the follow-on insulation systems. The tolerances were reviewed for practicality so that fabrication is possible with normal manufacturing methods, while still ensuring proper interfacing with other parts and components.

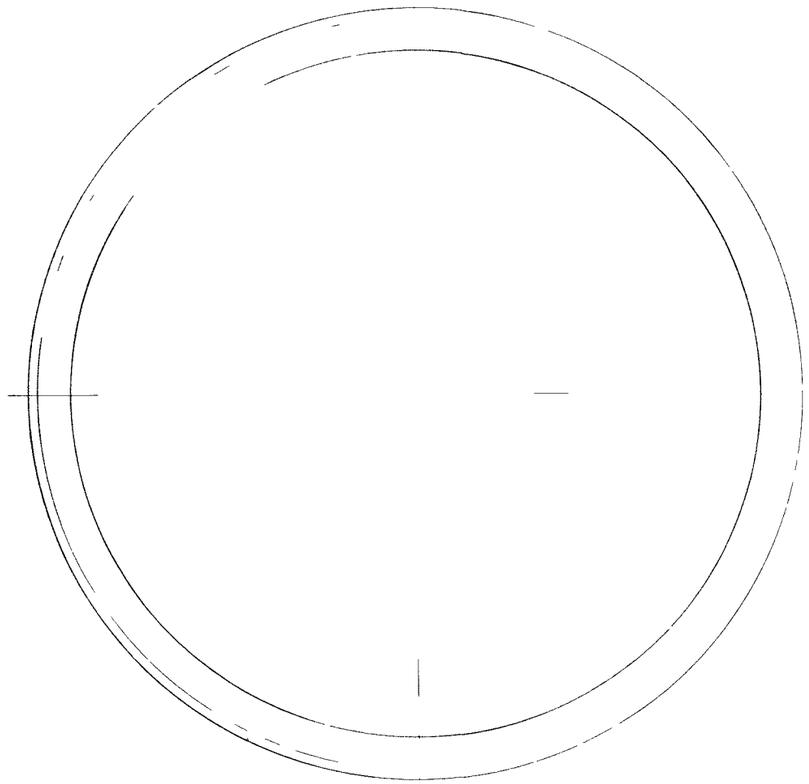

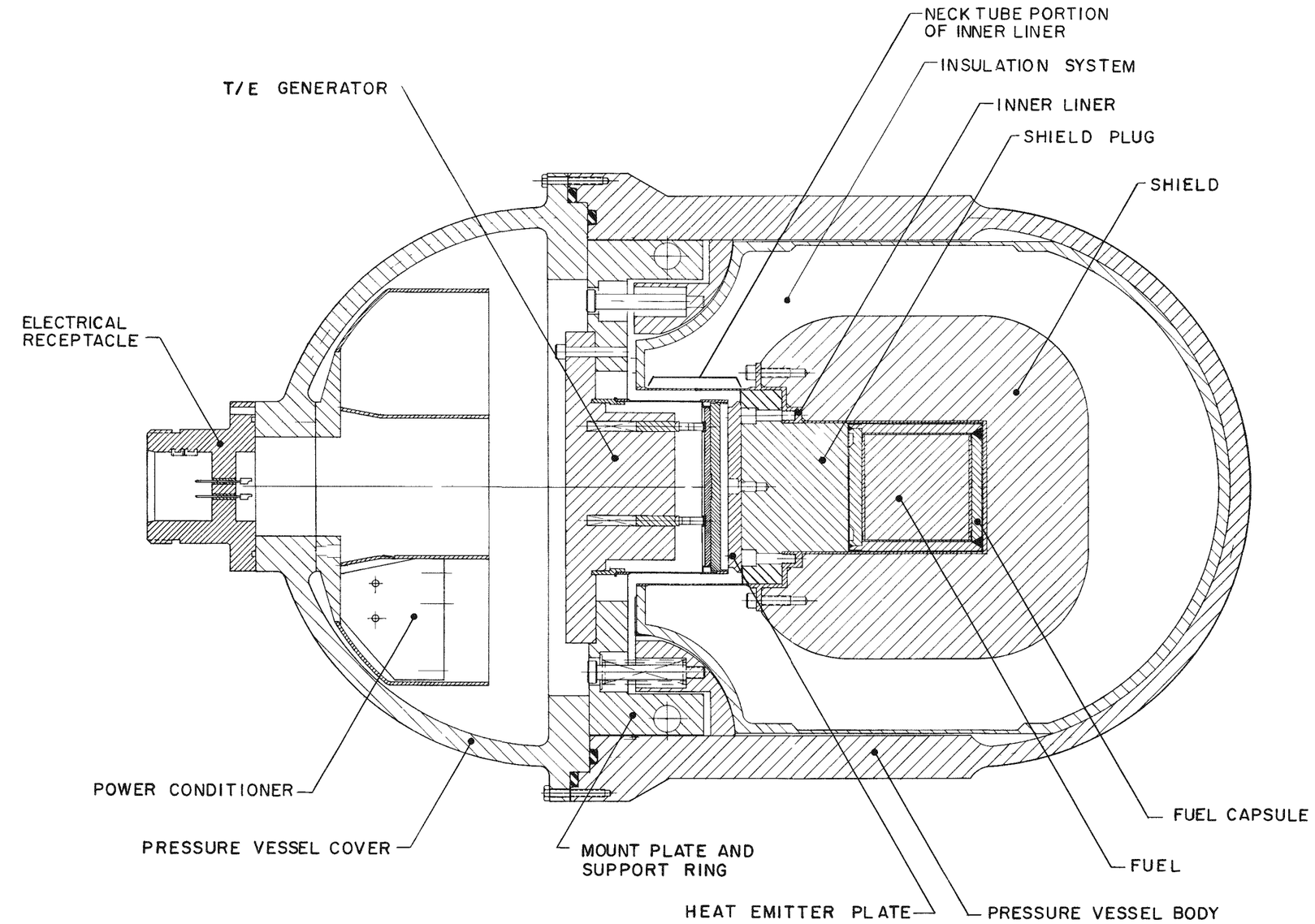

Figure 3-4. Schematic Diagram of 10-Watt System (No. 10 D-1)

3.4.1.3 Inner Liner (Figure 3-3)

The exterior of the part of the inner liner interfacing directly with the radiation shield was plated with 0.020-inch thick flame sprayed copper over a 0.003 - 0.005-inch molybdenum substrate. This coating will prevent a eutectic formation between the uranium-8 molybdenum alloy shield and the inner liner at the operating temperatures. A study of the inner liner temperatures was conducted to ensure clearance between the shield and the outside diameter of the inner liner at operating temperature, and during the start-up transient when the inner liner is at a higher temperature than the shield.

3.4.1.4 Biological Radiation Shield

The biological shield to be used for System 10 D-1 was redesigned to accept the flame sprayed inner liner. The thermal expansion of the shield material under operating temperatures was determined to ensure dimensional compatibility with the inner liner. The external configuration of the shield is the same as used in Phase I.

A preliminary shield design for the remaining 10-watt units was sufficiently completed for quotation purposes. The design can be finalized when the neck tube design and fuel requirements are defined.

3.4.1.5 Shield Bolts

The radiation shield is held in position in the insulation envelope by an inner liner. The shield and inner liner are fabricated separately and joined with eight 1/4-28 UNF bolts. The bolt material is uranium-8 molybdenum, the same material as the shield. Molybdenum was considered for the bolts but was not used because of a radiation shielding problem in the bolt holes. These bolts will be torqued to 24 inch-pounds to provide a preload of 480 pounds per bolt.

3.4.2 TASK II A, 20-WATT SYSTEM

The design analysis effort on the 20-watt system during this report period consisted of a study of different design concepts. In addition to the scaled-up 10-watt concept, Figure 3-5, established at the end of Phase I, three other concepts were investigated: 1) A twin 10-watt generator concept, 2) an external heat rejection concept and 3) a spherical concept. Concepts 1) and 2) are illustrated in Figures 3-6 and 3-7, respectively. An analysis of each concept from the standpoint of advantages, disadvantages and technical problems follows.

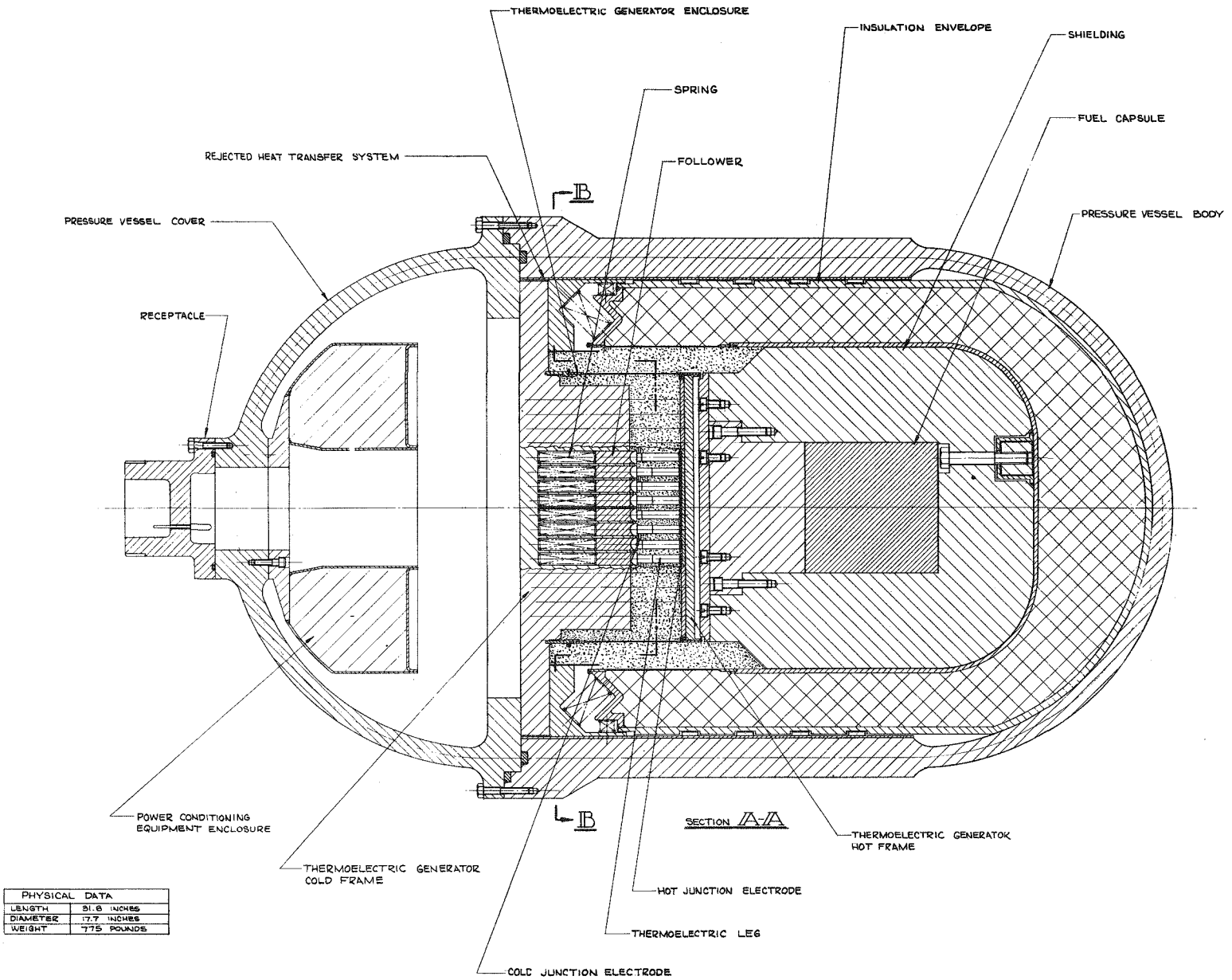

Figure 3-5. 20-Watt Configuration Proposed Under SNAP-21B Contract

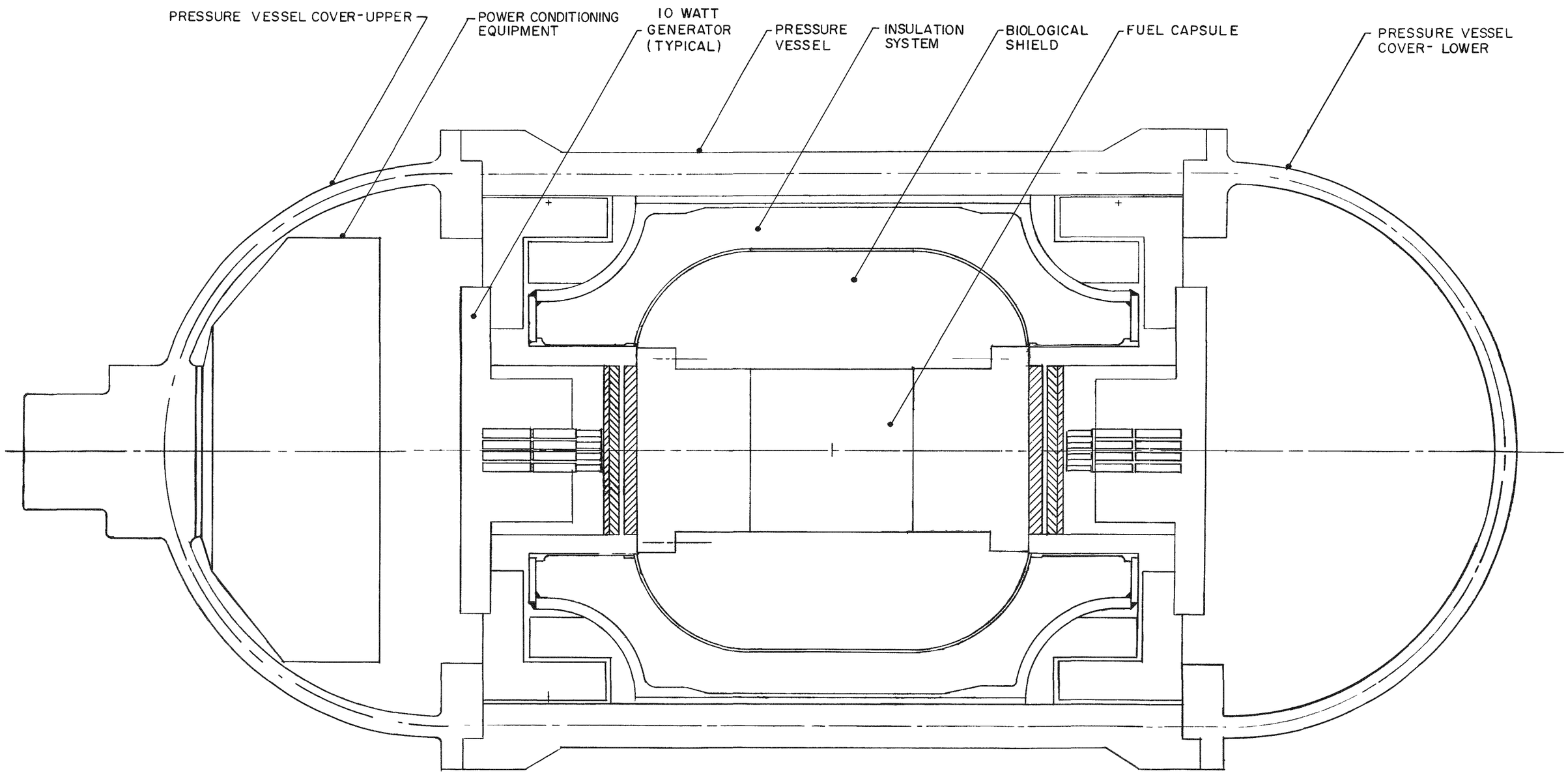

Figure 3-6. 20-Watt Conceptual Configuration Using Two 10-Watt Generators

3.4.2.1 Scaled-up 10-Watt Concept (Figure 3-5)

This concept was originally submitted at the end of the SNAP-21B contract as a feasible method of constructing a 20-watt generator which would be consistent with the specifications. The concept consists of a flat plate generator with twice the number of thermoelectric legs as the original 10-watt generator. The super insulation system is similar to the 10-watt system, but the method of heat rejection from the cold frame was modified in an attempt to reduce the temperature drop from what it was on the 10-watt system. An obvious consequence of this concept is that the larger thermoelectric generator will require a larger pressure vessel diameter which in turn requires increased thickness and more weight per unit length.

This concept offers the advantage of utilizing much of the 10-watt system technology; however, it does present some assembly problems because of generator size and is limited in growth potential.

3.4.2.2 Twin 10-Watt Generator Concept (Figure 3-6)

This concept consists of an existing 10-watt generator located on each end of a cylinderical heat source which is surrounded by a super insulation system. The generator and generator support system are based on the SNAP-21 10-watt system design. A preliminary analysis of energy requirements, size, and weight is shown below. Critical stress calculations for the thin-walled neck tube are shown in Appendix C.

Energy Requirements for two 10-watt Generators (192 elements at 0.1875 in. diameter) at beginning of life.

Component	Energy Required
Generator Legs	273.6 watts
Neck Tube (Insulation System)	40.1
Outer Case (Thermoelectric Generator)	20.0
MIN-K Insulation (Thermoelectric Generator)	17.6
Super Insulation (Insulation System)	7.6
Reduced Insulation Thickness at Getter Capsule	0.5
8% added per correlation between measured and calculated data on SNAP 21-B (estimated)	28.8
Total (estimated)	388.2 watts

Component	Weight (pounds)
Fueled Capsule	10
Biological Shield	400
Pressure Vessel (Body and Covers)	183
Super Insulation System	60
Generator	50
Power Conditioning Equipment	5
Centering Ring and Generator Mounting Plate	46
Receptacle	3
Miscellaneous	24
Total (estimated)	781 pounds

Some technical problems of this concept which require solution are: a) location of getter capsule, b) providing a method of leading wires from the bottom generator to the power conditioning equipment, and c) providing for a means of expansion of the inner shell, which will be hot, without inducing compressive stress in the neck tube.

Areas where further study is required to determine validity of evaluations, which were conducted by analytical procedure, are:

- The pressure vessel is a cylinder with a dome on each end. Structural strength and integrity of "O" ring seals require further study.
- Assumptions were made as to the loading and method of support of the neck tube. This area should be investigated to determine whether the assumptions are realistic.

Advantages and disadvantages of this concept are:

- The thermoelectric generator has been developed in the SNAP-21B program. A minimum amount of work would be required in this area.
- The heat is removed from both ends which allows use of smaller generators. The generator outer case and insulation neck tube are of smaller diameter, allowing less heat loss.
- The fuel capsule and biological shield is supported by a neck tube at each end. The bending moment is therefore half as great as would be experienced with a cantilevered type construction. The wall thickness is therefore small, reducing heat loss.
- Using two generators of small diameter, the over-all diameter of the pressure vessel does not have to be increased. The wall thickness is therefore unchanged. This would indicate less weight per unit length than the scaled-up 10-watt concept. However, this weight advantage is cancelled out, in part, by the increased length required.
- There are more components to assemble, and, with the power having to be transferred from the bottom generator to the power conditioning equipment the assembly will be more complicated. The greater number of components would also have an adverse effect on reliability.

3.4.2.3 External Heat Rejection System (Figure 3-7)

The objective of this concept is to provide better heat rejection by providing a direct heat path from the generator cold frame to the heat sink (sea water). In this concept this is achieved by connecting the cold frame directly to sea water with a ring of copper. Since

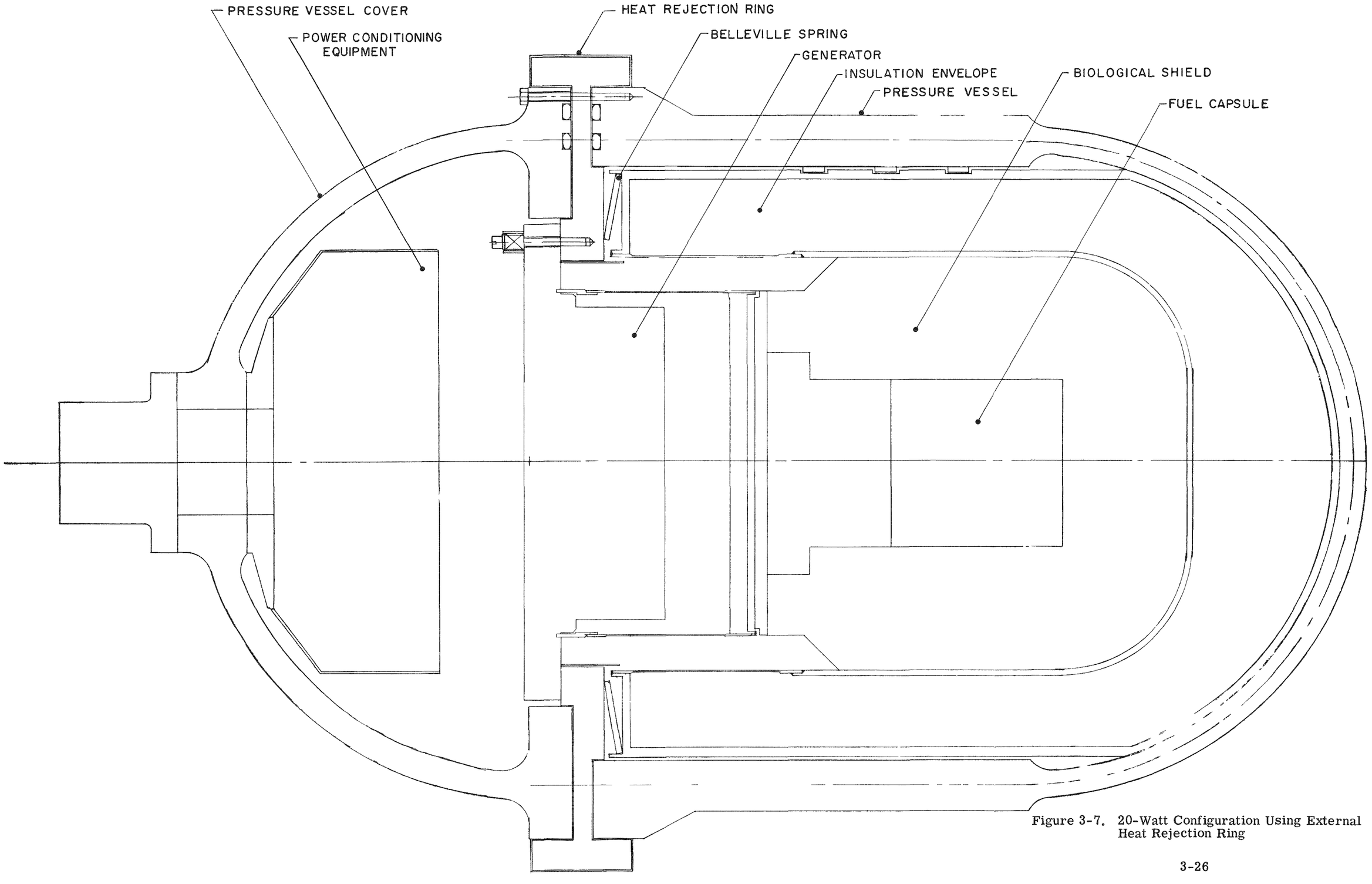

Figure 3-7. 20-Watt Configuration Using External Heat Rejection Ring

the copper ring would be in contact with both sea water and the titanium vessel, it would have to be coated with a metal compatible with titanium in a salt water medium. Spring loaded capscrews will hold the cold frame to the heat rejection ring. A belleville spring is used to hold the insulation system in place. Although heat transfer calculations are not yet complete, it is expected that the temperature at the cold end of the thermoelectric legs will be reduced considerably.

The following technical problems remain unresolved with this concept:

- Method of coating copper with a material compatible with titanium and salt water.
- A structural evaluation will be required to determine whether interaction between the vessel, ring, and cover can be achieved without introducing discontinuity stresses.

The following advantages would be obtained:

- Heat rejection from the system would be more direct, thereby lowering the cold end temperature of the legs. The efficiency of the generator would increase and power output per unit of heat would be increased.
- The belleville spring concept would be easy to assemble and would require a smaller number of parts than the current 10-watt concept.
- The pressure vessel would be approximately one inch shorter, consequently the weight of the pressure vessel would be reduced. This weight advantage would, however, be balanced by the added weight of the heat rejection ring.

The main disadvantage is that the heat rejection ring is located outside of the pressure vessel and is therefore large in diameter. This increases the over-all weight of the system.

3.4.2.4 Spherical Concept

An investigation was made of a spherical concept. It was determined that due to physical size requirements, it would not be practical to use one generator. An attempt was made to mount six generators around the center cube of fuel. This system would make economical use of the space and permit the use of a spherical pressure vessel. However, some of the

fabrication and assembly problems appear difficult to solve. A six-generator system would probably not adapt well to a 20-watt power requirement.

Some problems with this design approach are:

- Transferring heat from the generator to the pressure vessel would be done with spherical spring loaded segments. It would be difficult to get more than 50 percent contact between these spherical surfaces and therefore heat transfer would not be efficient.
- All spherical segments would have different configurations since they would be bearing against different segments of the super insulation system. These segments would be difficult to fabricate.
- The super insulation system would have an irregular configuration which would be difficult to manufacture. The system would probably have to be fabricated in several sections so that it could be assembled. The problem of insulating between sections to reduce heat loss would also have to be solved.
- With all of the spherical segments being spring loaded outward against the vessel, difficulty would be encountered in assembling the two halves of the pressure vessel.
- A method of running wires from the individual generators to the power conditioning equipment would have to be developed.

Because of the above problems, the spherical pressure vessel was, for the present, ruled out as a method to be used for this system. Further investigation has been discontinued.

3.5 PROCUREMENT AND FABRICATION

The effort devoted to procurement and fabrication during this quarter was primarily involved with the ordering of long lead time items and evaluation of materials to meet component requirements. Work was initiated to define the materials and fabrication requirements for tooling and fixturing. Following is a discussion of procurement and fabrication activity for various major system components.

3.5.1 INNER LINER (INSULATION SYSTEM)

Four possibilities were examined for the material to be used for the inner liner: Hastelloy X, Inconel 750, Inconel 625, and Inconel 600. The selection of the inner liner material was to be a joint effort of the subcontractor, Linde Company, and 3M Company. While the final selection was pending, two billets each of Hastelloy X and Inconel X750 were ordered so that material would be available when the final design was determined. Hastelloy X was ordered because it appeared the most promising of the new alloys. Inconel X750 was ordered because it was used during Phase I. These billets have been received. All candidate materials have similar properties, however, some variations do exist in their weldability, availability, and stress rupture strength. The inner liner must be hermetically sealed by fusion welding in the insulation system, therefore, Inconel X625 was not considered to be a satisfactory choice because it would create the most welding problems. At the present there is no commercial weld rod available for this alloy. It is also the least available of the alloys with a quoted delivery of 21 weeks.

The final selection of material was Hastelloy X. Reasons for this selection have been discussed previously in this report in paragraph 3.2.2.2. A total of 130 inches of Hastelloy X billet stock was ordered, 60 inches to be delivered by 31 October 1966 and the balance to be held in an intermediate stage of forging for later delivery.

3.5.2 THERMOELECTRIC GENERATOR

Enough tellurium copper for the entire program has been ordered. This is used in fabricating the thermoelectric couples. In addition, enough electrolytic tough-pitch copper for 20 cold frames has been ordered.

3.5.3 FUEL CAPSULE

Hastelloy C used in the fuel capsule, was ordered. Stainless steel, Type 321, to be used as test material in the development of ultrasonic inspection of the fuel capsule weld, was also ordered. Fuel capsule inner liner material of Type 347 or 316 stainless steel is now in the process of being procured.

3.5.4 BIOLOGICAL SHIELD

Procurement of the biological shield must precede fabrication of the insulation envelope, since in the insulation system fabrication sequence the biological shield is completely surrounded by the insulation system. Normal procurement time for similar shields has been approximately 8 weeks ARO. The Linde insulation development program calls for delivery of the first new shield about November 1, 1966.

Because of the high cost of this component, quotations have been requested from three qualified vendors. Adding this quotation phase to the procurement cycle may cause a slip in the November 1 delivery schedule.

3.5.5 COMPATIBILITY TESTING MATERIALS

Materials to be used for coating compatibility tests, uranium-8 molybdenum, and Hastelloy X washers, have been ordered.

3.5.6 PROCUREMENT SUMMARY

Following is a list of materials ordered this quarter with the promised or expected delivery date:

Material Description	Date Received or Promised
Copper Plate - (Cold Frame Material)	9-30 (received)
Hastelloy "X" Bar Stock (Inner Liner Material)	9-19: 2 billets (received) 10-31: 60-inch bar stock 70-inch 3M Co. to specify delivery
Inconel 750 Bar Stock (Inner Liner Material)	9-19: 2 billets (received)

Material Description	Date Received or Promised
Tellurium Copper Wire (Cold Cap Material)	9-24 (received)
Hastelloy "C" Bar Stock (Fuel Capsule Material)	11-15
321 Stainless Steel Sheet (Ultrasonic Test Weld Development)	Out for quotation
321 Stainless Steel Tubing (Ultrasonic Test Weld Development)	Out for quotation
Hastelloy "X" Bar Stock (Compatibility Test Material)	10-10
Uranium-8 Molybdenum Alloy Washers, Bolts and Nuts (Compatibility Test Material)	Waiting delivery date
Molybdenum Wire (For Securing Biological Shield Bolts)	10-3
Uranium-8 Molybdenum Alloy (Biological Shield and Bolts)	Out for quotation
Uranium-8 Molybdenum Samples (Linde Company's Compatibility Studies)	10-10

It is planned that the balance of the long lead time items, such as the pressure vessel, thermoelectric legs, and biological shields, along with other items necessary to meet scheduled delivery will be ordered and delivery dates established during the next quarter. Tooling and fixturing will have been identified and fabrication of leading items will have started.

3.6 ASSEMBLY AND PROCESSING

The effort devoted to assembly and processing during this quarter was primarily involved with refurbishment of the biological shield from Phase I and developing the copper flame spray coating on the inner liner. This process was developed to coat the inner liner for the first development insulation system, made from Phase I residual parts. Details of this effort are presented in the following paragraphs.

3.6.1 PROCESS DEVELOPMENT

3.6.1.1 Inner Liner Flame Sprayed Copper Coating

At the system operating temperature of approximately 1300-1400° F, it is possible for a eutectic reaction to occur between the high temperature alloy of the inner liner and the uranium-8 molybdenum biological shield. It was therefore necessary to develop a barrier coating for the inner liner. The material selected was a coating consisting of 0.003 to 0.005 molybdenum substrate with a 0.020-inch thick copper overlay. Copper was selected as the coating material because of previous experience with it on SNAP-21 and SNAP-23, and for its ease of application.

Before coating the first inner liner to be delivered to Linde for the first Phase II insulation system, it was necessary to establish the methods and techniques required for applying the coating. This first inner liner is a residual component from Phase I and is made from Inconel X750. It was also necessary to determine the adequacy of the bond between the base metal versus substrate and substrate versus copper coating.

The flame spray development was conducted on a test piece consisting of a 304 stainless steel tube, 3-inch O.D. by 0.065-inch thick wall and 18-inch long. The test piece was mounted between lathe centers and rotated during the spraying operation.

Surface preparation of the test piece consisted of sandblasting the entire outer surface with SiO_2 sand.

The flame spraying gun used was a "METCO" type GF. The spray material used was 1/8-inch diameter molybdenum and copper wire. The spraying gas mixture was acetylene and oxygen with flow meter settings of 30 and 32 respectively.

The test piece was initially sprayed with a 0.003 to 0.005-inch thick substrate of molybdenum. It was then masked off into six 2-inch long sections so that the coating thickness could be varied from section to section. Spraying of the test piece with copper was then initiated. Sections 1 and 2 were individually sprayed to obtain 0.005-inch and 0.010-inch of copper, respectively. Thickness of the coating was controlled by taking O.D. micrometer measurements.

After spraying, it was noted that the tube temperature had risen enough to cause oxide discoloration of the copper coating. The last four sections of the test piece were built up to 0.015, 0.020, 0.025 and 0.030, respectively, by spraying all four sections in successive passes. Between passes, time was allowed to permit the test piece to cool to prevent excessive oxidation of the copper coating. The thickness of coating was controlled by O.D. micrometer measurements.

One sample of each coating thickness was sectioned longitudinally and metallographically examined for laminations, voids, and mechanical bond between the base metal, substrate, and copper coating. In all cases a good mechanical bond was obtained at both interfaces. The molybdenum substrate was not continuous nor as thick as anticipated, actually only 0.001 to 0.002-inch thick where covered, rather than the 0.003-0.005 inch measured previously. This was probably due to micrometer measurement error caused by the initial expansion of the test piece being heated to the working temperature. The thicker layers showed laminations and some layer separation, probably caused by the spraying technique. Most thicknesses showed discontinuous porosity and dispersed oxides.

Photomicrographs of typical cross sections of the coatings are shown in Figures 3-8 through 3-13.

The average coating thickness was measured from the photomicrographs with the following results:

Sample No.	Desired Thickness	Obtained Thickness
1	0.005	0.006
2	0.010	0.010
3	0.015	0.018
4	0.020	0.020
5	0.025	0.026
6	0.030	0.030

(These results show very close dimensional control with the exception of Sample No. 3.)

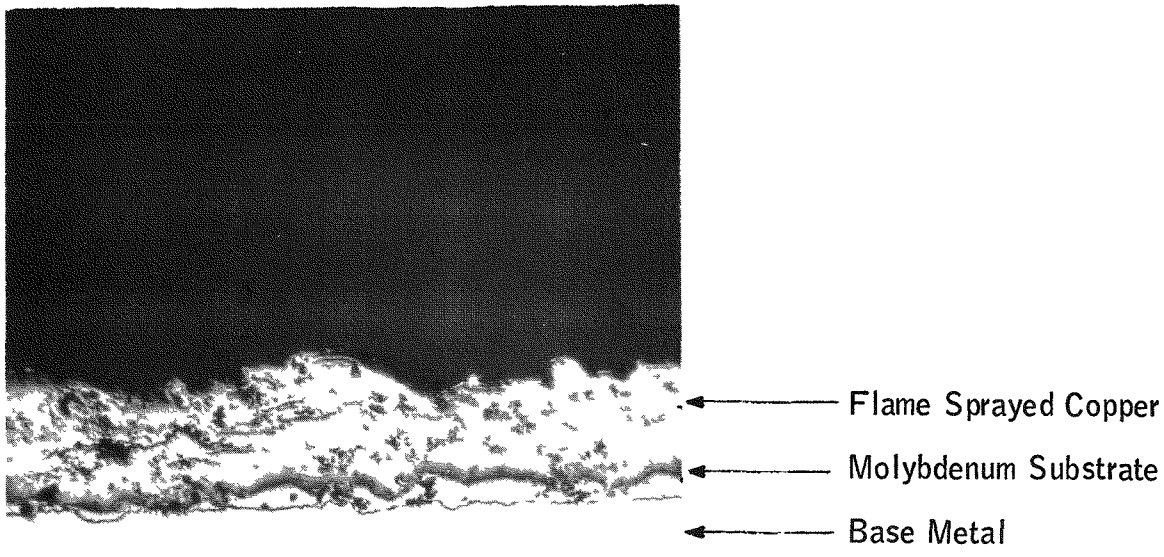

Figure 3-8. Cross Section of Flame Sprayed Sample Sample No. M1599-1, 100X Magnification (0.005 in. thick copper plus molybdenum substrate)

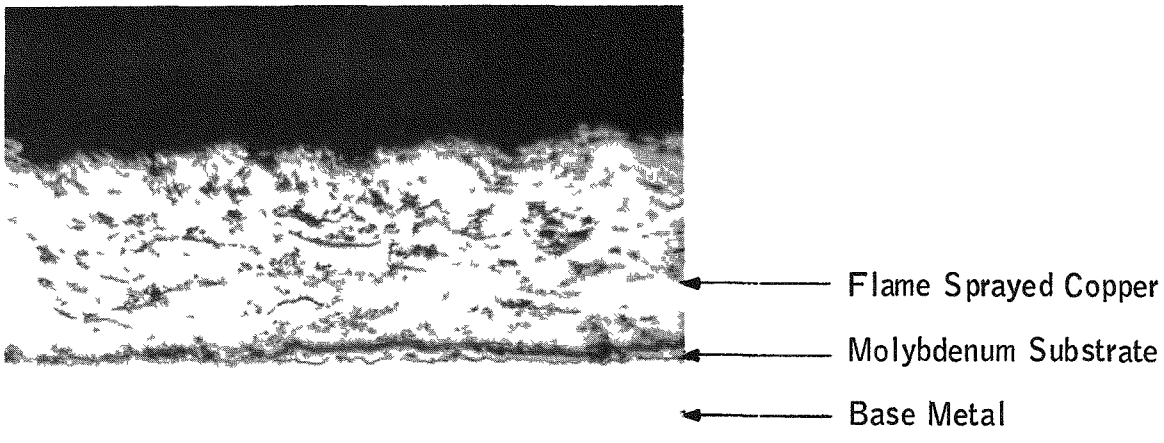

Figure 3-9. Cross Section of Flame Sprayed Sample Sample No. M1599-2, 100X Magnification (0.010 in. thick copper plus molybdenum substrate)

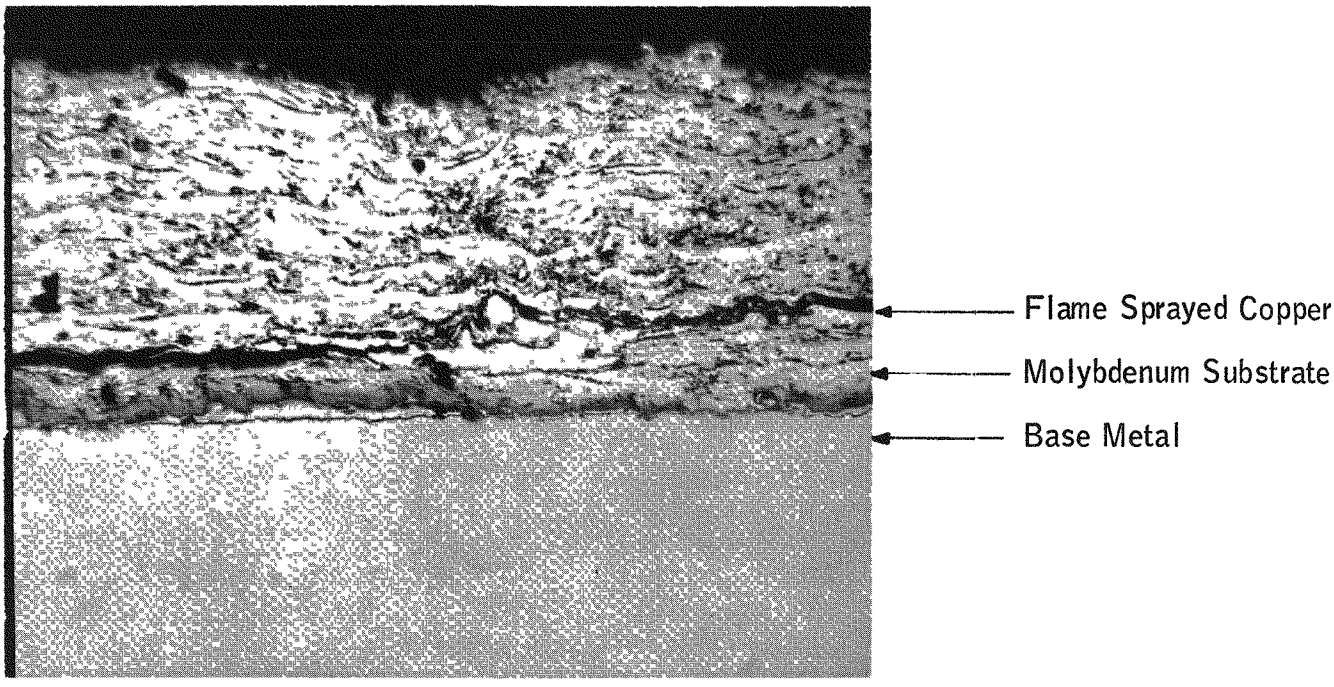

Figure 3-10. Cross Section of Flame Sprayed Sample Sample No. M1599-3, 100X Magnification (0.015 in. thick copper plus molybdenum substrate)

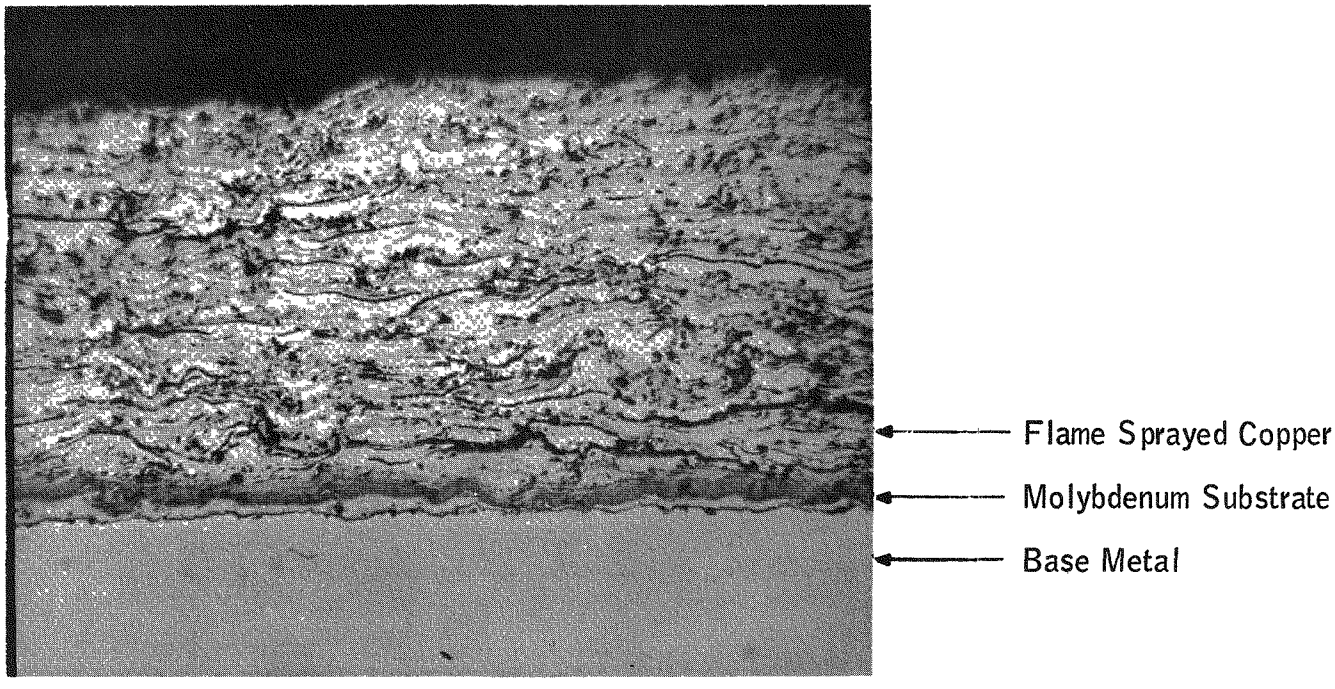

Figure 3-11. Cross Section of Flame Sprayed Sample Sample No. M1599-4, 100X Magnification (0.020 in. thick copper plus molybdenum substrate)

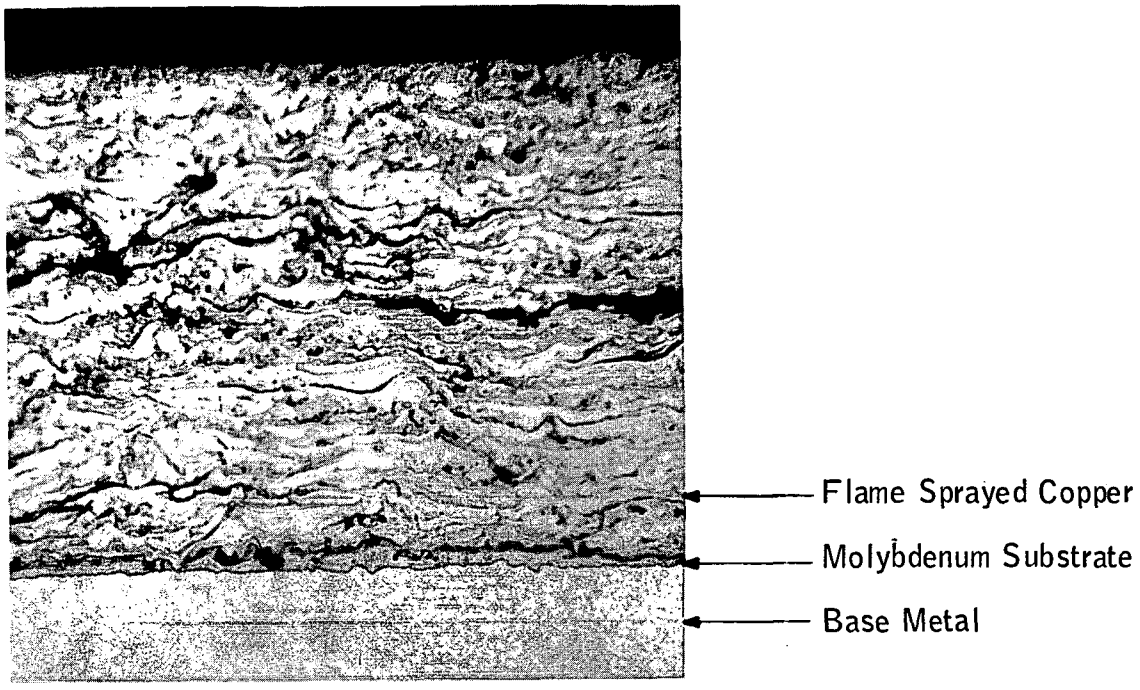

Figure 3-12. Cross Section of Flame Sprayed Sample Sample No. M1599-5, 100X Magnification (0.025 in. thick copper plus molybdenum substrate)

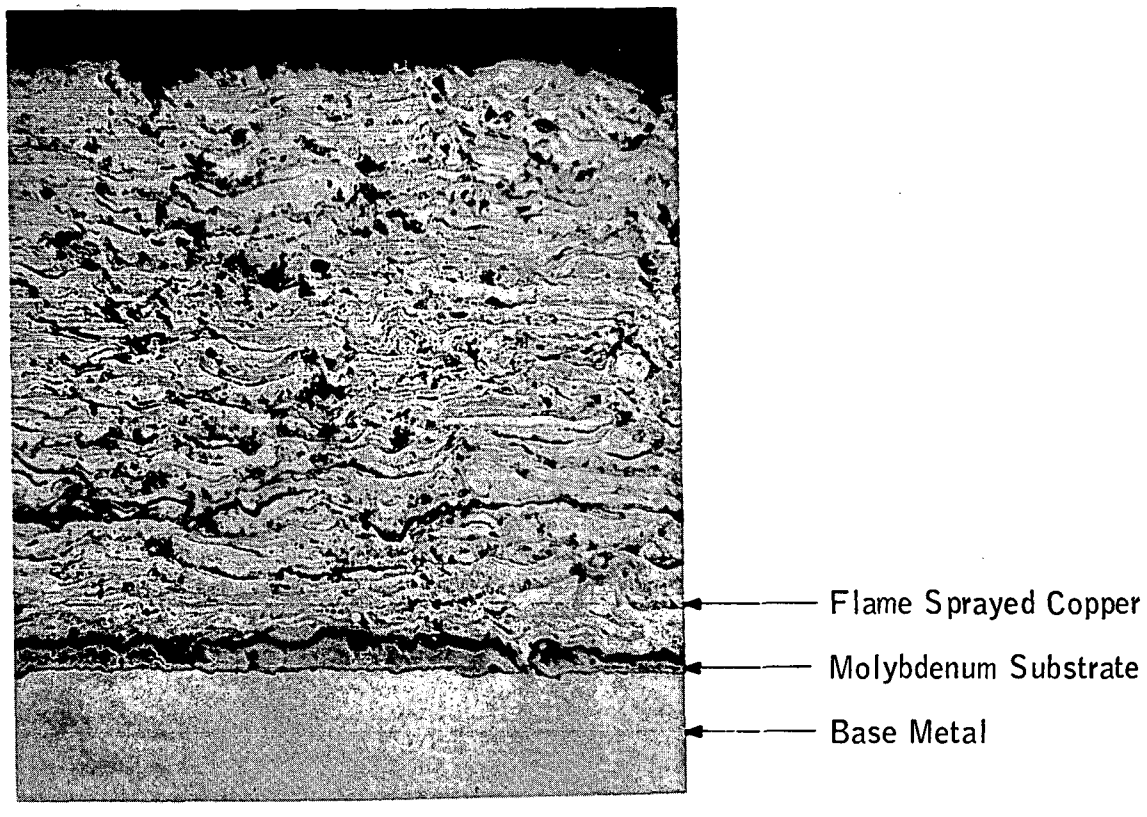

Figure 3-13. Cross Section of Flame Sprayed Sample Sample No. M1599-6, 100X Magnification (0.030 in. thick copper plus molybdenum substrate)

To determine coating integrity during its most severe environment, (the temperature transients experienced during processing, checkout, and fueling) samples 1/2-inch wide by 2 inches long were thermally cycled to determine their blistering and spalling characteristics. These samples were prepared by degreasing in trichloroethylene, then placed in a vycor tube which was evacuated to less than 25 microns. Subsequently they were heated to 1400° F in a radiant wall type furnace. Evacuation of the tube was continuous throughout the heating cycle. Furnace temperature was controlled by an instrumented test sample attached to the outside of the vycor tube.

The first set of samples were cycled three times from ambient to 1400° F. The results showed no spalling or blistering, but copper had evaporated and was redeposited on the inside surface of the vycor tube.

It was hypothesized that the surface of the samples had been at a higher temperature than that indicated by the instrumented sample outside the tube, due to the radiant heating effect, and that this higher temperature caused the copper evaporation. That is, the instrumented sample whose temperature was being measured, was placed outside the tube in the furnace atmosphere. However, the test sample was in the evacuated tube and all heat transferred to it was radiative, from the atmosphere and walls. The furnace walls, being at a higher temperature, would then cause the surface of the specimen to reach a higher temperature. The temperature would be nearer to that of the walls than to the atmosphere, since conductive heat loss from the sample in the evacuated tube is minimal. To verify this, samples were tested in an asbestos wrapped vycor tube. These samples were free from copper evaporation and showed no blistering or spalling effect. In view of this, it was assumed that the excessive radiant heating had caused the vaporization. New samples were prepared for more complete thermal cycling, using the same asbestos wrapped vycor tubing technique. To help eliminate the possibility of surface overheating, the temperature was raised from ambient to 1400° F over a four-hour period. Examination of the samples following this test cycle again showed copper evaporation and redeposition on the tube wall. This indicated that some phenomenon other than surface overheating was taking place.

The next potential problem source evaluated was the sample preparation technique. New samples were prepared by degreasing in isopropyl alcohol, rinsing in de-ionized water, and drying in a furnace at 250° F for 45 minutes. Samples were placed in two vycor tubes, one asbestos wrapped and one not wrapped. Both were placed in the furnace, evacuated, and reheated at a slow heating rate. After five thermal cycles samples from both tubes

were free from copper evaporation and from any spalling or blistering. This evidence suggests that a reaction was taking place between the halogen in the trichloroethylene and the copper coating. Further evaluation during the next quarter will be necessary to prove this hypothesis.

3.6.1.2 Compatibility Testing

To investigate the reaction between the copper coating on the inner liner and the U-8 Mo shield, compatibility studies will be undertaken to determine the adequacy of the barrier coating for the system lifetime.

A preliminary test program has been established. Test samples will consist of U-8 Mo washers, Hastelloy X washers, copper coated Hastelloy X washers, and U-8 Mo bolts and nuts. The test washers will be placed on the bolts in a sequence duplicating the actual interfaces obtained in system assembly. The pressure applied will be equivalent to the inner liner to biological shield bolt torque of 24 inch-pounds. Samples of bare Hastelloy X to U-8 Mo will also be a part of the test.

Program duration tests are planned which will run for the life of the program at the operating temperature of 1375° F. Short term tests will be run at various times and temperature. The times will be 200, 500, 1000, 1500 and 2000 hours with test temperatures varying from 1375° F to 1800° F. This test program will be firmly established and testing started during the next quarter.

3.6.2 INNER LINER COATING (INSULATION SYSTEM)

Two inner liners were copper coated by flame spraying, using the method described above. These two inner liners were made from Inconel 750 and were residual from the Phase I SNAP-21 Program. The first inner liner to be flame sprayed was used to establish dimensional control during the processing, and to develop techniques for spraying this configuration.

A complete pre-coating dimensional check of the inner liner was made by measuring the cylindrical portion to be coated on both the O.D. and I.D. in five planes perpendicular to the longitudinal axis to establish base points. Three diameter measurements were taken at each plane. These dimensions were again inspected after spraying to determine if distortion occurred during the spraying operation and to establish coating thickness.

The inner liner was prepared for spraying by masking non-coated areas and only sand-blasting those areas to be coated. The liner was then placed in a lathe in preparation for spraying. The same spraying equipment and wire size was used as that used in the test samples. The spray gas proportions were changed slightly to help prevent excessive oxidation.

The new gas settings on the flow meters were 31 for oxygen and 32 for acetylene. Dimensional control of the coatings was again controlled by in-process micrometer readings. Although the heat buildup on the liner was not as high as on the test samples, it was considered in obtaining the final thickness of coating. It was particularly difficult, because of the angle of spray to obtain uniform coating thickness on the I.D. of the holes in the flange section of the liner, therefore special attention was given to them. The balance of the configuration did not appear to be difficult to spray.

A complete dimensional inspection after spraying showed no distortion. The bottom of the liner showed an excessive buildup of material. This was attributed to the spraying technique. Two of the stepped O.D.'s showed larger diameters. This was due to over-spray while attempting to spray the bottom of the flange and first step. The flange holes did not have enough coating on the I.D. surface nearest the outer rim of the flange, and were oval because of the problem of hitting the flange holes with the spraying cone of metal.

The second liner was flame sprayed using the same methods as employed on the first liner, but changing technique to compensate for and correct the dimensional variation noted on the first liner. All dimensional requirements were met on the second liner, with the exception of the bolt holes. In this case the holes showed ovality, but the minimum coating thickness was satisfied. It was necessary to ream the bolt holes to remove excess copper. The excess was caused by the overspraying necessary to obtain the minimum coating thickness in hard to reach places. Figure 3-14 shows two views of the as-sprayed inner liner, ready for insertion into the biological shield with the exception of the bolt hole machining.

3.6.3 REFURBISHMENT OF PHASE I RADIATION SHIELD

As a means of accelerating development of the SNAP-21 System, it was necessary to use a residual shield fabricated in the Phase I effort of the program. This shield was of a different configuration from that of the present design; however, it could be re-machined to conform to the new configuration. This shield was part of the last insulation system

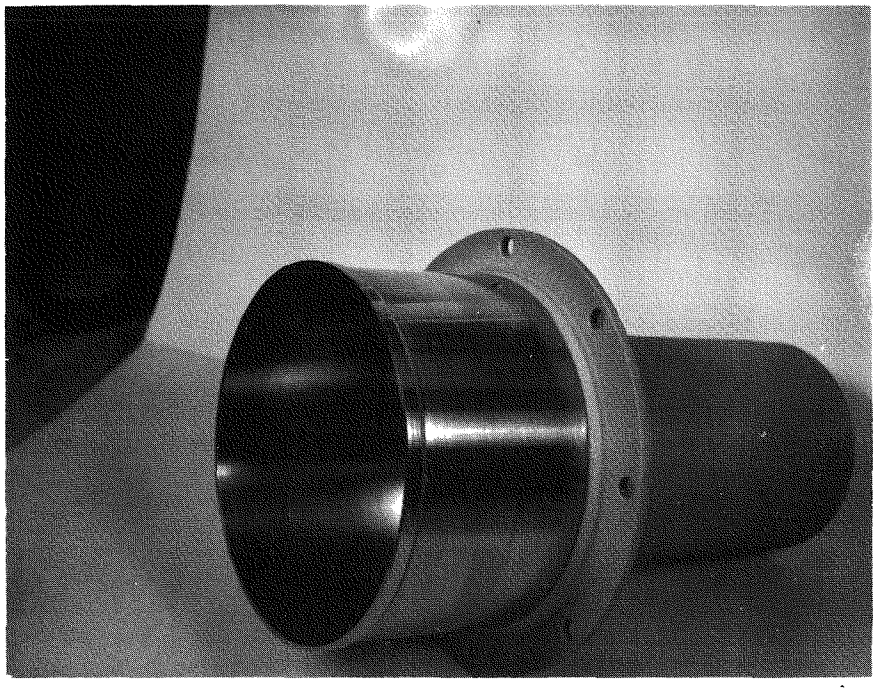

(a)

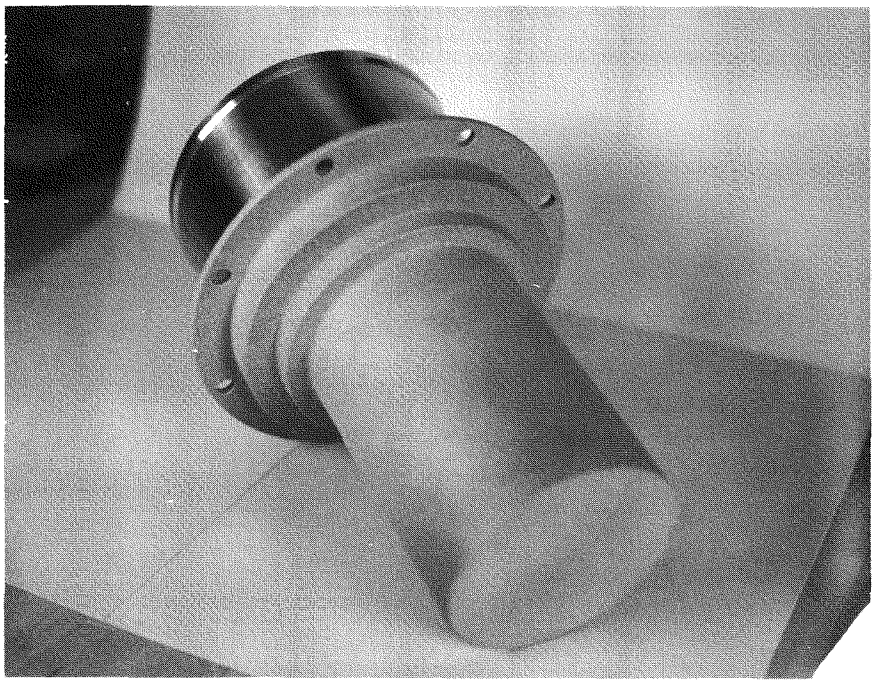

(b)

Figure 3-14. Flame Sprayed Inner Liner

(Unit No. 3) to be fabricated by Linde during Phase I, which was defective because of a vacuum leak. Because of the radioactive nature of the shield material, it was sent to the Nuclear Metals Division of the National Lead Company for refurbishing. The outside insulation envelope was removed at 3M, but because the vacuum leak had caused considerable oxidation of the shield during the several reheating cycles experienced in processing the insulation system, it was decided to remove the inner liner of the envelope at National Lead. Examination of the shield surface showed that much of its copper plated surface had blistered (Figure 3-15). The cladding appeared to have effectively prevented inter-reaction of the shield alloy with the inner liner. Prior to machining, the copper cladding was stripped chemically. Some difficulty was encountered with dissolution of the copper in the sulfuric acid.

Examination of the shield revealed that a tap had been broken off in a bolt hole, but it was removed without difficulty. An attempt was made to plug the old bolt holes; however, it was not successful and it was necessary to machine out the bolt circle and shrink fit a new ring in the cavity. After machining was completed, electroplating a 0.003-inch thick copper cladding was started. This work is scheduled for completion the first week in October, with shipment to Linde by October 10th.

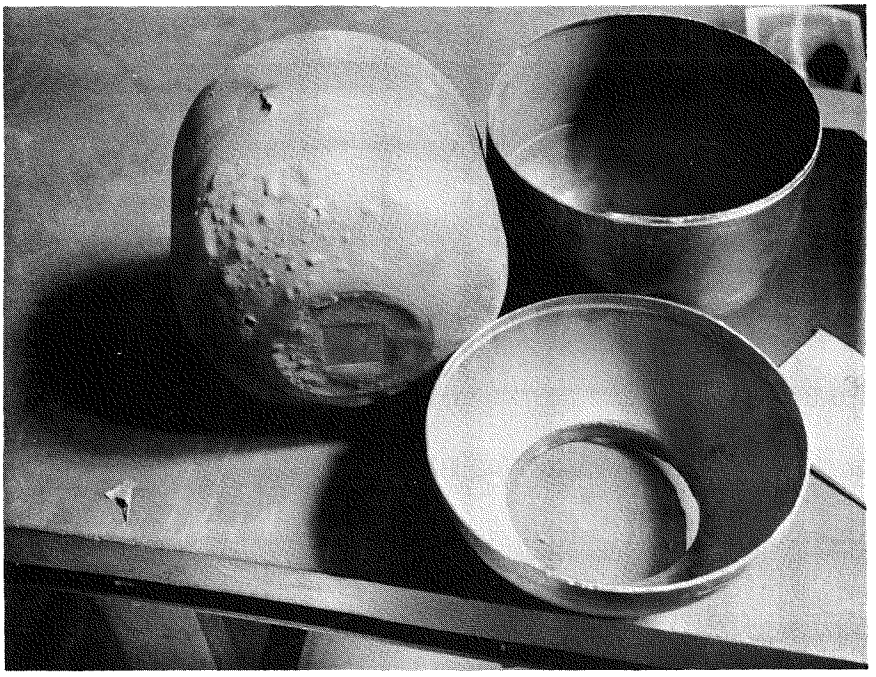

(a)

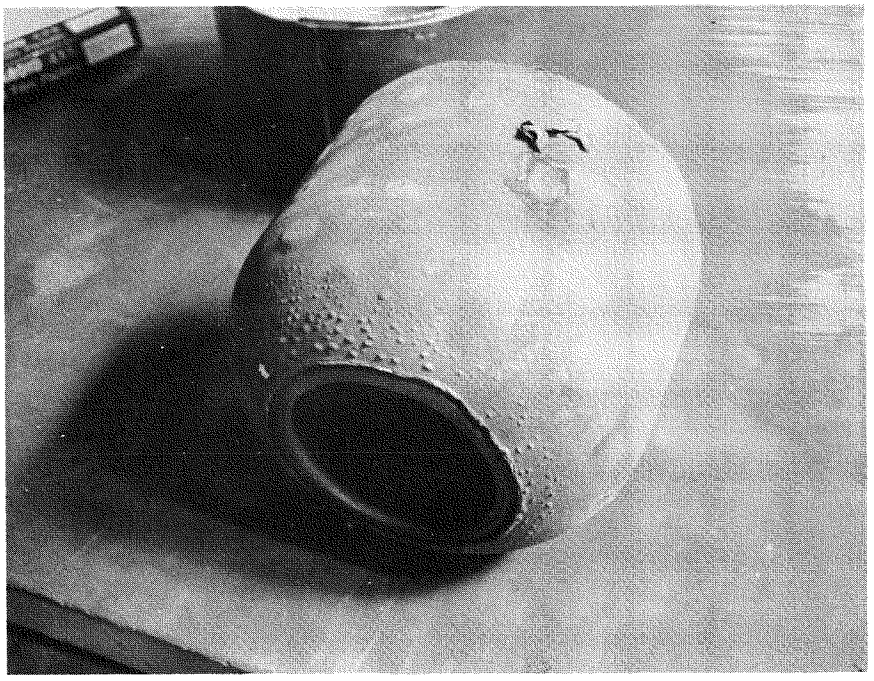

(b)

Figure 3-15. Phase I Biological Shield Showing Blisters in Copper Cladding

3.7 TEST AND ANALYSIS

3.7.1 TASK I, 10-WATT SYSTEM

Test and analysis effort on the 10-watt system was concerned with preparing an insulation system for dynamic testing and failure analysis of its components following disassembly. The insulation system used was a Phase I residual system from Linde. This insulation system (Unit No. 3) was the last to be fabricated during Phase I. It was inoperative because a vacuum leak of unknown size and location prevented it from being evacuated to a level required for operation.

Since this unit contained a biological shield of the same material, U-8 Mo, and was of the approximate size as the Phase II units, it was to be salvaged for use in the first Phase II development insulation system. Because the neck tube of this unit was dimensionally representative of the Phase II neck tube, it was decided to dynamically test the unit to destruction under controlled conditions to obtain experimental data that could be used to verify an analytical design.

Dynamic testing of this unit was not performed because the neck tube was damaged during transportation because of improper handling procedures.

Prior to shipping the system to the dynamic test vendor, the test plan called for the unit to be evacuated by dynamic vacuum pumping, and then brought to operating temperature to make the test conditions simulate actual conditions as close as possible. An attempt was made to evacuate the system; however, the vacuum leak was greater than pump capacity. Consequently, the pumping effort was abandoned. The unit was heated to 1250° F using electric heaters and a procedure that simulated the actual thermal transient experienced by the SNAP-21 System. Thermocouples were mounted on the system to monitor various temperatures during the heat-up cycle. A photograph of the complete system is shown in Figure 3-16.

After the inadvertent neck tube failure, the system was dismantled. The first step was to remove the outer shell and cut away the thermal radiation shields and spacers. A photograph of the unit after this operation is shown in Figure 3-17.

Following this, the biological shield, encased in the inner shell, was removed. Examination of the inner shell revealed two raised bumps at the bottom. Four cracks radiated

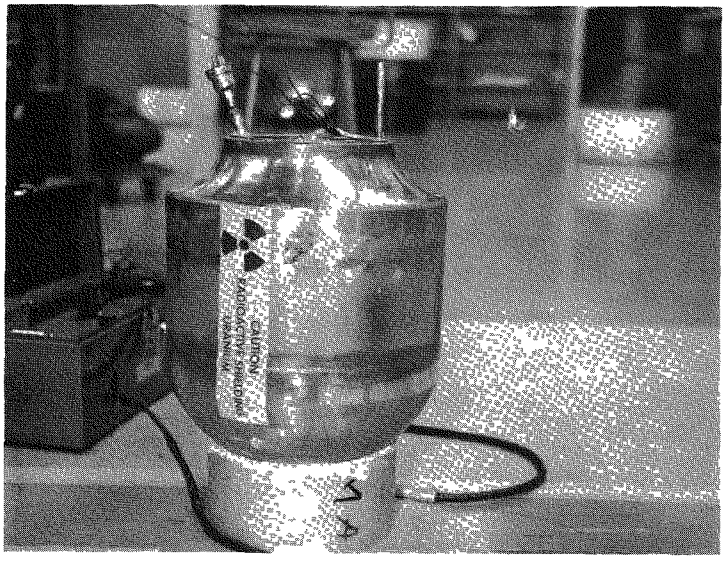

Figure 3-16. Insulation System (Unit No. 3) During Electrical Heating Cycle

Figure 3-17. Sectioned View of Partially Dismantled SNAP-21 Insulation System

from each bump. A leak check of these two spots revealed that they were the source of the vacuum leak. Figures 3-18, 3-19, and 3-20 show the location and leak check of these spots. Figure 3-21 is a schematic showing actual dimensions of the failure zone.

Removal of the inner shell from the shield revealed that a 2-inch by 2-inch by 1/4-inch thick square spacer had been spot welded to the interior of the inner shell. The spacer was used as a shim to facilitate assembly. Differential thermal expansion of the shield and shell created excessive stresses and caused the protrusions and cracking. Figures 3-22 and 3-23 show the shim and separated shell.

3.7.2 PHASE I CONTINUATION TESTING

During this report period thermoelectric and electronic test work initiated during Phase I continued to be monitored and analyzed. The test units are:

1) 6-couple modules: Units A1, A3, and A4
2) Prototype generators: Units P3, P5, P6, and P7
3) SNAP-21B, Mock-up System Test
4) Electronic components: power conditioners MPB and MPC, test fixture regulator, and automatic selector switch

The performance of 5-couple modules A1, A3, and A4 is shown in Figures 3-24, 3-25, and 3-26 respectively. In these figures the 6-couple open circuit voltage and power delivered to load are plotted as a function of test time. The only significant change in performance is noted for Module A4 at 16,200 hours. On August 12, 1966, this module was observed to have a broken current lead resulting in an open circuit load condition. At constant input power this would result in a hot electrode temperature considerably above the beginning of life (B.O.L.) design point of 1100° F. Although it is not known how long the module was open circuited, it could conceivably have been since July 18, 1966 (about 700 hours). The decrease in power output appears to be principally associated with a resistance increase in the P-legs or their contacts.

Normalized performance data for the four prototype generators continuing on bench test (Prototypes P3, P5, P6, and P7) is shown in Figures 3-27 through 3-30. In these figures the following nomenclature is used:

E_x - experimental open circuit voltage

E_c - computer predicted open circuit voltage

R_x - experimental internal resistance

R_c - computer predicted internal resistance

P_x - experimental power to load

P_c - computer predicted power to load

Examination of the data shows all four prototype generators to be operating satisfactorily with no recent significant changes in performance.

Performance data for the system evaluation test is shown in Tables 3-1 and 3-2. This data shows the system to be performing satisfactorily after over 12,000 hours of continuous operation. It should be noted that on June 26, 1966 the input power to the system was decreased from 230 to 224 watts. This was done to simulate the reduction in thermal power which the SR-90 isotopic fuel would experience after one year. Similar input power decreases were performed on the 6-couple modules and prototype generators.

Life tests of electronic components (power conditioners, regulators, and automatic selector switch) are continuing. Test data shows no significant change in performance.

NOTE

On June 27-28, 1966 the SNAP-21 6-couple modules, prototype generators, system test, and electronic tests were moved from one facility to another. All tests except the electronic components were moved electrically hot. There were two minor incidents:

1) A small amount of MIN-K 1301 thermal insulation was lost from the external test container of Prototype No. 3. This was due to a loose external cover.

2) The isolation transformer on the SNAP-21B burned out. The system was moved with a maximum hot electrode temperature decrease of 100° F.

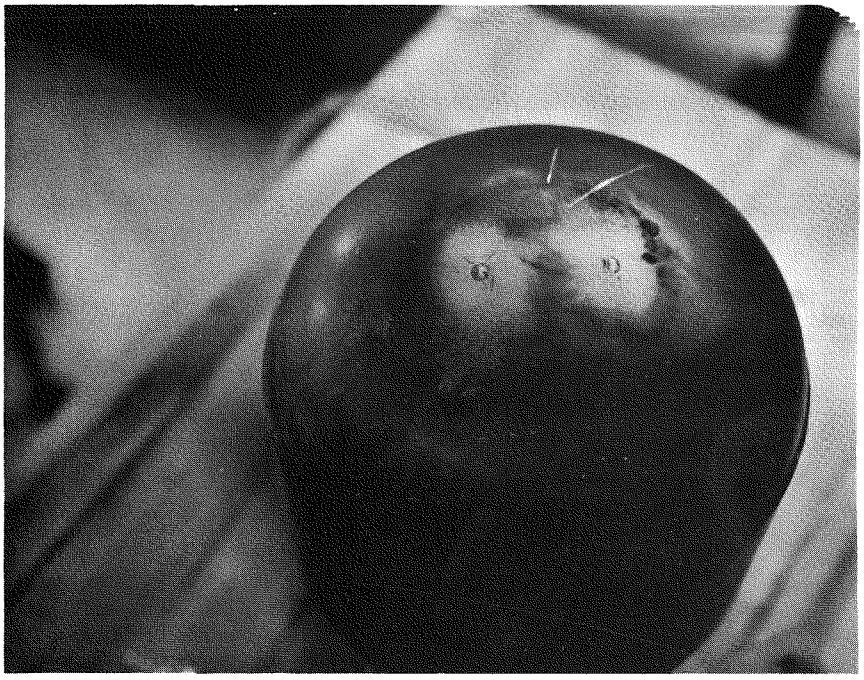

Figure 3-18. Biological Shield in Inner Shell Showing Two Failure Zones

Figure 3-19. Leak Checking Inner Shell (Internally Pressurized)

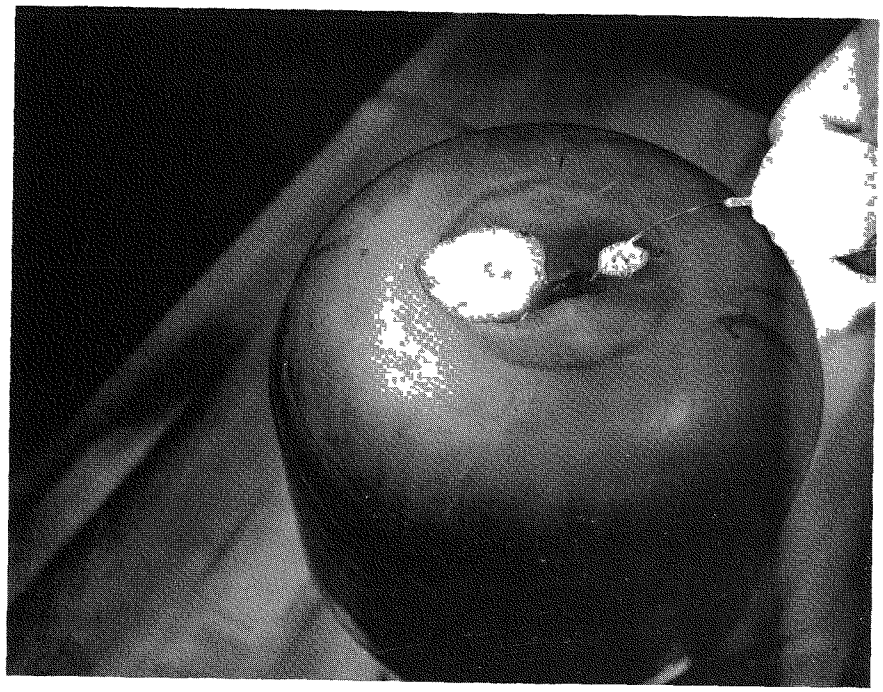

Figure 3-20. Result of Pressurized Shell Leak Check

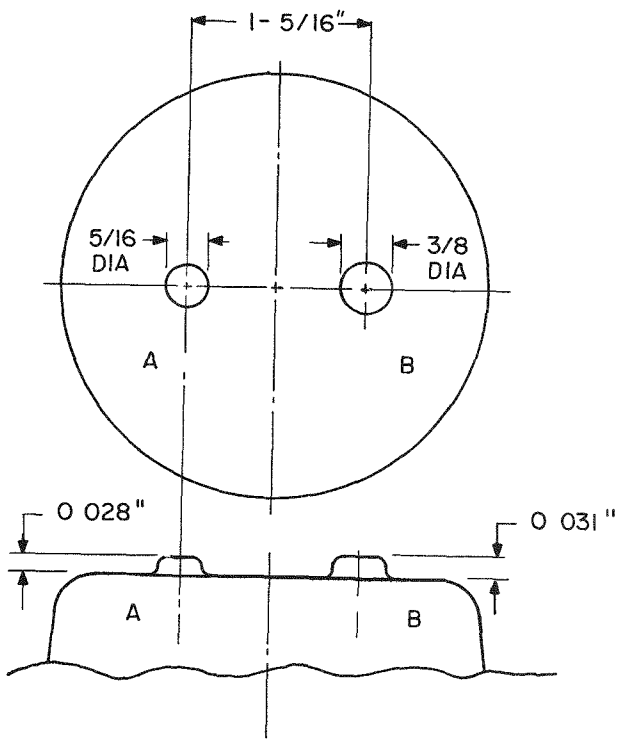

Figure 3-21. Schematic Showing Actual Dimensions of Inner Shell Failure Zone

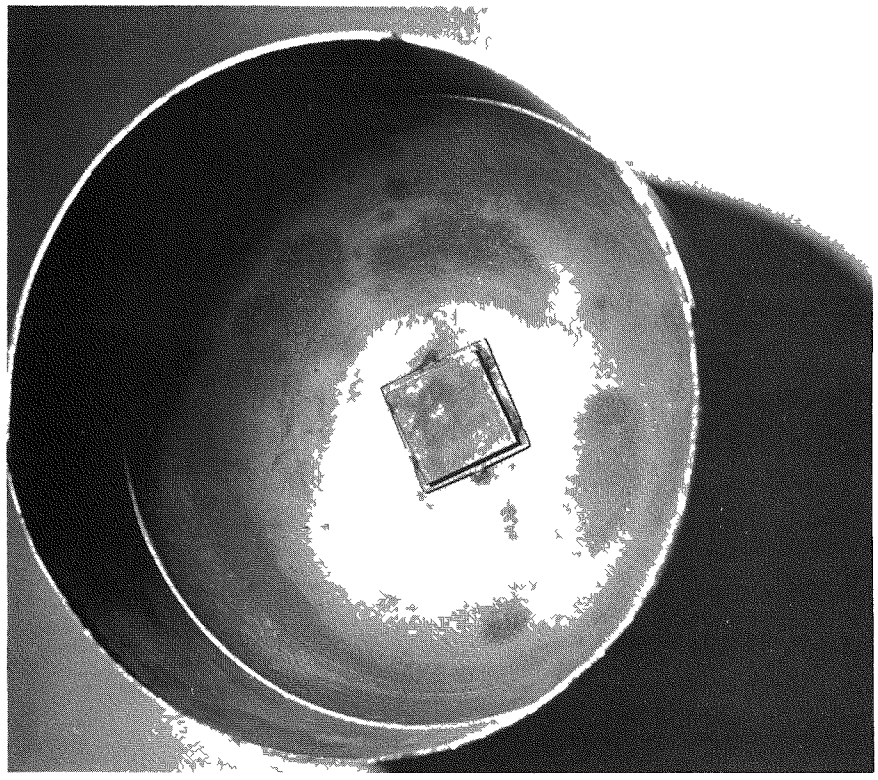

Figure 3-22. Lower Half of Inner Shell Showing Shims

Figure 3-23. Inner Shell Following Separation

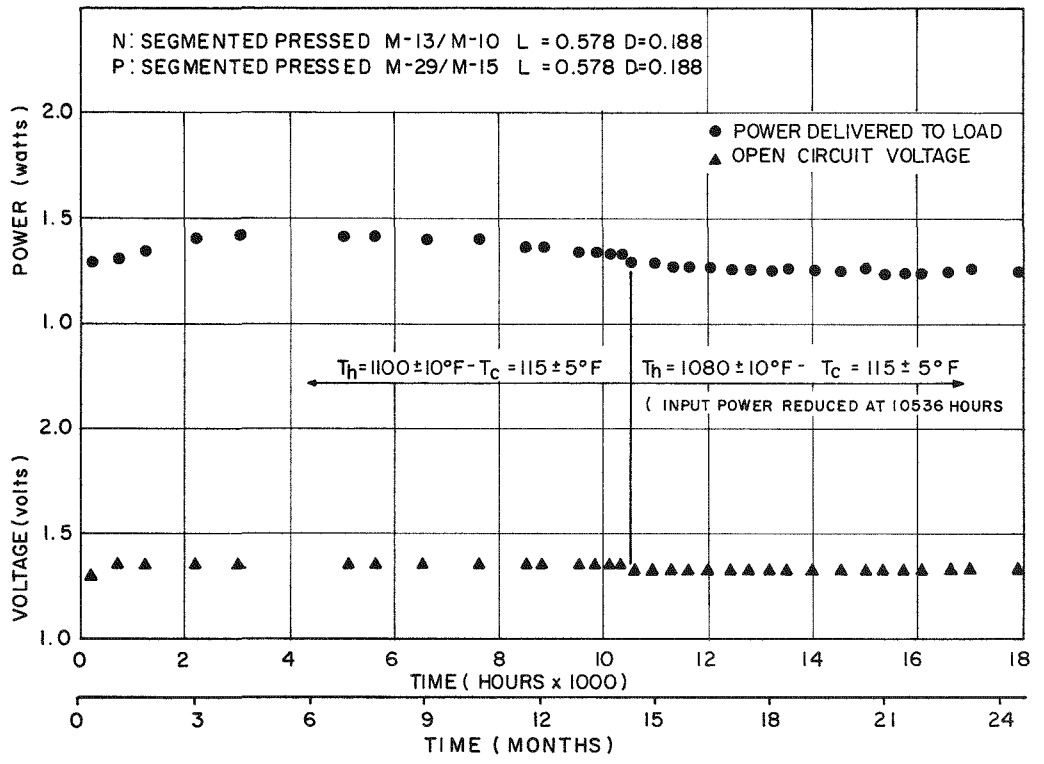

Figure 3-24. SNAP-21B 6-Couple Module A1 Performance

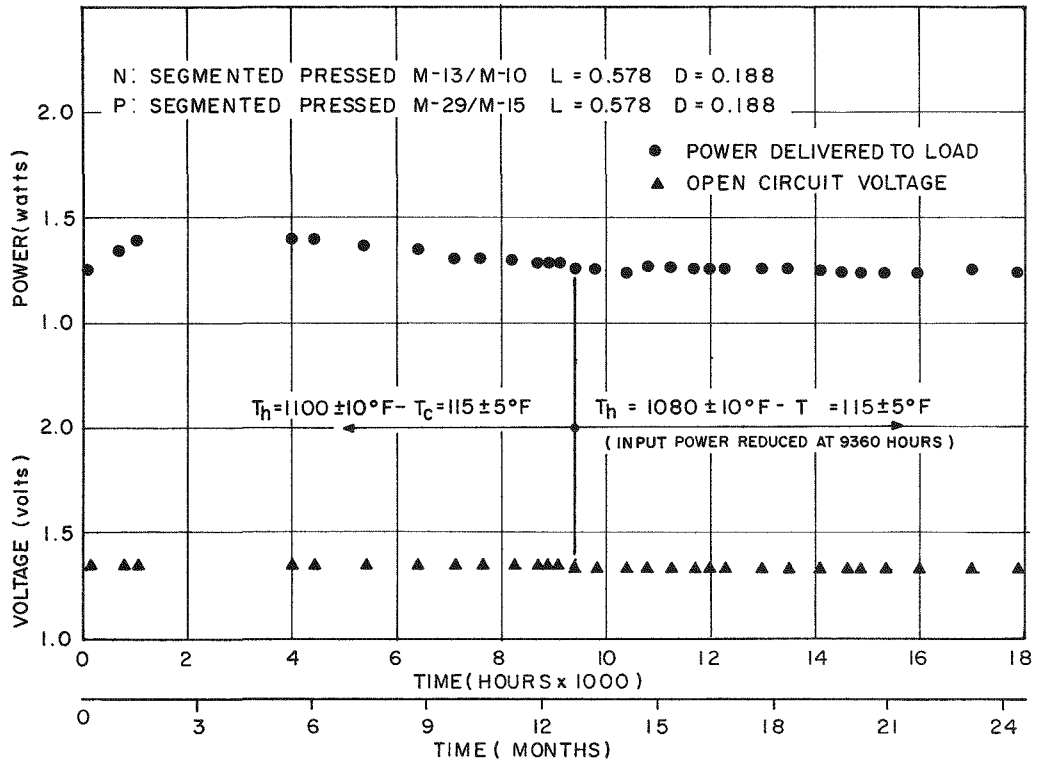

Figure 3-25. SNAP-21B 6-Couple Module A3 Performance

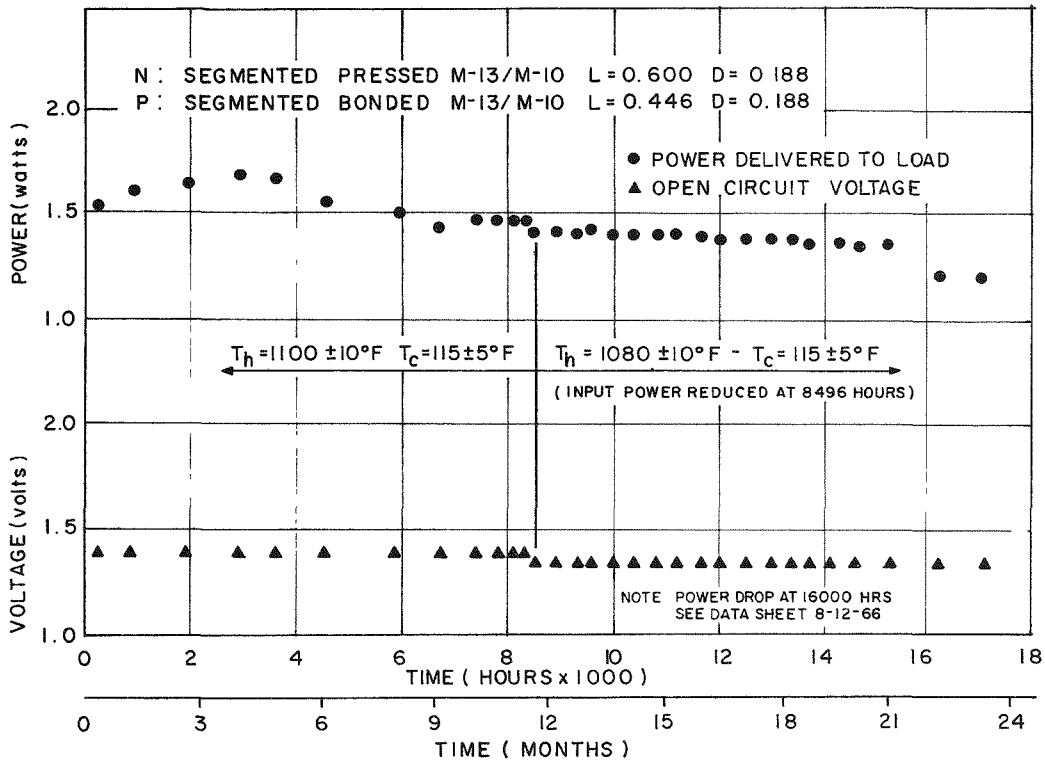

Figure 3-26. SNAP-21B 6-Couple Module A4 Performance

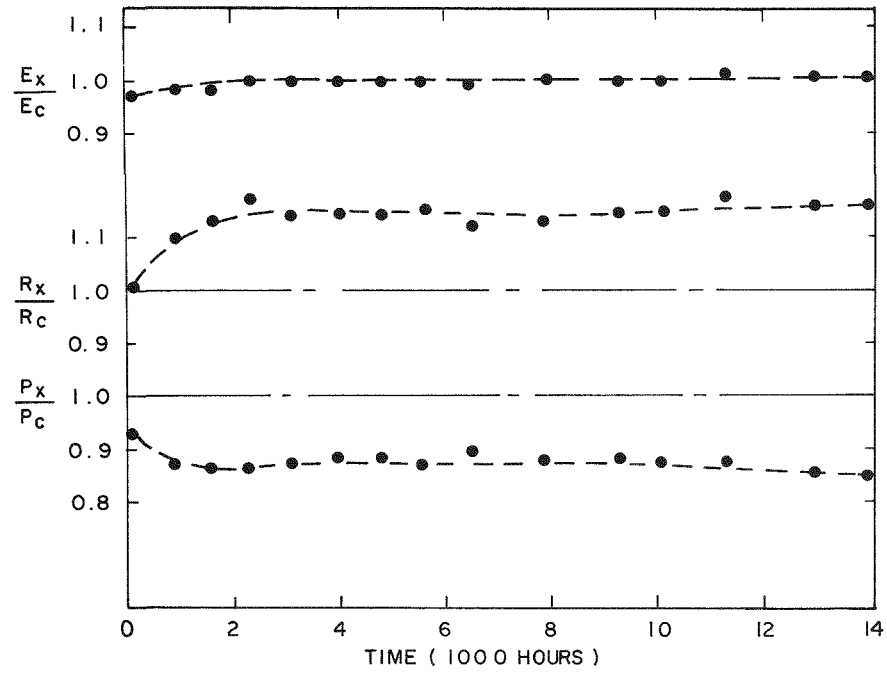

Figure 3-27. Performance of Prototype 48-Couple Generator 3M-37-P3 (E = voltage, R = resistance, P = power, x = experimental, c = computer)

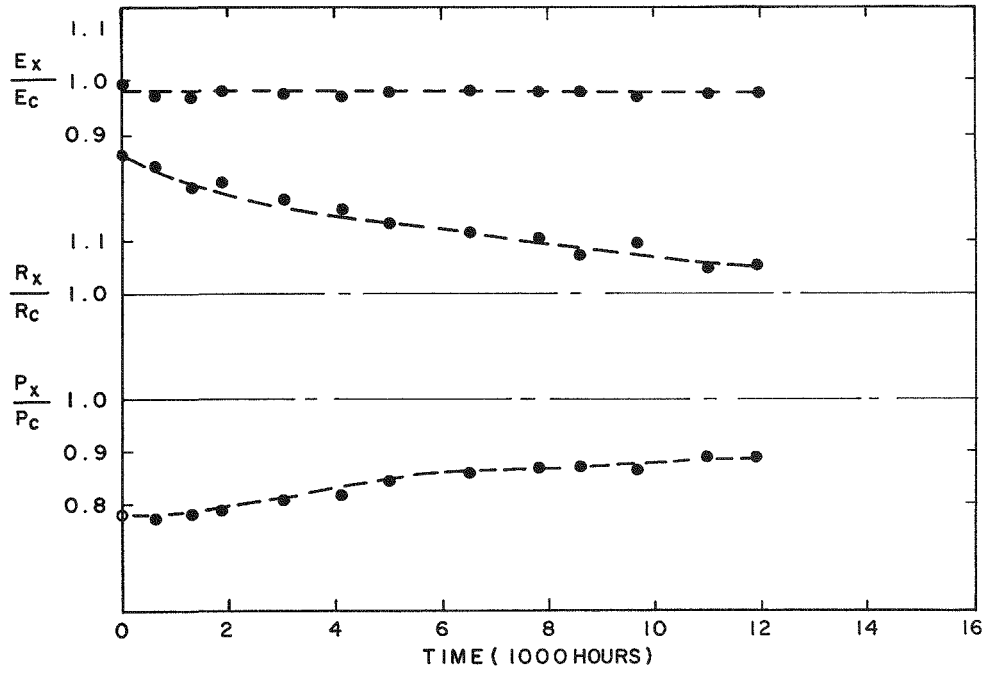

Figure 3-28. Performance of Prototype 48-Couple Generator 3M-37-P5 (E = voltage, R = resistance, P = power, x = experimental, c = computer)

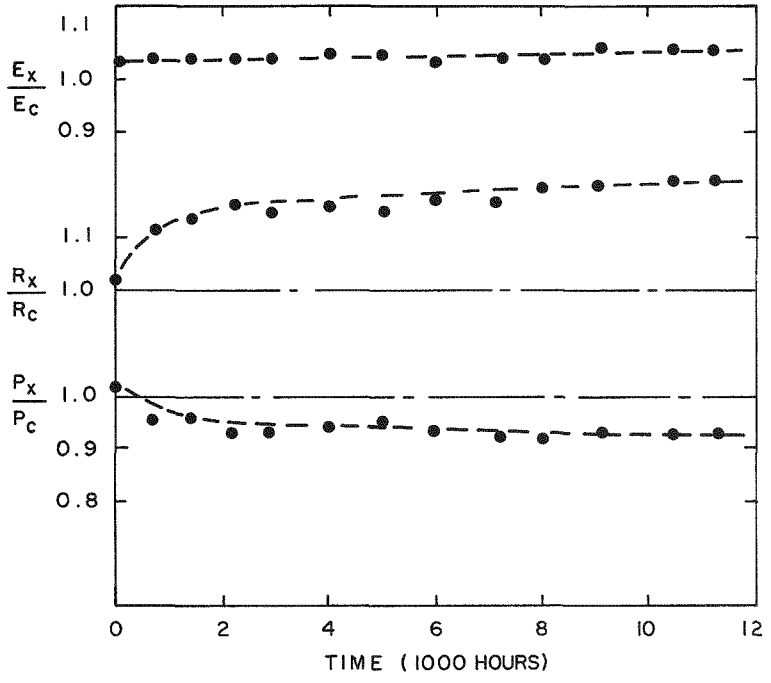

Figure 3-29. Performance of Prototype 48-Couple Generator 3M-37-P6 (E = voltage, R = resistance, P = power, x = experimental, c = computer)

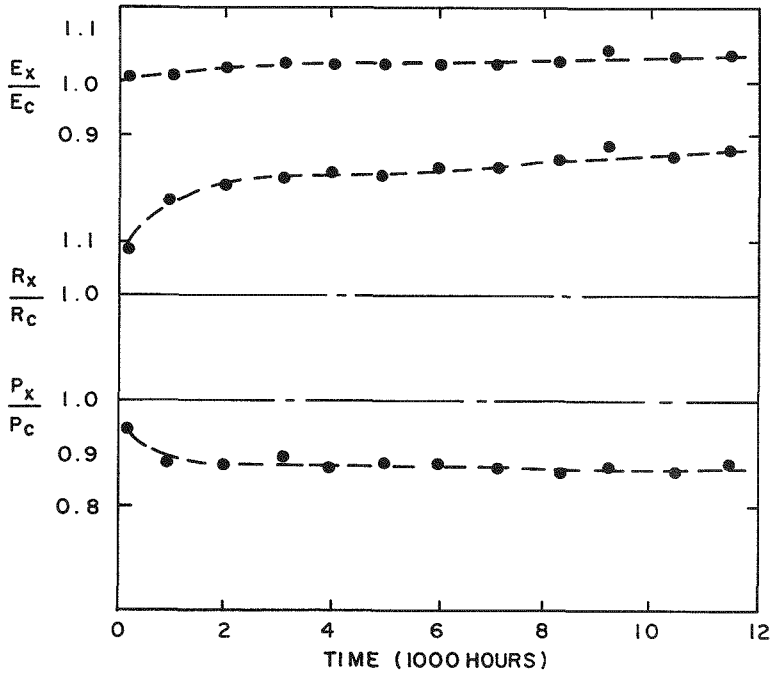

Figure 3-30. Performance of Prototype 48-Couple Generator 3M-37-P7 (E = voltage, R = resistance, P = power, x = experimental, c = computer)

Table 3-1. SNAP-21B-1 SYSTEM TEST Summary of Data-System Test Circuit

Date	6/17/65[5]	9/7/65	10/8/65	11/8/65	11/30/65	12/30/65
Generator hot electrode temperature (°F)	1100	1091	1087	1087	1093	1090
Generator cold electrode temperature (°F)	179	181	179	181	181	180
Water temperature (°F)	39	39	38	38	39	39
Generator load voltage (volts)[1]	5.23	5.23	5.22	5.22	5.22	5.22
Generator load current (amps)[1]	2.48	2.46	2.44	2.43	2.43	2.42
Generator total power output (watts)	13.08	12.98	12.85	12.79	12.79	12.73
Conditioner load voltage input (volts)[1]	4.90	4.89	4.89	4.89	4.88	4.88
Conditioner load current input (amps)[1]	2.48	2.46	2.44	2.43	2.43	2.42
Conditioner total power input (watts)	12.24	12.12	12.02	11.97	11.95	11.89
System load voltage (volts)	24.00	24.00	24.00	24.00	24.00	24.00
System load current (amps)	0.45	0.45	0.44	0.44	0.45	0.44
System power output (measured)(watts)	10.90	10.80	10.68	10.68	10.73	10.57
System power output (corrected)(watts)[2]	11.65	11.67	11.46	11.39	11.59	11.36
System power input (measured)(watts)	230	230	229	230	230	231
System power input (corrected)(watts)[3]	226	226	225	226	226	227
Conditioner efficiency (percent)	89	89	89	89	89	89
System efficiency (percent)[4]	5.2	5.2	5.1	5.0	5.1	5.0
Hours on test (start test 4/29/65)	1,176	3,144	3,888	4,632	5,160	5,880

Table 3-1. SNAP-21B-1 SYSTEM TEST Summary of Data-System Test Circuit (Continued)

Date	1/11/66	2/28/66	3/12/66	4/28/66[6]	5/26/66	6/23/66[7]
Generator hot electrode temperature (°F)	1090	1089	1086	1079	1090	1069
Generator cold electrode temperature (°F)	180	180	180	179	180	180
Water temperature (°F)	40	39	41	37	39	39
Generator load voltage (volts)	5.22	5.22	5.22	5.20	5.22	5.20
Generator load current (amps)	2.41	2.40	2.38	2.38	2.37	2.32
Generator total power output (watts)	12.69	12.64	12.50	12.46	12.48	12.06
Conditioner load voltage input (volts)	4.89	4.88	4.88	4.86	4.84	4.86
Conditioner load current input (amps)	2.41	2.40	2.38	2.38	2.37	2.32
Conditioner total power input (watts)	11.88	11.80	11.68	11.54	11.56	11.29
System load voltage (volts)	24.00	24.00	24.00	24.00	24.00	24.00
System load current (amps)	0.44	0.44	0.43	0.43	0.43	0.43
System power output (measured)(watts)	10.58	10.54	10.42	10.37	10.37	10.20
System power output (corrected)(watts)	11.39	11.29	11.20	11.06	11.07	10.89
System power input (measured)(watts)	230	231	230	230	230	225
System power input (corrected)(watts)	226	227	226	226	226	221
Conditioner efficiency (percent)	89	89	89	89	89	90
System efficiency (percent)	5.0	5.0	5.0	4.9	4.9	4.9
Hours on test (start test 4/29/65)	6,168	7,320	7,608	8,712	9,384	10,059

Table 3-1. SNAP-21B-1 SYSTEM TEST Summary of Data-System Test Circuit (Continued)

Date	7/29/66[8]	8/9/66	9/15/66	10/1/66
Generator hot electrode temperature (°F)	1065	1061	1075	1062
Generator cold electrode temperature (°F)	179	178	181	181
Water temperature (°F)	40	40	39	37
Generator load voltage (volts)	5.18	5.18	5.19	5.15
Generator load current (amps)	2.30	2.27	2.30	2.30
Generator total power output (watts)	12.01	11.86	12.08	11.95
Conditioner load voltage input (volts)	4.87	4.87	4.87	4.84
Conditioner load current input (amps)	2.30	2.27	2.30	2.30
Conditioner total power input (watts)	11.29	11.14	11.29	11.22
System load voltage (volts)	24.00	24.00	24.00	24.00
System load current (amps)	0.42	0.42	0.42	0.42
System power output (measured)(watts)	10.08	9.96	10.08	10.08
System power output (corrected)(watts)	10.66	10.66	10.69	10.63
System power input (measured)(watts)	224	224	224	225
System power input (corrected)(watts)	220	220	220	221
Conditioner efficiency (percent)	89	90	90	90
System efficiency (percent)	4.8	4.8	4.9	4.8
Hours on test (start test 4/29/65)	10,923	11,187	12,075	12,531

1. Primary circuit only.
2. Corrected for measured instrumentation losses.
3. Corrected for estimated instrumentation losses.
4. Based on corrected power input and output.
5. Based on average of data from 6/17/65, 6/18/65, 6/21/65 and 6/22/65.
6. Power failure for approximately 17 hours, March 26 and 28, 1966.
7. The input power was reduced from 230 watts to 224 watts on May 26, 1966.
8. The system test was moved from T.C.A. to Space Center 6/28/66.

Table 3-2. SNAP-21B-1 SYSTEM TEST Electrical Data-Generator Test Circuit[1]

Date	6/17/65[2]	9/7/65	10/8/65	11/8/65	11/30/65	12/30/65
Open Circuit Voltage (volts)	10.48	10.40	10.34	10.36	10.36	10.38
Load Voltage (volts)	5.23	5.23	5.22	5.22	5.22	5.22
Load Current (amps)	2.50	2.50	2.46	2.45	2.47	2.44
Internal Resistance (ohms)	2.10	2.07	2.08	2.10	2.08	2.11
Power Output (watts)	13.08	13.08	12.84	12.78	12.89	12.74
Hours on Test (start test 4/29/65)	1,176	3,144	3,888	4,632	5,160	5,880
	1/11/66	2/28/66	3/12/66	4/28/66[3]	5/26/66	6/23/66[4]
Open Circuit Voltage (volts)	10.36	10.42	10.36	10.29	10.30	10.20
Load Voltage (volts)	5.22	5.22	5.22	5.20	5.22	5.10
Load Current (amps)	2.45	2.43	2.41	2.38	2.36	2.37
Internal Resistance (ohms)	2.10	2.14	2.14	2.13	2.15	2.15
Power Output (watts)	12.78	12.68	12.54	12.38	12.32	12.09
Hours on Test (start test 4/29/65)	6,168	7,320	7,608	8,712	9.384	10.059
	7/29/66[5]	8/9/66	9/15/66	10/1/66		
Open Circuit Voltage (volts)	10.10	10.04	10.20	10.15		
Load Voltage (volts)	5.18	5.18	5.19	5.15		
Load Current (amps)	2.30	2.30	2.32	2.30		
Internal Resistance (ohms)	2.14	2.11	2.16	22.17		
Power Output (watts)	11.91	11.91	12.04	11.85		
Hours on Test (start test 4/29/65)	10,923	11,187	12,075	12,531		

1. The thermal conditions which correspond to these electrical data are the same as those shown for the respective test date in the Summary of Data-System Test Circuit table.
2. Based on average of data from 6/17/65, 6/18/65, 6/21/65 and 6/22/65.
3. Power failure for approximately 17 hours, March 26 and 28, 1966.
4. The input power was reduced from 230 watts to 224 watts on May 26, 1966.
5. The system was moved from T.C.A. to the Space Center 6/28/66.

3.8 PLANNED SAFETY ANALYSIS AND TESTING

3.8.1 TASK I - 10-WATT SYSTEM

Although effort was expended on system safety from an analytical standpoint during Phase I, additional investigation and testing is required. In particular, material compatibility at shield interfaces must be determined. Long term interface compatibility testing will be started using mock-up samples exposed to operating temperatures under controlled atmospheric conditions (vacuum) and at expected interface pressures. Diffusion characteristics and changes in parent material properties, as well as susceptibility to eutectic formation, will be evaluated. A radiation shield will be tested for shielding effectiveness using a fueled capsule.

Development efforts to perfect a nondestructive method of fuel capsule weld evaluation using ultrasonic techniques will resume. Such a method allows examination of the weld of the fueled units. Previously, the welds have been evaluated using destructive methods on control capsules welded during the fueling sequence. Dummy capsules will be prepared for welding and subsequent ultrasonic testing by the fueling facility.

A sea environment testing program will be drafted and initiated with NRDL. Electrolytic and chemical corrosion testing of a simulated system assembly at equilibrium temperature in sea water will be started. Special emphasis will be placed on capsule weld stress cracking and shield erosion in sea water.

3.8.2 TASK IIA - 20-WATT SYSTEM

The major safety effort next quarter will be concerned with the design-development area. Material compatibility, structural requirements, operational-temperatures, etc., will be reflected in the design.

3.9 QUALITY ASSURANCE

The Quality Assurance Program Plan has been prepared in rough draft form and is being reviewed. This plan provides procedures for fulfilling the requirements of MIL-Q-9858A, Quality Program Requirements.

The quality organization has participated in configuration control meetings to assist in organizational plans and definitions needed to formulate the SNAP-21 Program configuration control policies and procedures. A procedure has been implemented which insures review by Quality Engineering personnel of purchase documents prior to issue. The assigned Quality Engineer reviews the documents to assure that all necessary quality clauses are provided, such as: material certification, Government Source Inspection Options, vendor inspection or quality control requirements, and packaging and shipping instructions. The Quality Control Manual and Preliminary Quality Control Plan from the Linde Company were reviewed. Recommended changes to the plan are being prepared. These changes will insure that the plan will meet the requirements of MIL-Q-9858A and 3M program definitions.

The Materials Control Office is preparing a list of qualified vendor names and addresses for procurement of materials and services for the SNAP-21 program.

4.0 PLANNED EFFORT NEXT QUARTER

This section presents significant work which will be performed or initiated during the next quarterly period.

4.1 PROGRAM MANAGEMENT

The Configuration Control Plan for Phase II will be prepared to establish technical document control for the program.

4.2 DESIGN AND ANALYSIS

4.2.1 10-WATT SYSTEM

Design efforts for optimizing the inner liner neck tube for heat transfer and structural integrity will be continued. A thermal analysis of thermoelectric generator cold frame and cold end hardware will be performed to improve heat transfer characteristics. Materials for use in the pressure vessel will be re-evaluated. Design of the larger cover and redesign of the old pressure vessel, if required, will be based on final material selection. Encapsulation details of the radiation shield plug will be completed.

4.2.2 20-WATT SYSTEM

Conceptual studies for the entire system design will continue. The most promising design will be selected for preliminary design development. Design of major components will be initiated.

4.3 PROCUREMENT AND FABRICATION

Early in the quarter a vendor will be selected for the biological shield, and the purchase order will be placed. Fabrication techniques will be directed toward maintaining dimensions within tolerances on the spherical radius interface between the hard-coated aluminum follower and cold cap of the thermoelectric generator. Purchase orders for the pressure vessels will be placed after material selection and design changes have been made. Dummy electrically heated fuel capsules will be fabricated for use in the sea environment testing program. Work will be initiated to improve the segmented leg fabrication procedure.

4.4 TEST AND ANALYSIS

Verification tests will be performed on neck tube design. One neck tube will be tested for direct column buckling and one for bending. Cold end heat transfer tests will be conducted to evaluate modified couple design. Shield alloy compatibility tests will be initiated to determine performance characteristics of various cladding materials. System materials samples will be submitted to NRDL for sea environment effects testing.

4.5 QUALITY ASSURANCE

Following the 3M Company in-plant review of the rough draft Quality Assurance Program Plan, all pertinent comment information will be incorporated and a formal preliminary plan will be prepared for transmittal to AEC. This will be accomplished early in the next quarter.

APPENDIX A

NECK TUBE AND OUTER SHELL STRESS ANALYSIS

1) Vertical position (neck tube, open end up)

Combined tension and internal pressure:

The weight (W) on the neck tube acting downward under 3g of acceleration is:

$$W = 3 \times 264 = 792 \text{ lbs.}$$

The stresses at the hot end of the tube:

The tensile stress due to W (σ_t) is:

$$\sigma_t = \frac{W}{A} = \frac{4W}{\pi (Do^2 - Di^2)} = \frac{4 \times 792}{\pi (4.922^2 - 4.900^2)} = 4669 \text{ psi}$$

The circumferential or the hoop stress due to 2 atmospheres inside pressure (σ_1) is:

$$\sigma_1 = \frac{PR}{t} = \frac{2 \times 14.7 \times 2.461}{1011} = 6577 \text{ psi}$$

The longitudinal stress (σ_2) is:

$$\sigma_2 = \frac{PR}{2t} = 3288 \text{ psi}$$

The maximum stress in the longitudinal direction, σ_{max}:

$$\sigma_{max.} = \sigma_t + \sigma_2 = 4669 + 3288 = 7957 \text{ psi}$$

The safety factor based on the maximum stress theory, SF

$$SF = \frac{\sigma_{yield}}{\sigma_{max.}} = \frac{38,920}{7957} = 4.8$$

σ_{yield} = 38,920 psi for Hastelloy X at 1325°F (Bibliography, Ref. (1))

At the cold end of the tube the safety factor will be larger because both the cross sectional area and the yield strength is increased. For 1 atmosphere internal pressure the maximum tensile strength will be decreased which will also result in a higher safety factor.

2) Upside down vertical position

a) Combined Compression and Internal Pressure (at hot end of neck tube)

The compressive stress due to W is:

$$\sigma_c = \frac{W}{A} = \frac{792}{0.1696} = 4669 \text{ psi}$$

The longitudinal stress due to 1 atmosphere internal pressure:

$$\sigma_2 = \frac{PR}{2t} = \frac{14.7 \times 2.461}{2 \times 1011} = 1644 \text{ psi}$$

The net compressive stress in the longitudinal direction:

$$\sigma_{max.} = \sigma_c - \sigma_2 = 4669 - 1644 = 3025 \text{ psi}$$

The safety factor in compression based on the yield strength.

$$SF = \frac{\sigma_{yield}}{\sigma_{max.}} = \frac{38,920}{3025} = 12.8$$

b) Buckling in Combined Compression and Internal Pressure (at hot end of neck tube)

Using Figure A1 attached, for 1 atmosphere pressure:

$$\frac{\frac{PR}{Et}}{0.007} = \frac{\frac{14.7 \times 2.461}{21.2 \times 10^6 \times 0.011}}{0.007} = 0.0221$$

$E = 21.2 \times 10^6$ psi at 1325°F (Bibliography, Ref. (1))

$$\frac{L}{R} = \frac{2.497}{2.461} = 1.01$$

$$\frac{R}{t} = \frac{2.461}{0.011} = 237.2$$

The straight line for $\frac{R}{t} + 237$ shown on Figure A1 was determined by extrapolating $\frac{\sigma_{ccr}}{E_r}\frac{R}{t}$ for values of $\frac{R}{t}$ less than 500.

Knowing $\frac{PR}{Et} \Big/ 0.007$ and having the design curve for $\frac{R}{t} = 237$, the value of $\frac{\sigma_{ccr}}{Er}\frac{R}{t}$ is is now obtained from Figure A1.

$$\frac{\sigma_{ccr}}{Er}\frac{R}{t} = 0.27$$

$$\sigma_{ccr} = (0.27)\frac{t}{R} Er = 0.00113\ Er$$

To calculate σ_{ccr} we need to know the reduced modulus of elasticity corresponding to the maximum compressive stress. Using a trial-error solution first, we assume a modulus of elasticity and calculate a maximum compressive stress. If the modulus of elasticity at the calculated maximum compressive stress is different from the assumed value, the calculation is repeated with a corrected modulus of elasticity until the modulus of elasticity used to calculate σ_{ccr} is the same as that of the material corresponding to the computed maximum compressive stress.

Using the stress-strain curve for Hastelloy X given in Ref. (1), Bibliography, stress-versus modulus of elasticity was plotted and is shown on Figure A2. Results of the trial-error solution gives:

$E \times 10^6$	$\sigma_{ccr} - \sigma_2$	$Er \times 10^6$ (From Figure A2)
25	28,250 - 1644 = 26,606	20
24	27,120 - 1644 = 25,476	22.8
23	25,990 - 1644 = 24,346	26.7
23.5	26,555 - 1644 = 24,910	24.7
23.6	26,668 - 1644 = 25,020	24.2
23.7 ✓	26,781 - 1644 = 25,137	23.8 ✓

$$\sigma_{ccr} = (0.27)\left(\frac{0.011}{2.461}\right)(23.7 \times 10^6) = 26,781 \text{ psi}$$

$$\text{Safety factor} = \frac{26,781}{3025} = 8.8$$

3) Horizontal Position

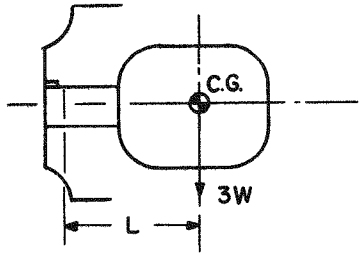

3W = 3 x 264 = 792 lbs.

L = 7"

(+) Tension

(-) Compression

Condition 3: t = 0.011

a) Combined Bending and Internal Pressure

The combined stress

$$c = \pm\frac{MC}{I} + \frac{PR}{2t}$$

The moment at the cold end of the neck tube:

$$M = 3WL = 792 \times 7 + 5544 \text{ in.-lbs.}$$

The section modulus:

$$Z = \frac{I}{C} = \pi R^2 t = \pi (2.455)^2 (0.011) = 0.2082 \text{ in.}^3$$

The bending stress:

$$\sigma_B = \pm \frac{MC}{I} = \frac{M}{Z} = \frac{5544}{0.2082} = 26,621 \text{ psi}$$

The maximum tensile stress for 2 atmospheres internal pressure:

$$\sigma_t = + \frac{MC}{I} + \frac{PR}{2t} = + 26,621 + \frac{2 \times 14.7 \times 2.461}{2 (0.011)} = 26,621 + 3288 = 29,909 \text{ psi}$$

The safety factor based on the maximum stress theory:

$$SF = \frac{\text{yield stress}}{\text{max. applied stress}} = \frac{50,500}{29,909} = 1.67$$

σ_{yield} = 50,500 psi for Hastelloy X at 150°F (Bibliography, Ref. (1))

b) Shear Stresses

$$\tau = \frac{3W \sin \alpha}{\pi Rt} = \frac{792 (1)}{\pi 2.455 (0.011)} = 9317 \text{ psi (shear)}$$

Taking the yield strength of Hastelloy X in shear as $\tau_{yield} = 1/2\ \sigma_{yield} = 1/2\ 50,500 = 25,250$

$$SF = \frac{25,250}{9317} = 2.7$$

c) Buckling in Combined Bending and Internal Pressure

Determine critical bending stress using Figure A3 (from Ref. (3), Bibliography)

p = 1 atmosphere internal pressure

t = 0.011"

E = $28.3\ 10^6$ psi (cold end of neck tube)

Er: (see Figure A2) Reduced Modulus of Elasticity, psi

$$\frac{P}{E}\left(\frac{r}{t}\right)^2 = \frac{14.7}{28.3 \times 10^6}\ \frac{(2.461)^2}{(0.011)^2} = 0.0259$$

$$\frac{\sigma_{CR}}{Er}\ \frac{r}{t} = 0.34$$

$$\sigma_{CR} = (0.34)\frac{t}{r};\ Er = (0.34)\ \frac{0.011}{2.461};\ Er = 0.001519\ Er$$

$$E \times 10^{-6} = 19.0\checkmark;\ \sigma_{CR} - \frac{PR}{2t} = 28,870 - 1654 = 27,216;\ Er = 19.1 \times 10^6$$

$$SF = \frac{\sigma_{BCR}}{M/Z} = \frac{28,870}{26,621} = 1.08$$

Critical buckling stresses and safety factors were calculated for various wall thicknesses ranging from 0.011 to 0.018". Results are shown on Figure A4.

Determine critical bending stress using Figure A5 from (Ref. (2), Bibliography):

p = 1 atmosphere internal pressure

t = 0.011"

E = $28.3\ 10^6$ psi (cold end of neck tube)

Er: see Figure A2

The straight line for $\frac{R}{t} = 237$ (Figure A5) was obtained by extrapolation.

$$\frac{\frac{PR}{Et}}{0.007} = \frac{\frac{14.7 \times 2.461}{28.3 \times 0.011}}{0.007} = 0.0166$$

From Figure A5:

$$\frac{\sigma_{BCR}}{Er} \quad \frac{R}{t} = 0.26$$

$$\sigma_{BCR} = (0.25)\frac{t}{R} Er = 0.25 \frac{0.011}{2.461} Er = 0.001117\, Er$$

By trial-error solution

$$E \times 10^{-6} = 24.1 \checkmark ; \sigma_{CR} - \frac{PR}{2t} = 26,926 - 1644 = 25,282; \quad ER \times 10^{-6} = 24 \checkmark$$

$$\sigma_{BCR} = 26,926$$

$$SF = \frac{\sigma_{BCR} + \frac{PR}{2t}}{M/Z} = \frac{26,926 + 1644}{26,621} = 1.07$$

Critical bending stresses and safety factors were calculated for various wall thicknesses ranging from 0.011 to 0.018". Results are shown on Figure A4.

d) Buckling in Combined Transverse Shear and Internal Pressure

Determine the critical shear stress by using Figure A6 from Ref. (2), Bibliography:

$$\frac{PR}{Et} = \frac{14.7 \times 2.461}{21.4 \times 10^6 \times 0.011} = 153 \times 10^{-6} = 0.153 \times 10^{-3}$$

$E = 21.4 \times 10^6$ psi for Hastelloy X at 1325°F (see Figure A4).

Since $\frac{PR}{Et} < 10^{-3}$, the internal pressure does not affect the torsion buckling stress.

From Figure A6:

$$\frac{\tau_{CR}}{Er} \times 10^3 = 0.56$$

The same result can be obtained from Figure A4, for the buckling stress in pure torsion:

$$\tau_{CR} = (0.56)\ 10^{-3}\ Er = 0.00056\ 21.4 \times 10^6 = 11,984 \text{ psi}$$

The shear buckling stress:

$$\tau_{SCR} = K\ \tau_{CR}\ (\text{Torsion}) = (1.25)(11.894) = 14,980 \text{ psi}$$

The applied shear stress:

$$\tau_{applied} = \frac{3W \sin \alpha}{\pi Rt} = \frac{792\ (1)}{\pi\ 2.455\ (0.011)} = 9317 \text{ psi}$$

Safety factor in combined shear and internal pressure:

$$SF = \frac{14,980}{9317} = 1.6$$

Safety factors were calculated for various wall thicknesses ranging from 0.011 to 0.016. Results are shown on Figure A7.

VIBRATION AND SHOCK ANALYSIS

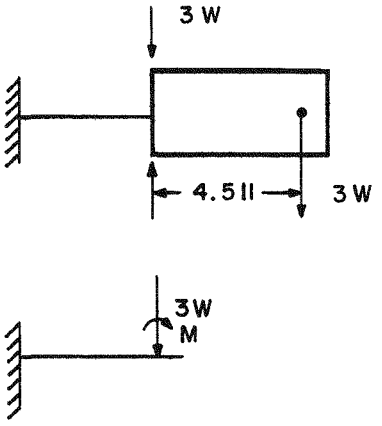

a) Vibration Analysis

The vibration model for the cantilever beam is:

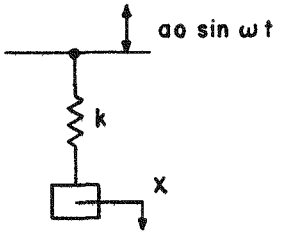

The equation for resonance for the case of forced vibration without damping, from Ref. (4), Bibliography, Equation 2.26, P. 45, is:

$$\frac{yo}{ao} = \frac{\frac{(\omega)^2}{(\omega n)}}{1 - (\omega/\omega_n)^2}$$

where:

yo = the relative motion between the mass and the fixed end of the spring,

ao = the amplitude of motion at the fixed end of the spring;

ω = frequency of motion at fixed end;

ωn = natural frequency of spring mass system.

The maximum vibration frequency is 50 cps at 3g peak acceleration as specified in the dynamic vibration test.

The amplitude of motion at 50 cps and 3g peak acceleration is calculated from the relationship:

$$X = ao \sin \omega t$$

$$\dot{X} = ao\, \omega \cos \omega t$$

$$\ddot{X} = -ao\, \omega^2 \sin \omega t$$

$$3g = ao\, \omega^2$$

Then:

$$ao = \frac{3g}{\omega^2} = \frac{3g}{(2\pi f)^2} = \frac{3 \times 32.2 \times 12}{4\pi^2\, 50^2} = 0.01175 \text{ in.}$$

The natural frequency of the system:

$$\omega_n = \frac{k}{M}$$

The spring constant for the system is taken as the force acting at the free end of the cantilever divided by the total deflection at the end of the cantilever. The total deflection is due to the force and moment acting on the beam plus the deflection of the cantilever (neck tube) due to the deflection of the flange.

Deflection due to the load 3W:

$$\delta_1 = 1/3 \frac{P\ell^3}{E_{AV} I_{av}} = \frac{792\ (2.497)^3}{3\ (24.8)\ 10^6\ (0.628)} = 0.000263 \text{ in.}$$

where:

$$I_{av} = \frac{\text{I cold + I hot end}}{2}$$

For 0.0115" wall thickness at the hot end:

$$\text{I hot end} = \frac{\pi}{64} (D^4 - d^4) = \frac{\pi}{64} (4.923^4 - 4.900^4) = 0.5347 \text{ in.}^4$$

For 0.0155" wall thickness at the cold end:

$$\text{I cold end} = \frac{\pi}{64} (D^4 - d^4) = \frac{\pi}{64} (4.931^4 - 4.900^4) = 0.7226 \text{ in.}^4$$

$$I_{av} = \frac{0.5347 + 0.7226}{2} = 0.6286 \text{ in.}^4$$

$$E_{av} = \frac{\text{E cold end + E hot end}}{2} = \frac{28.3 + 21.4}{2} = 24.8$$

The deflection due to the moment

$$\delta_2 = 1/2 \frac{M\ell^2}{E_{av} I_{av}} = 1/2 \frac{3572\ (2.497)^2}{24.8 \times 10^6\ (0.6286)} = 0.000714 \text{ in.}$$

$$M = 3W\ell = 792\ (4.511) = 3572 \text{ in./lbs.}$$

The deflection of the neck tube due to the deflection of the flange δ_3 = 0.00008 in. using 0.375" thick flange. See stress calculations in flange, page A-21.

The total deflection of the beam is:

$$\delta_{tot} = \delta_1 + \delta_2 + \delta_3 = 0.000263 + 0.000714 + 0.00008 = 0.001057 \text{ in.}$$

The natural frequency of the system

$$\omega_n = \frac{3W/\delta_{tot}}{M} = \left[\frac{792 \times 32.2 \times 12}{(0.001057)(264)}\right]^{1/2} = 1047 \frac{\text{rad}}{\text{sec}}$$

$$\omega = 2\pi f = 2\pi \ 50 = 314 \frac{\text{rad}}{\text{sec}}$$

$$\frac{\omega}{\omega_n} = \frac{314}{1047} = 0.2999$$

$$\frac{yo}{ao} = \frac{\left(\frac{\omega}{\omega_n}\right)^2}{1 - \left(\frac{\omega}{\omega_n}\right)^2} = \frac{(0.2999)^2}{1 - (0.2999)^2} = 0.09882$$

$$yo = ao \frac{(yo)}{(ao)} = (0.01175)(0.9882) = 0.00116 \text{ in.}$$

The force acting on the end of the neck tube due to the vibration:

$$P = k\,yo = \frac{792}{0.001057} (0.00116) = 869.1 \text{ lbs.}$$

The equivalent acceleration at the end of neck tube is:

$$a = \frac{P}{W} = \frac{869.1}{264} = 3.292g \approx 3.3g$$

Magnification factor $= \frac{869.1}{792} = 1.097 \approx 1.1g$

The Model A (heavy wall):

$$\delta_1 = \frac{P\ell^3}{3 E_{av} I_{av}} = \frac{792\ (2.497)^3}{3 \times 24.8 \times 10^6\ (0.7226)} = 0.000229 \text{ in.}$$

For 0.0135" wall thickness at the hot end:

$$I \text{ hot end} = \frac{\pi}{64}(D^4 - d^4) = \frac{\pi}{64}(4.927^4 - 4.900^4) = 0.6285 \text{ in.}^4$$

For 0.0175" wall thickness at the cold end:

$$I \text{ cold end} = \frac{\pi}{64}(D^4 - d^4) = \frac{\pi}{64}(4.935^4 - 4.900^4) = 0.8167 \text{ in.}^4$$

$$I_{av} = \frac{0.6285 + 0.8167}{2} = 0.7226$$

$$\delta_2 = \frac{M\ell^2}{2 E_{av} I_{av}} = \frac{3572\ (2.497)^2}{2\ (24.8)\ 10^6\ (0.7226)} = 0.000621 \text{ in.}$$

$$\delta_{tot} = 0.000229 + 0.000621 + 0.00008 = 0.00093 \text{ in.}$$

The natural frequency of the system:

$$\omega_n = \sqrt{\frac{3W/\delta_{tot}}{M}} = \left[\frac{792 \times 32.2 \times 12}{0.00093 \times 264}\right]^{1/2} = 1116 \frac{\text{rad}}{\text{sec}}$$

$$\frac{\omega}{\omega_n} = \frac{314}{1116} = 0.281$$

$$\frac{yo}{ao} = \frac{\left(\frac{\omega}{\omega_n}\right)^2}{1-\left(\frac{\omega}{\omega_n}\right)^2} = \frac{(0.281)^2}{1-(0.281)^2} = 0.0859$$

$$yo = ao\frac{(yo)}{(ao)} = (0.01175)(0.0859) = 0.00101 \text{ in.}$$

$$P = k\,yo = \frac{792}{0.00093}(0.00101) = 860.1 \text{ lbs.}$$

$$a = \frac{P}{W} = \frac{860.1}{264} = 3.258 \quad 3.26g$$

$$\text{Magnification factor} = \frac{860.1}{792} = 1.086 \approx 1.09$$

b) Shock Analysis

The maximum shock level which the unit has to withstand is: (see dynamic shock test specifications)

td = nominal duration of shock = 6 ms

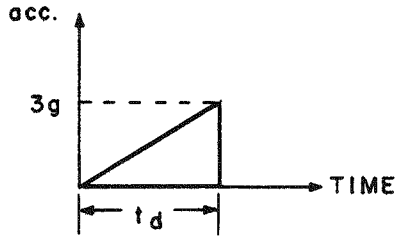

Determine shock response by Figure 5.9, P. 117, Ref. (5), Bibliography

Model A neck tube

$$fn = \frac{\omega_n}{2\pi} = \frac{1047}{2\pi} = 166.72 \text{ cps}$$

$$2 \times fn \times td = 2\,(166.72)\ 6 \times 10^{-3} = 2.00 \text{ cycles}$$

The acceleration, from Figure 5.9, Ref. (5):

$$a = 1.05 \times 3g = 3.15g$$

Model A (heavy wall)

$$fn = \frac{\omega_n}{2\pi} = \frac{1116}{2\pi} = 177.70 \text{ cps}$$

$$2 \times fn \times td = 2 \times 177.70 \times 6 \times 10^{-3} = 2.13 \text{ cycles}$$

From Figure 5.9, Ref. (5):

$$a = (0.95)\ 3g = 2.85g$$

To increase the abscissa to 5, the required time durations to reduce the amplification factor to nearly 1.0, will be:

$$td = \frac{5}{2 \times 166.72 \times 10^{-3}} = 14.9 \approx 15 \text{ ms}$$

Model A heavy wall

$$td = \frac{5}{2 \times 177.70 \times 10^{-3}} = 14.0 \text{ ms}$$

Heat leak calculations through straight and tapered neck tubes

1) Straight neck tube

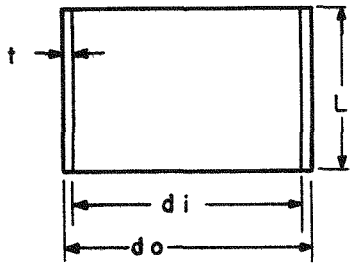

L = 2.497 in.

di = 4.900 in.

do = 4.922 in.

t = 0.011

$A = 0.1696 \text{ in.}^2 = \frac{0.1696}{144} \text{ ft}^2$

$$9 = -k(T) A \frac{dT}{dx}$$

k vs. temperature plot for Hastelloy X is shown on Figure A8.

The equation of the straight line on Figure A8 is:

$$y = \frac{y_2 - y_1}{x_2 - x_1} (x - x_1) + y_1$$

where:

x_1 = 150°F

$y_1 = k_1$ = 71 BTU-in/ft^2-hr-°F } Cold End

x_2 = 1325°F

$y_2 = k_2$ = 161 BTU-in/ft^2-hr-°F } Hot End

then:

$$y = k = \frac{161 - 71}{1325 - 150} (T - 150) + 71 = 0.07659T + 59.511$$

$$k = aT + b \qquad \text{where } a = 0.07659, \quad b = 59.511, \quad A = \frac{\pi}{4}$$

$$q = -(aT + b)\, A \frac{dt}{dx}$$

$$\int_0^L q\, dx = \int_{150}^{1325} -(aT + b)\, A\, dt$$

$$q = -\left[\frac{aT^2}{2} + bT\right]_{150}^{1325} \frac{A}{L}$$

$$q = -\left[\frac{(0.076595)\ 1325^2}{2} + (59.511)(1325) - \frac{(0.076595)\ 150^2}{2} - (59.511)(150)\right] \frac{0.1696}{2.497 \times 144} = -72.71 \text{ BTU/hr}$$

$$q = -72.71 \left[\text{BTU/hr}\right] \times \frac{1}{3.41} \left[\frac{\text{Watts Hr}}{\text{BTU}}\right] = -21.3 \text{ Watts}$$

2) Tapered necktube

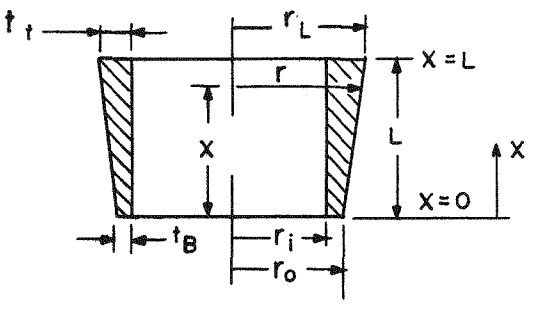

r_i = 2.450 in.
r_o = 2.461 in.
r_L = 2.462 in.
t_{bottom} = 0.011 in.
t_{top} = 0.012 in.

$r = ax + b$

The boundary conditions are:

$$x = 0 \qquad r = r_o = 2.461 = b$$

$$X = L \qquad r = r_L = 2.462 = aL + 2.461$$

$$a = \frac{2.462 - 2.461}{2.497} = \frac{0.001}{2.497} = 0.0004004857$$

$$A(x) = [(ax + b)^2 - r_i^2] \frac{\pi}{144} = \frac{\pi}{144} [(ax + 2.461)^2 - 2.450^2]$$

$$q = -k(t) \; A(x) \frac{dt}{dx}$$

$$\int \frac{d(x)}{A(x)} = \frac{144}{\pi} \int \frac{dx}{(ax + 2.461 + 2.450)(ax + 2.461 - 2.450)}$$

From Table of Integrals

$$\int \frac{dx}{(ax - b_1)(cx + d)} = \frac{1}{b_1 c - ad} \ln \frac{cx + d}{ax + b}$$

$$a = c = 0.0004004859$$

$$b_1 = 2.461 + 2.450 = 4.911$$

$$d = 2.461 - 2.450 = 0.011$$

$$\int \frac{dx}{A(x)} = \frac{144}{\pi} \frac{1}{4.911 (0.0004004857 - 0.0004004857 (0.011)} x$$

$$\ln \frac{0.001 + 0.011}{0.001 + 4.911} - \ln \frac{0.011}{4.911} = 2026.13$$

$$q = -\frac{\int k(t)\ dt}{\int \frac{dx}{Ax}}$$

Using the results of $\int k(t)\ dt$ from the calculations for a straight neck tube:

$$q = -\frac{154,148.7468}{2026.1371 \times 3.413} = -22.29 \text{ watts}$$

Heat leaks through straight and tapered neck tubes were calculated for various top and bottom wall thicknesses and results are shown in Figure A5.

Heat leak for Model A neck tube:

Bottom thickness	0.0115"
Top thickness	0.0155"

$q = 25.94 \approx 26$ watts

Heat leak for Model A (heavy wall) neck tube:

Bottom thickness	0.0135"
Top thickness	0.0175"

$q = 29.96 \approx 30$ watts

RUPTURE LIFE OF NECK TUBE

Stress rupture life for Hastelloy X is shown in Figure A6.

The bending moment at the hot end of the neck tube under 1 g acceleration is

$$M = W \times L = 264 \times 4.511 = 1190 \text{ in.-lbs.}$$

Allow a total oxidation of 0.001" over the 5-year life for Hastelloy X based on Figures A3 and A9. To determine the average stress which the neck tube will be subjected to during the five years as the wall thickness is gradually decreasing, we will use the mean thickness of the neck tube corresponding to 0.0005" average oxidation for stress calculations.

The thickness of the Model A neck tube at the hot end, including the loss of 0.0005" due to oxidation, is:

$$t = 0.0115" - 0.0005" = 0.011"$$

The maximum tensile strength in the neck tube when it is in the horizontal position is the sum of the bending and tensile stresses.

$$\sigma = \frac{M}{Z} + \frac{PR}{2t} = \frac{1190}{0.2082} + \frac{2 \times 14.7 \times 2.461}{2 \times 0.011} = 9004 \text{ psi}$$

$$Z = \pi R_{ave}^2 t = \pi \left(\frac{2.461 + 2.450}{2} \right)^2 (0.011) = 0.2082 \text{ in.}$$

From Figure A6, the rupture strength for 5-year life was 9300 psi, obtained by extrapolating the stress rupture line beyond 1000 hours.

OUTER SHELL - TOP FLANGE DESIGN

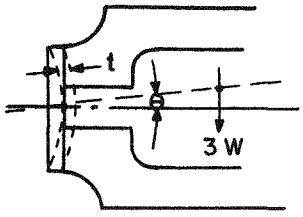

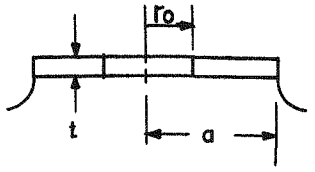

a = 3.74 in.

r_o = 2.52 in.

t = ?

The rotation of the neck tube due to the deflection of the flange is calculated by the equation from Ref. (6) Bib., Table X, Case 10, p. 216:

$$\text{Max } \theta = \frac{M}{\alpha E t^3} \quad \text{(at center)}$$

$$\frac{r_o}{a} = \frac{2.52}{3.74} = 0.674$$

From Ref. (6) p. 216, $\alpha = 44$

The maximum θ was found for several flange thicknesses. It was found that for 3/8" flange thickness, the rotation of the neck tube due to the deflection of the flange is negligible compared with the deflection of the neck tube due to the force and moment acting on it.

t = 0.375"

$$\text{Max } \theta = \frac{M}{\alpha E t^3} = \frac{7.3(792)}{44(28 \times 10^6)(0.375)^3} = 0.000033 \text{ rad}$$

$E = 28 \times 10^6$ psi for 304 Stainless Steel at 200°F (Ref. (7) Bib.)

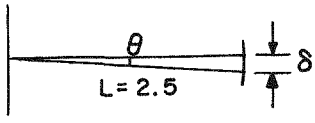

$\delta = 0.000033 \times 2.5 = 0.00008$ in.

The rotation δ of the neck tube with flange thickness less than 3/8" was calculated as follows:

t	0.312"	0.250"	0.187"
δ	0.00038"	0.00075"	0.00179"

It can be seen that for flange thicknesses less than 3/8", the rotation of the neck tube will be in the same magnitude as the deflection of the neck tube due to the force and moment, which would lower the natural frequency of the system resulting in a higher resonance g loading on the mass supported by the neck tube. (See vibration analysis.)

The stresses in the top flange were checked for 0.375" flange thickness.

The loading conditions are:

1) Uniform outside pressure

2) Moment, unit being in horizontal position

3) Uniform load along the inner edge of the flange due to inside pressure in the neck tube.

1)

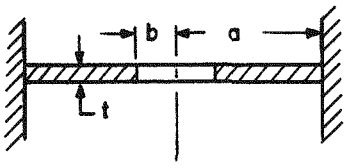

Ref. 6, Table X, Case 17, p. 199

a = 3.74
b = 2.52
t = 0.375

Maximum radial stress at the outer edge:

$$S_r = \frac{3W}{4t^2}\left[a^2 - 2b^2 + \frac{b^4(m-1) - 4b^4(m+1)\ln\frac{a}{b} + a^2b^2(m+1)}{a^2(m-1) + b^2(m+1)}\right]$$

w = uniform load (lbs/in^2) = 2 x 14.7 = 29.4 lbs/in^2

$$m = \frac{1}{\gamma} = \frac{1}{0.28} = 3.57$$

m = reciprocal of γ, Poisson's ratio

γ = 0.28 (Ref. 7)

$$S_r = \frac{3 \times 29.4}{4 \times (0.375)^2}\left[3.74^2 - 2(2.52)^2 + \frac{2.52^4(2.57) - 4(2.52)^4(4.57)\ln\frac{3.74}{2.52} + (3.74)^2(2.57)^2(4.57)}{(3.74)^2(2.57) + (2.52)^2(4.57)}\right]$$

$S_r = 773$ psi

2)

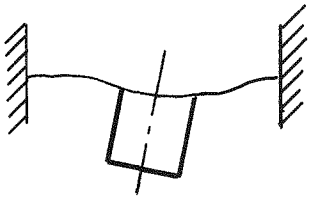

Ref. 6, Bib.: Table X, Case 10, p. 216

Maximum stress $S = \frac{\beta M}{at^2}$ at center

$\frac{r_o}{a} = 0.673$

$\beta = 0.568$ see p. 216, Ref. (7)

$$S = \frac{(0.568)(7.3)(792)}{3.74\ (0.375)^2} = 6243 \text{ psi}$$

3)

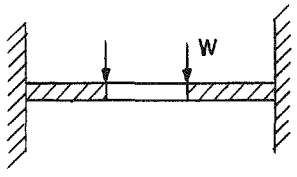

Ref. (7) Bib.: Table X, Case 18, p. 199

Maximum stress occurs at outer edge when $\frac{a}{b} < 2.4$

$$\frac{a}{b} = \frac{3.74}{2.52} = 1.48 < 2.4$$

The maximum stress at the outer edge,

$$S_{max} = \frac{3w}{2\pi t^2}\left[1 - \frac{2mb^2 - 2b^2(m+1)\ln\frac{a}{b}}{a^2(m-1) + b^2(m+1)}\right]$$

$$w = \frac{\text{vacuum load}}{\text{inner edge perimeter}} = \frac{2 \times 14.7 \times \pi 2.52^2}{\pi 2(2.52)} = 37 \text{ lbs/in.}$$

$$S_{max} = \frac{3(37)}{2\pi(0.375)^2}\left[1 - \frac{2(3.57)(2.52)^2 - 2(2.52)^2\, 4.57(0.392)}{(3.74)^2(2.57) + (2.57)^2(4.57)}\right] = 82 \text{ psi}$$

Maximum stress by superposition

$$S_{max} = 773 + 6243 + 82 = 7098 \text{ psi}$$

$$\text{Safety factor} = \frac{\text{yield strength}}{\text{max. applied stress}} = \frac{33,000}{7098} = 4.6$$

Outer Shell Upper Head Calculations

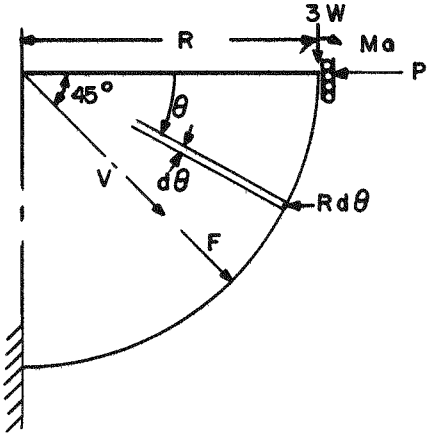

R = 2.45 in.
V = Vacuum Load
F = Spring Force
P = Flange Force
W = Weight of shield plus vacuum load on top flange

Assume the upper head may be treated as a beam with unit width. Including the force P from the flange, the problem becomes statically undeterminate.

By Castigliano's Theorem: Ref. (8), Bib.

$$\delta_p = \int \frac{M}{EI} \frac{\partial M}{\partial P} dx = 0$$

Consider the flange completely stiff in the radial direction $\delta_p = o$ and solve for P.

The moment between $0 < \theta < \frac{\pi}{4}$

$$M = Ma + WR(1 - \cos\theta) - PR \sin\theta$$

$$\frac{\partial M}{\partial P} = -R \sin\theta$$

The moment between $\frac{\pi}{4} < \theta < \frac{\pi}{2}$

$$M = Ma + WR(1 - \cos\theta) - PR \sin\theta + (F + V) R \sin(\theta - 45)$$

$$\frac{\partial M}{\partial P} = -R \sin\theta$$

$$\partial p = 0 = \int \frac{M}{EI} \frac{\partial M}{\partial P} Rd\theta$$

$$= \int_o^{\frac{\pi}{4}} [Ma + WR(1 - \cos\theta) - PR \sin\theta] (-R \sin\theta) Rd\theta +$$

$$+ \int_{\frac{\pi}{4}}^{\frac{\pi}{2}} [Ma + WR(1 - \cos\theta) - PR \sin\theta + (F + V) R \sin(\theta - 45)] (-R \sin\theta) Rd =$$

$$= \int_o^{\frac{\pi}{4}} (-R^2 \sin\theta Ma - WR^3 (1 - \cos\theta) \sin\theta + PR^3 \sin^2\theta) d\theta +$$

$$+\int_{\frac{\pi}{4}}^{\frac{\pi}{2}} [-R^2 \sin\theta \, Ma - WR^3 (1 - \cos\theta) \sin\theta + PR^3 \sin^2\theta -$$

$$- (F + V) R^3 \sin(\theta - 45) \sin\theta] \, d\theta$$

From Table 4 Integrals

$$\int -R^2 \sin\theta \, Ma \, d\theta = R^2 \, Ma \cos\theta$$

$$\int -WR^3 \sin\theta \, d\theta = WR^3 \cos\theta$$

$$\int WR^3 \cos\theta \sin\theta \, d\theta = WR^3 \, 1/2 \sin^2\theta$$

$$\int PR^3 \sin^2\theta \, d\theta = PR^3 [1/2 \, \theta - 1/4 \sin 2\theta]$$

$$\int -(F + V) R^3 \sin(\theta - \tfrac{\pi}{4}) \sin\theta \, d\theta = \int -(F + V) R^3 (\sin^2\theta \cos 45 -$$

$$\int - \sin 45 \sin\theta \cos\theta) \, d\theta = -(F + V) R^3 (0.7071) \int \sin^2\theta - \cos\theta \sin\theta) \, d\theta$$

$$= -(F + V) R^3 (0.7071) [1/2 \, \theta - 1/4 \sin 2\theta - 1/2 \sin^2\theta]$$

$$0 = R^2 \, Ma \, [\cos\theta]_0^{\pi/4} + WR^3 \, [\cos\theta + 1/2 \sin^2\theta]_0^{\pi/4} +$$

$$+ PR^3 \left[\frac{\theta}{2} - \frac{\sin 2\theta}{4}\right]_0^{\pi/4} + R^2 \, Ma \, [\cos\theta]_{\pi/4}^{\pi/2} +$$

$$+ WR^3 \, [\cos\theta + 1/2 \sin^2\theta]_{\pi/4}^{\pi/2} + PR^3 \left[\frac{\theta}{2} - \frac{\sin^2\theta}{4}\right]_{\pi/4}^{\pi/2} -$$

$$- (F + V) R^3 (0.7071) \left[\frac{\theta}{2} \; \frac{\sin^2\theta}{4} \; \frac{\sin^2\theta}{2}\right]_{\pi/4}^{\pi/2} =$$

$$= R^2 \, Ma(0.7071 - 1) + WR^3 [0.7071 - 1 + 1/2 \, (0.7071)^2] + PR^3 \left(\frac{\pi}{8} - \frac{1}{4}\right) +$$

$$+ R^2 \, Ma \, (-0.7071) + WR^3 \left[-0.7071 + \frac{1 - (0.7071)^2}{2} \right] +$$

$$+ PR^3 \left[\frac{\pi}{4} - \frac{\pi}{8} + \frac{1}{4} \right] - (F+V) \, R^3 (0.7071) \left[\frac{\pi}{4} - \frac{\pi}{8} + \frac{1}{4} - \frac{1}{2} + \frac{(0.7071)^2}{2} \right]$$

Solve for P

$$P = \frac{Ma + (0.5) \, WR + (0.277) \, (F+V)R}{(0.643)R}$$

Calculate Ma from the Max. stress in the flange, Sr max = 7099 psi

$$Ma = Sr \, Z = 7099 \, \frac{1 \times (0.375)^2}{6} = 166 \, \frac{\text{in.-lbs}}{\text{in.}}$$

$$WR = (3 \times 264 + 3.74^2 \pi 29.4) \, 2.45 = 5104 \text{ in.-lbs.}$$

$$\frac{WR}{\text{perimeter}} = \frac{5104}{\pi 2(3.74)} = 217 \, \frac{\text{in.-lbs}}{\text{in.}}$$

$$\frac{V}{\text{perimeter}} = \frac{29.4(6.19^2 - 3.74^2)}{2\pi 4.965} = 72 \, \frac{\text{lbs}}{\text{in.}}$$

$$\frac{F}{\text{perimeter}} = \frac{2400}{2\pi(4.965)} = 76.9 \, \frac{\text{lbs}}{\text{in.}}$$

$$P = \frac{166 + (0.5) \, 217 + (0.277) \, (72 + 76.9) 2.450}{0.643(2.450)} = 238 \, \frac{\text{lbs}}{\text{in.}}$$

$$P = 238 \frac{\text{lbs}}{\text{in.}}$$

$$W = 88.5 \frac{\text{lbs}}{\text{in.}}$$

$$Ma = 166 \frac{\text{lbs}}{\text{in.}}$$

$$V+F = 148.9 \frac{\text{lbs}}{\text{in.}}$$

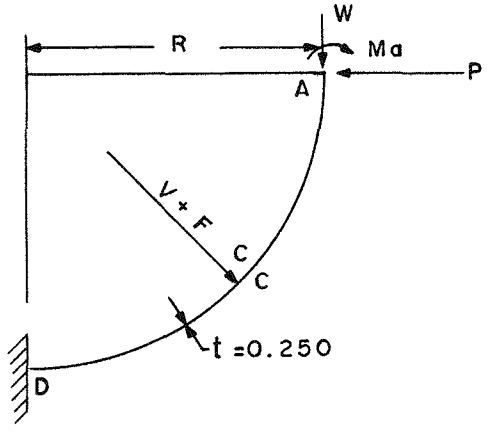

Bending stress at the top:

$$\sigma_B = \frac{Ma}{Z} = \frac{166}{0.0104} = 15,961 \text{ psi}$$

$$Z = \frac{1 \times 0.250^2}{6} = 0.0104$$

$$SF = \frac{33,000}{15,961} = 2.06$$

Bending stress at the center:

$$M_c = -P\,R \sin 45 + WR(1-\cos 45) + Ma =$$

$$= -238(2.450)(0.7071) + (88.5)(2.45)(1-0.7071) + 166 + 182 \frac{\text{in.-lbs}}{\text{in.}}$$

$$\sigma_B = \frac{Mc}{Z} = \frac{182}{0.0104} = 17,575 \text{ psi}$$

$$SF = \frac{33,000}{17,575} = 1.8$$

Bending stress at the bottom:

$$M_D = Ma + WR + (V+F)\,R\cos 45 - PR =$$

$$= 166 + 217 + (148.9)(2.45)(0.7071) - 238 \times 2.45 = 57 \frac{\text{in.-lbs}}{\text{in.}}$$

$$\sigma_D = \frac{57}{0.0104} = 5480 \text{ psi}$$

$$SF = \frac{33,000}{5,480} = 6.0$$

Shear stresses at the top:

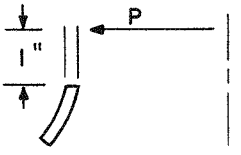

$$\tau = \frac{238}{1 \times (0.250)} = 952 \text{ psi}$$

Outer Shell Cylindrical Wall

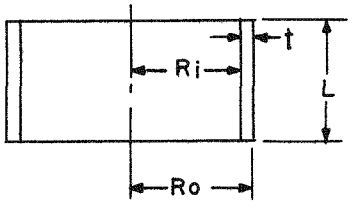

Ri = 6.101 in.
Ro = 6.21 in.
L = 7.988 in.
t = 0.109 in.
Do = 12.42 in.

Loadings

1) 2 atm outside pressure (compression);

2) Weight on neck tube (compression);

3) Spring force holding unit in place.

1) Stress due to outside pressure (compression)

$$\sigma_1 = \frac{PR}{2t} \quad \frac{2 \times 14.7 \times 6.21}{2(0.109)} = 837 \text{ psi}$$

2) and 3) Stresses due to weight and spring force

$$P = W + F = 792 + 2400 + 3192 \text{ lbs.}$$

Cross sectional area of cylinder.

$$A = (Ro^2 - Ri^2)\,\pi = (6.21^2 - 6.101^2)\pi = 4.21 \text{ in}^2$$

$$\sigma_{comp} = \frac{3192}{4.21} = 757 \text{ psi}$$

Total compressive stress

$$\sigma_{T\ comp} = 757 + 837 = 1594 \text{ psi}$$

Buckling in compression with no internal pressure (neglect outside radial pressure)

From Figure A8

$$\frac{L}{R} = \frac{7.988}{6.155} = 1.29$$

$$\frac{R}{t} = \frac{7.988}{0.109} = 73.2$$

$$\frac{\sigma cr}{Er} = 240 \times 10^{-5} \text{ for} \frac{R}{t} = 100$$

$$\frac{\sigma cr}{Er} \frac{R}{t} = 240 \times 10^{-5} \times 100 = 0.24$$

$$\sigma cr = (0.24)\frac{t}{R} Er = (0.24)\frac{0.109}{7.988} Er = 0.0032\ Er$$

$$\sigma cr = 29,300 \text{ psi}$$

Where $Er = E - 8.9 \times 10^6$ was used (see Figure A10):

$$SF = \frac{29,300}{1,594} = 18.3$$

Buckling under external pressure

Ref. (9), ASME Boiler and Pressure Vessel Code.

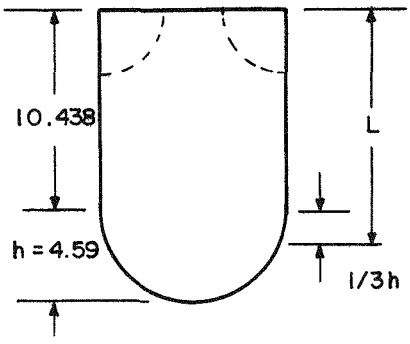

$$L = 10.438 + \frac{4.59}{3} = 11.96 \text{ in.}$$

$T = 150°F$

$Do = 12.42$ in.

Step 1.

$$\frac{L}{Do} = \frac{11.96}{12.42} = 0.962$$

$$\frac{Do}{t} = \frac{12.42}{0.109} = 113.9$$

Step 2. Using Figure 11 (UHA 28.1) attached

$B = 10,000$

$$\text{Pallow} = \frac{B}{Do/t} = \frac{10,000}{12.42} \times (0.109) = 87.7 \text{ psi}$$

$$SF = \frac{87.7}{29.4} = \underline{\underline{2.98}}$$

Assume that the total axial load is evenly distributed over the heads and check cylinder in buckling.

The total load in the axial direction

$$L = 792 + 2400 + 2 \times 14.7 (6.21)^2 \pi = 6752 \text{ lbs.}$$

$$\text{Axial pressure} = \frac{6752}{(6.21)^2 \pi} = 55.7 \text{ psi}$$

Assuming that this axial pressure is acting all around the cylinder,

$$SF = \frac{87.7}{55.7} = 1.57$$

Outer Shell Lower Head

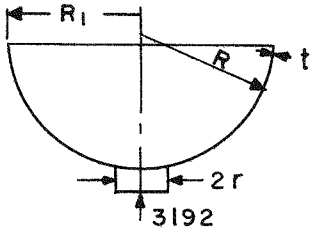

$R_1 = 6.21$

$R = 6.5$ in. $= L_1$

$t = 0.250$ in.

$r = 1$ in.

Determined stress at the bottom due to 3192 lb. load.

From Ref. (10), the parameters are

$$s = 1.82 \frac{r}{R} \sqrt{\frac{R}{t}} = 1.82 \frac{1}{6.21} \sqrt{\frac{6.21}{0.250}} = 1.45$$

From Figure A7:

$$M_x/P = 0.04 \qquad M_x = (0.4)\ 3192 = 127 \text{ in.-lbs.}$$

From Figure A8:

$$\frac{M_y}{P} = 0.025 \qquad M_y = 0.025\ (3192) = 80 \text{ in.-lbs.}$$

From Figure A5:

$$N_x/\frac{P}{t} = -0.085 \qquad N_x = (-0.085)\ \frac{3192}{0.250} = -1090 \text{ lbs.}$$

From Figure A6:

$$N_y/\frac{P}{t} = -0.03 \qquad N_y = -384 \text{ lbs}$$

The combined stress,

$$\sigma x = \frac{M_x}{Z} + \frac{N_x}{A} = \frac{127}{0.0104} + \frac{1090}{1 \times 0.250} = 16,570 \text{ psi}$$

Tension

$$Z = \frac{1 \times 0.250^2}{6} = 0.0104 \text{ in}^3$$

$$SF = \frac{33,000}{16.570} = 1.9$$

$$\sigma y = \frac{M_y}{Z} + \frac{N_y}{A} = \frac{80}{0.0104} + \frac{384}{1 \times 0.250} = 9228 \text{ psi}$$

$$SF = \frac{33,000}{9228} = \underline{3.57}$$

Buckling under external pressure:

Use ASME Code, Ref. (9), Page 10

$$\frac{L_1}{t_h} = \frac{6.5}{0.250} = 26$$

$$\frac{L_1}{100 t_h} = \frac{6.50}{0.250} = 0.26$$

From Figure A11:

$$Pa = \frac{12,500}{26} = \underline{480 \text{ psi}}$$

Assume the total load in the axial direction evenly distributed on the sphere.

The axial pressure, from the ASME Code,

$$Pa = 55.7 \text{ psi}$$

$$SF = \frac{480}{55.7} = 8.7$$

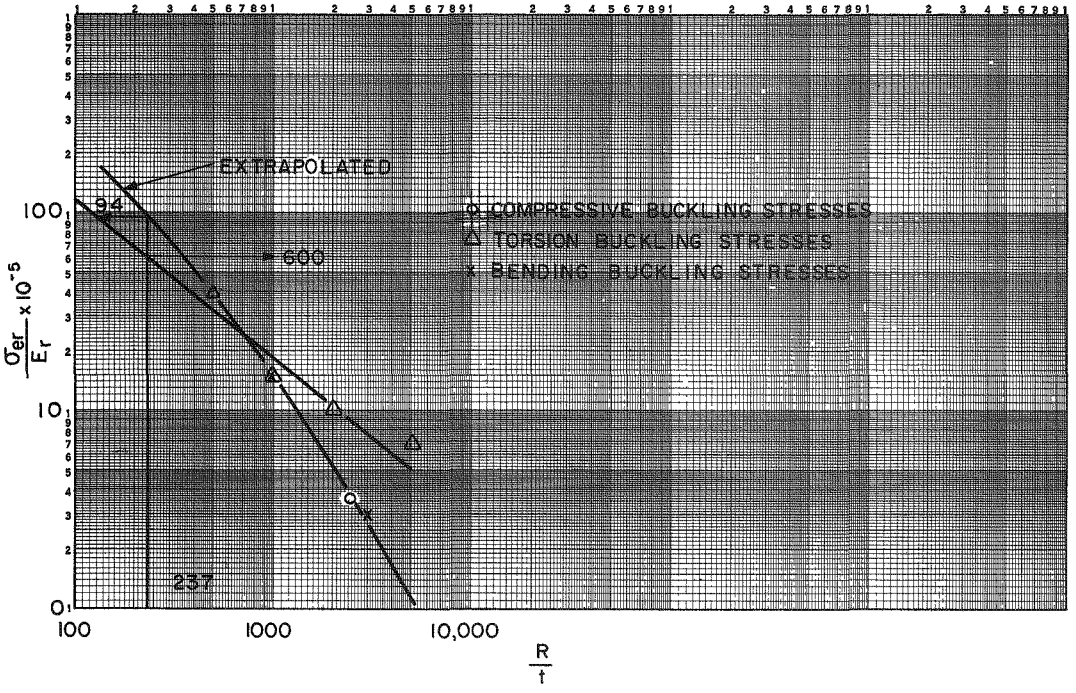

Figure A1. Critical Buckling versus $\frac{R}{t}$

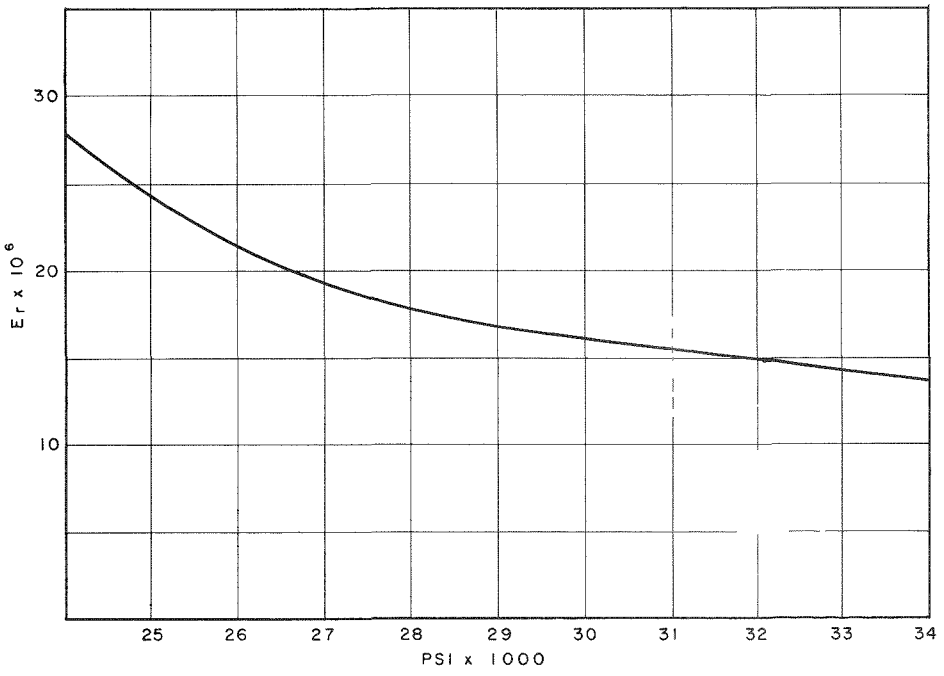

Figure A2. E_r versus σ for Hastelloy

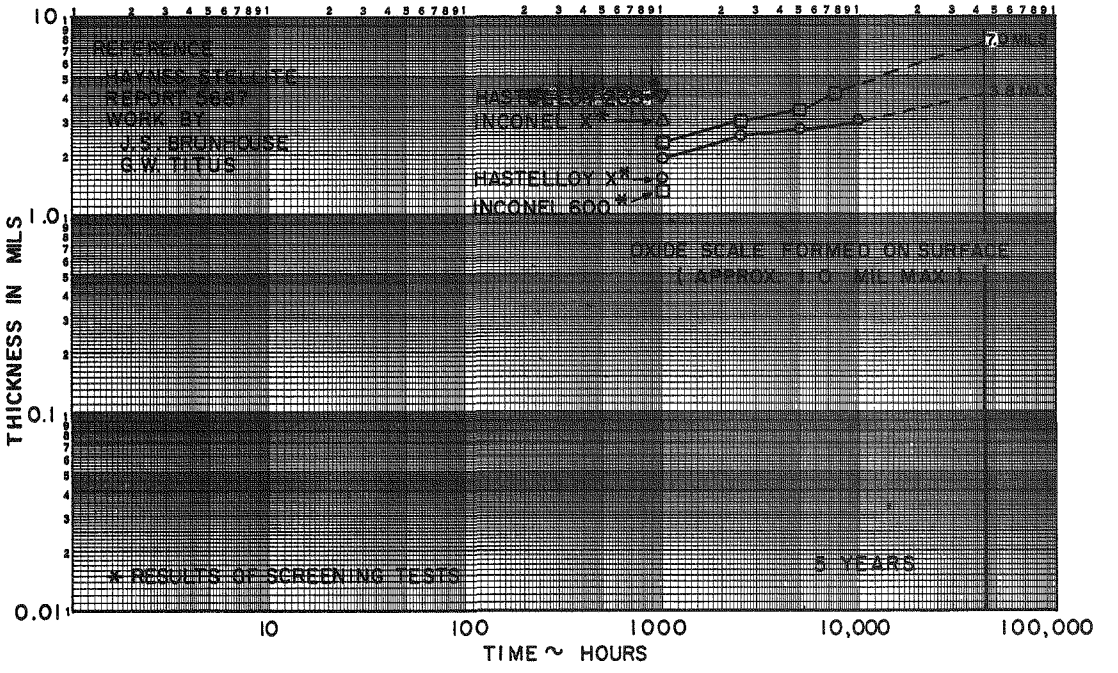

Figure A3. Oxidation Rates of Hastelloy X and Inconel 600 in Air at 1750°F, 300 psi

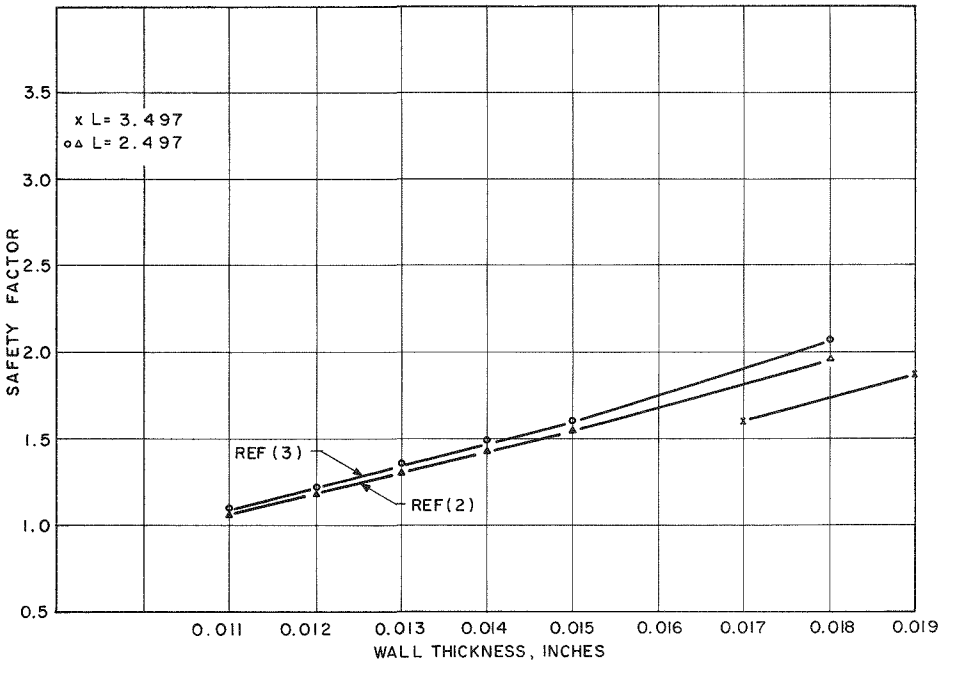

Figure A4. Safety Factor versus Wall Thickness for Neck Tube in Buckling in Combined Bending and Internal Pressure at the Cold End of the Neck Tube

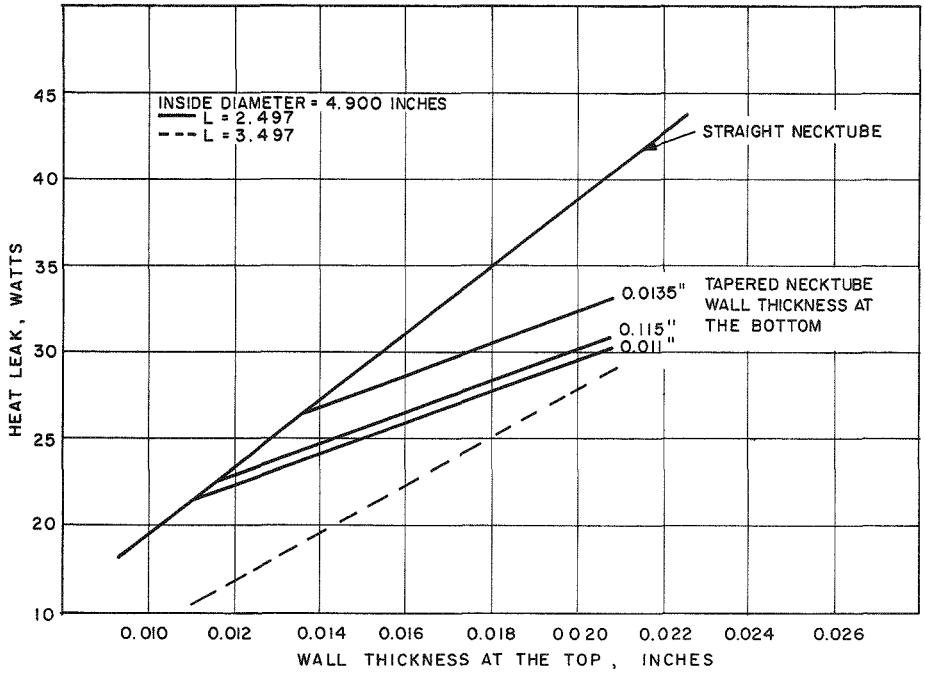

Figure A5. Heat Leak Through Neck Tube, Material Hastelloy X

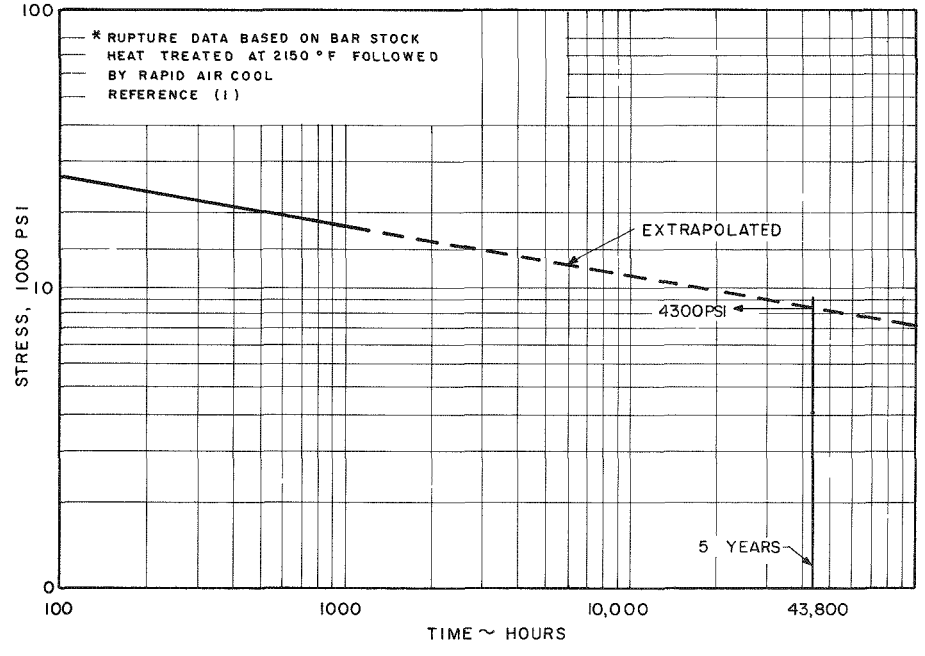

Figure A6. Stress Rupture Data for Hastelloy X*

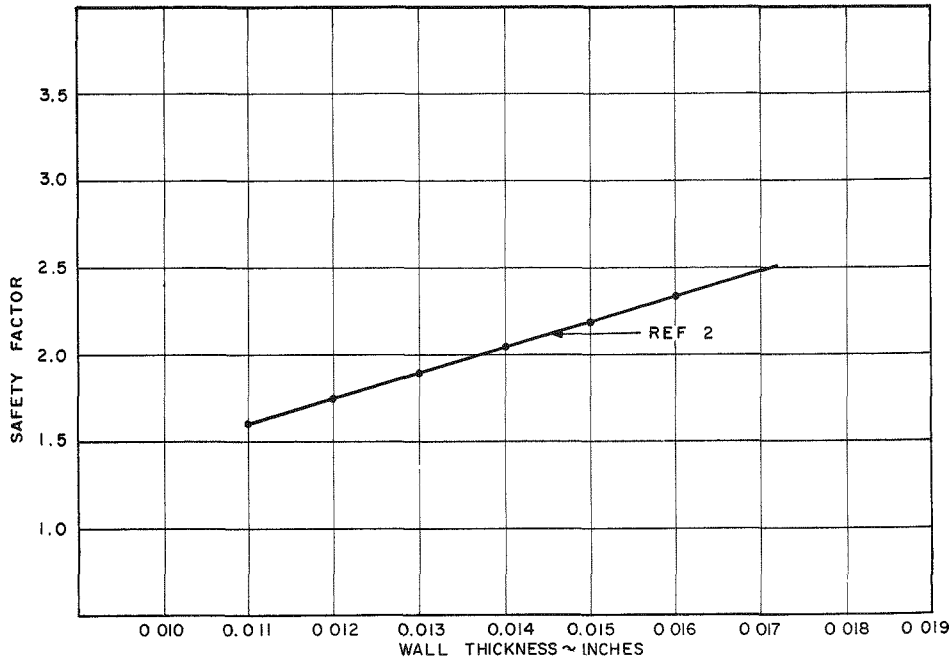

Figure A7. Safety Factor versus Wall Thickness for Neck Tube in Buckling in Combined Transverse Shear and Internal Pressure (1 atm) at the Hot End of the Neck Tube

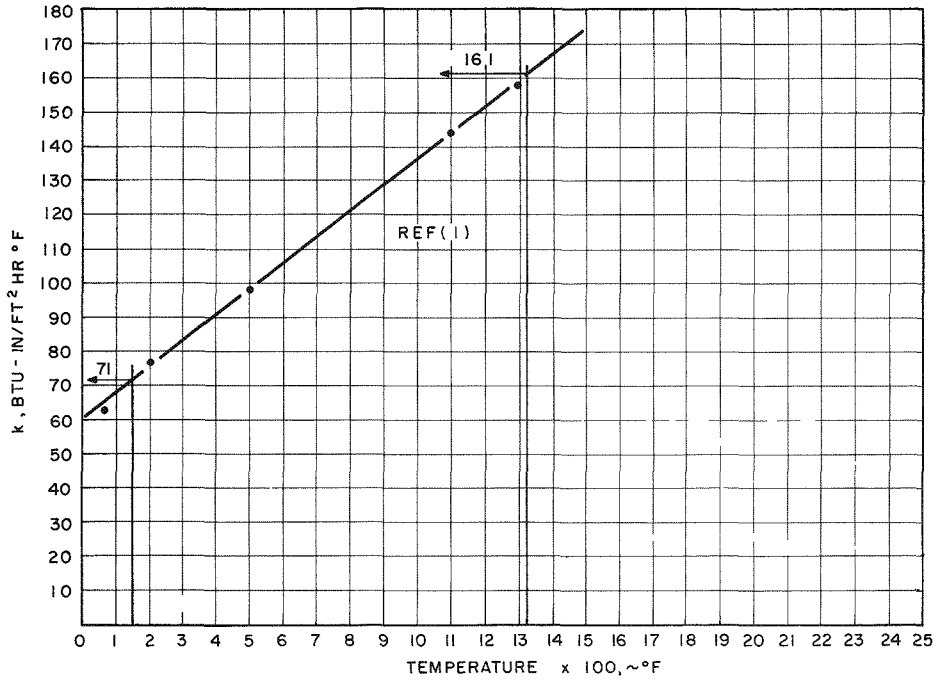

Figure A8. Thermal Conductivity versus Temperature for Hastelloy X

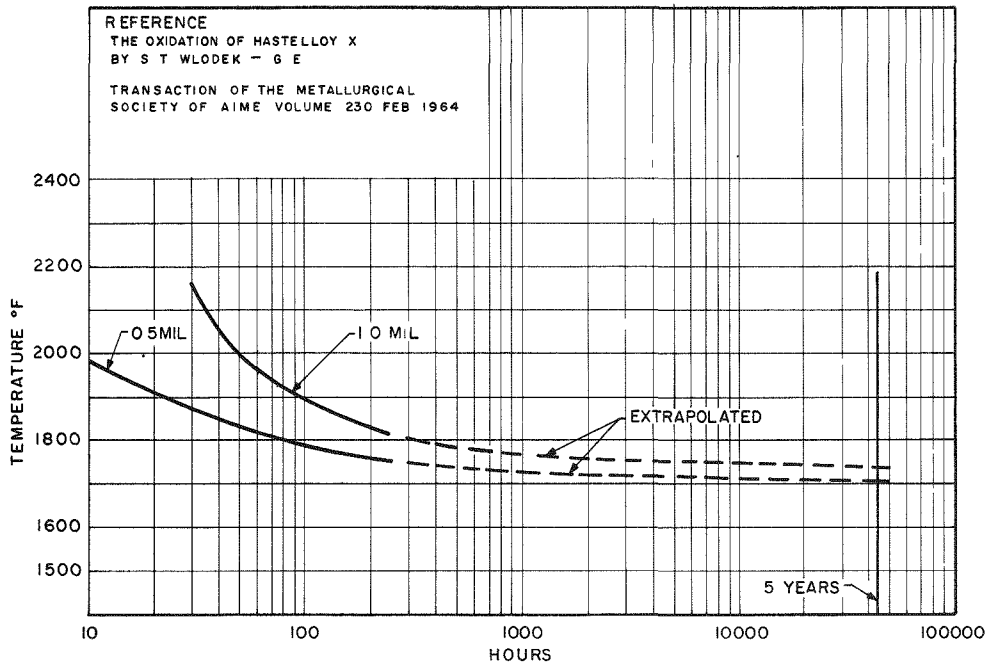

Figure A9. Hastelloy X Sub-scale Oxidation (Internal Oxidation Only)

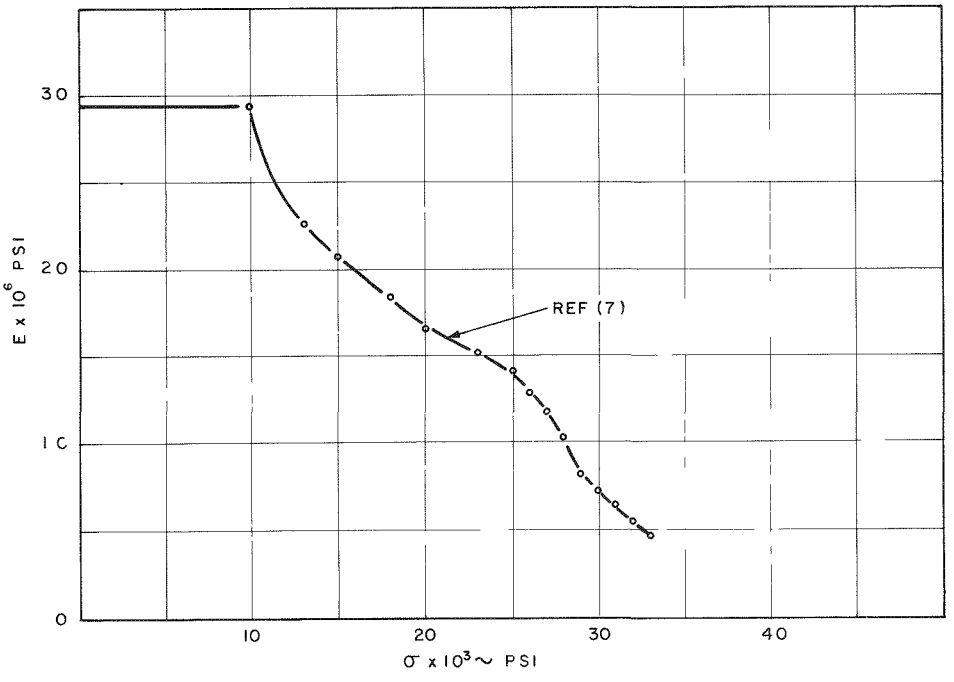

Figure A10. E versus σ for Type 304 Stainless Steel

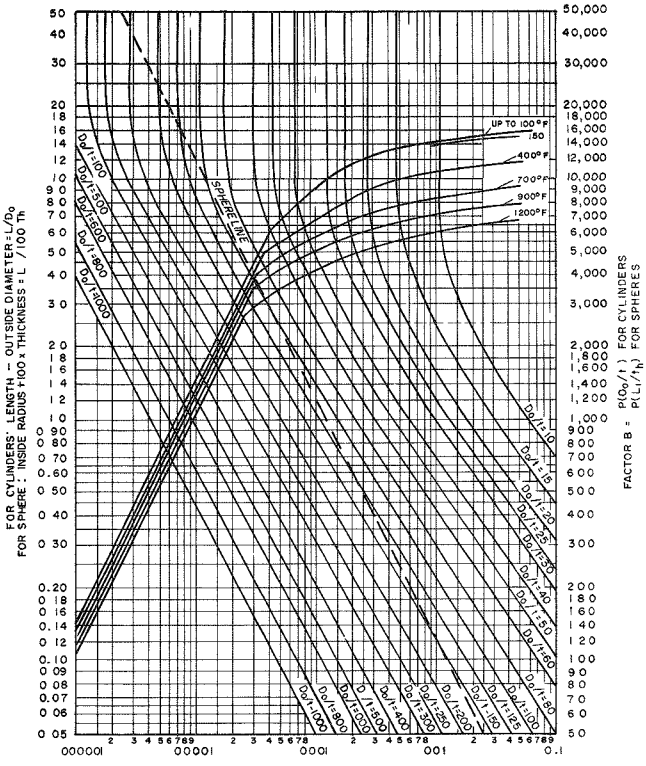

Figure A11. Chart for Determining Shell Thickness of Cylindrical and Spherical Vessels Under External Pressure When Constructed of Austenitic Steel (18 Cr-8 Ni, Type 304)

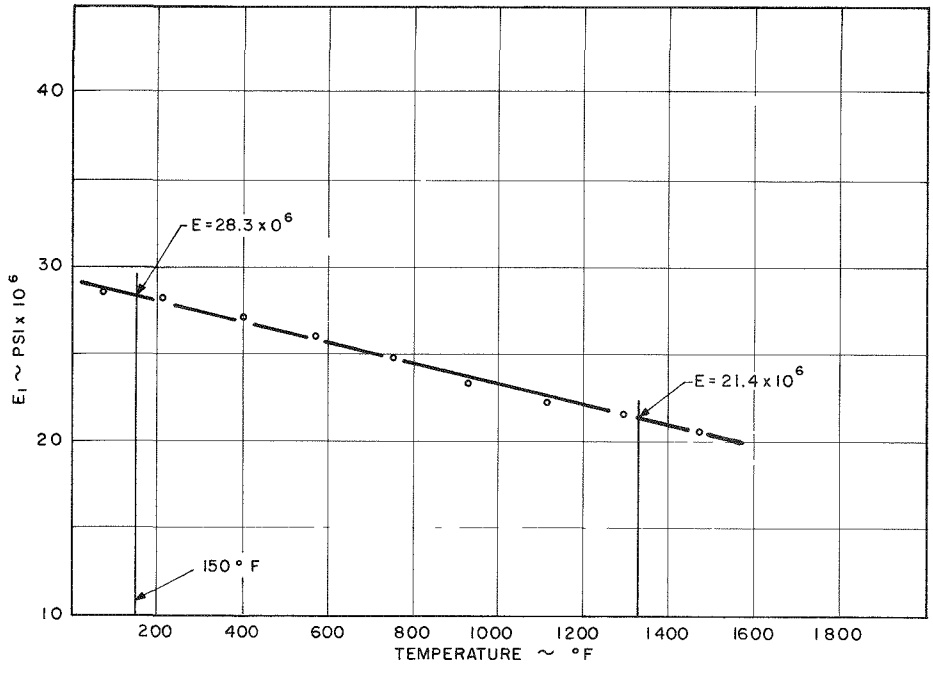

Figure A12. Modulus of Elasticity versus Temperature for Hastelloy X

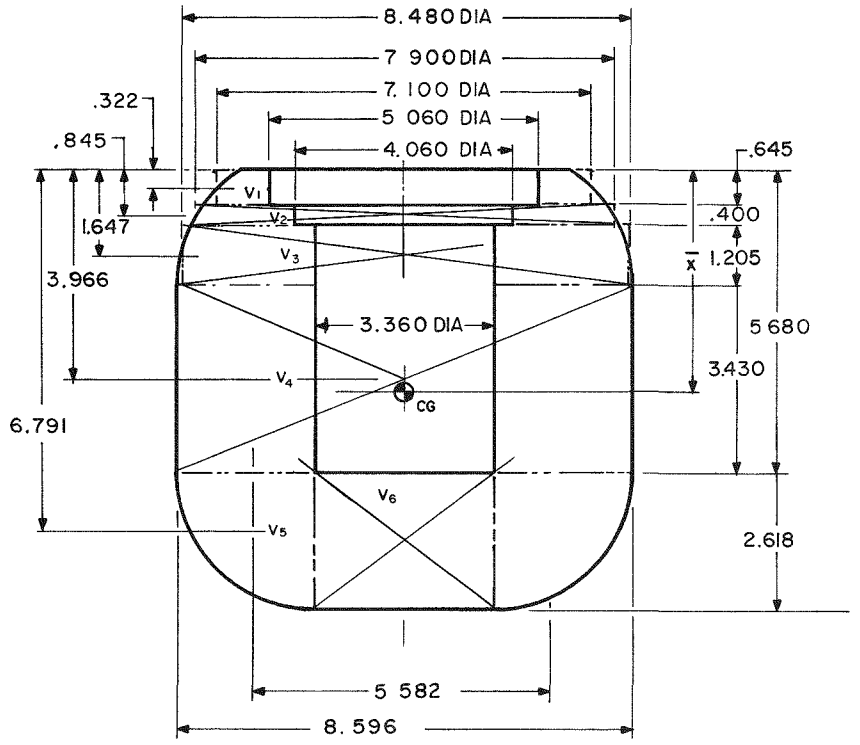

Calculation of Center of Gravity

$$V_1 = \frac{(7.100)^2 - (5.060)^2}{4}\pi(0.645) = \frac{50.410 - 25.600}{4}\,2.025 = 12.560$$

$$V_2 = \frac{(7.900)^2}{4}\pi(0.400) = \frac{62.410}{4}(1.256) = 19.596$$

$$V_3 = \frac{(8.480)^2}{4}\pi\ 1.205 = \frac{71.910}{4}(3.783) = 68.006$$

$$V_4 = \frac{(8.596)^2}{4}\pi\ 3.430 = \frac{73.891}{4}(10.770) = 198.943$$

V_5 = Area of quarter circle x path of the center of gravity

$= (2.618)^2 \pi/4 \times 5.582 = 6.853\ (0.7850)\ 17.527 = 94.277$

$$V_6 = \frac{(3.360)^2}{4} \pi 2.618 = 11.289\ (0.7850)\ 2.618 = 23.198$$

$$V_{TOT} = V_1 + V_2 + V_3 + V_4 + V_5 + V_6 = 416.580$$

$$\bar{X} = \frac{V_1\ (0.322) + V_2\ (0.845) + V_3(1.647) + V_4(3.965) + V_5(6.79 + V_6(6.489)}{V_{TOT}}$$

$= [12.56 \times (0.322) + 19.598\ (0.845) + 68.0\ (1.647) + 198.943\ (3.965) +$
$94.277\ (6.791) + 23.198\ (6.989)]/416.580$

$$= \frac{4.044 + 16.558 + 111.996 + 788.808 + 640.235 + 162.130}{416.580}$$

$$= \frac{1723.771}{416.580} = 4.137$$

Location of C.G. from cold end of neck tube = $3.156 + 4.137 = 7.293 \approx \underline{7.3}$

To beginning of 0.011" section $7.293 - 0.285 = 7.008$"

NOTE
Centroid at a quarter circle

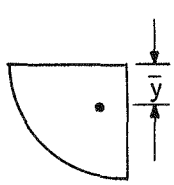

$$\bar{y} = \frac{4r}{3} = \frac{4 \times 2.618}{3} = \underline{1.111}$$

BIBLIOGRAPHY

(1) Union Carbide Corporation, Stellite Division, Catalog on Hastelloy Alloy X, October, 1964.

(2) Review of Design Information on Buckling of Unstiffened Thin-Walled Circular Cylindrical Shells by Bertraum Klein, ARS Journal, January, 1960.

(3) Harris, L.A., "The Bending Stability of Thin-Walled Unstiffened Circular Cylinders Including the Effects of Internal Pressure" T. Acron, Sci., Vol. 25. No. 5, May, 1958, pp 281-287.

(4) Den Hartog, Mechanical Vibrations McGraw-Hill, 1956.

(5) Charles T. Morrow, Shock and Vibration Engineering Vo. 1. John Wiley & Sons, Inc. 1963.

(6) Raymond J. Roark, Formulas for Stress and Strain McGraw-Hill, 1954.

(7) Mechanical and Physical Properties of Austenitic Chrmoium-Nickel Stainless Steels at Ambient Temperatures, The International Nickel Company, Inc. GM-3-64-3846(3) A-312.

(8) Advanced Mechanics of Materials, Seely, Smith, Wiley, 1957.

(9) ASME Boiler and Pressure Vessel Code Section VIII Unfired Pressure Vessels, 1965.

(10) Computatives of the Stresses from Local Loads in Spherical Pressure Vessels or Pressure Vessel Head, P. B. Bijlaard. Welding Research Council Bulletin 34, 1957.

APPENDIX B

STRUCTURAL ANALYSIS OF NECK TUBE
SNAP-21 PHASE II, TASK 1

The analysis presented in this report is based on an expression derived by Timoshenko in his book "Theory of Elastic Stability".

Assumptions:

1. The vessel is mounted in its shipping container in a vertical orientation.
2. No shock loadings will be encountered until the vessel is in the shipping container.
3. The stress in the tube due to the vacuum around the outside will not be added to the buckling stress since buckling will not occur at the point of restraint but rather some small distance from the end.

Check critical buckling stress (q_{cr}) in thin wall cylinder for 0.011 in. wall thickness

*

$$(1 - v^2)\, q_{cr} \frac{R}{Eh} = \frac{(1 - v^2)}{(n^2 - 1)\left(1 + \frac{n^2 L^2}{\pi^2 R^2}\right)^2} + \frac{h^2}{12R^2}\left(n^2 - 1 + \left(\frac{2n^2 - 1 - v}{1 + \frac{n^2 L^2}{\pi^2 R^2}}\right)\right)$$

in which

n = 2 Buckling modes
L = 2.47 Tube length, in.
R = 2.46 Tube radius, in.
v = 0.29 Poissons Ratio
E = 3.0×10^6 at 150°F, Modulus of Elasticity, psi
E = 21.2×10^6 at 1300°F, Modulus of Elasticity, psi

---

*Theory of Elastic Stability, Timoshenko; p. 450, Equation 270.

At 150°F

$$\frac{(1 - 0.29^2)\, q_{cr}\, (2.46)}{31.0 \times 10^6 \times 0.011} = \frac{(1 - 0.29^2)}{(2^2 - 1)\left(1 + \frac{(2^2)(2.47^2)}{(3.14^2)(2.46^2)}\right)} +$$

$$\frac{0.011^2}{(12)(2.46^2)}\left(2^2 - 1 + \frac{(2 \times 2^2) - 1 - 0.29}{\left(1 + \frac{(2^2) \times (2.47^2)}{(3.14^2) \times (2.46^2)}\right)}\right)$$

$$6.61 \times 10^{-6}\, q_{cr} = 0.154 + 0.0000129$$

$$q_{cr} = 23,300 \text{ psi at } 150°F$$

$$q_{cr} = 15,250 \text{ psi at } 1300°F$$

Determine I for various wall thicknesses

Try 0.015 in. thickness

$$I = \frac{\pi}{64}(4.900^4 - 4.870^4) = 0.0491\,(576.4801 - 562.4913)$$

$$I = 0.0491 \times 13.9888 = 0.6869 \text{ in.}^4$$

Try 0.016 in. thickness

$$I = \frac{\pi}{64}(4.900^4 - 4.868^4) = 0.0491\,(576.4801 - 561.5668)$$

$$I = 0.0491 \times 14.9133 = 0.7322 \text{ in.}^4$$

Try 0.017 in. thickness

$$I = 0.0491\,(576.4801 - 560.6477)$$

$$I = 0.0491 \times 15.8324 = 0.7774 \text{ in.}^4$$

Try 0.018 in. thickness

$$I = 0.0491 (4.900^4 - 4.864^4) = 0.0491 (576.4801 - 559.7246)$$

$$I = 0.0491 \times 16.7555 = 0.8227 \text{ in.}^4$$

Try 0.019 in. thickness

$$I = 0.0491 (4.900^4 - 4.862^4) = 0.0491 (576.4801 - 558.8023)$$

$$I = 0.0491 \times 17.6778 = 0.8680 \text{ in.}^4$$

Buckling stress due to flexture σ_B

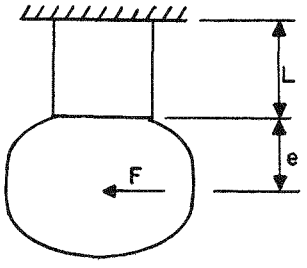

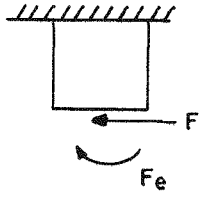

$F = 3 \times 276.86 = 831$ lbs

$e = 4.41$ in.

$L = 2.50$ in.

At cold end, try 0.018 in. wall thickness

$$\sigma_B = \frac{Mc}{I} = \frac{831 \times (4.41 + 2.50)\ 2.46}{0.8227}$$

$$\sigma_B = 17,200 \text{ psi}$$

Area of tube $= \pi \times 4.92 \times 0.018 = 0.278 \text{ in.}^2$

$$\sigma_T = \frac{P}{A} = \frac{276.86}{0.278} = 990 \text{ psi}$$

Since the vessel is mounted in a vertical orientation the tension stress subtracts from the buckling stress.

$$\sigma = 17,200 - 990 = 16,210 \text{ psi}$$

With 0.015 in. wall thickness check critical stress at cold end

$$\frac{6.61 \times 10^6 \, q_{cr} \times 0.011}{0.015} = 0.154$$

$$q_{cr} = \frac{0.154}{4.85 \times 10^6} = 31,800 \text{ psi}$$

at hot end

$$q_{cr} = 15,250 \times \frac{0.015}{0.011} = 20,800 \text{ psi}$$

at cold end

$$\sigma_B = \frac{Mc}{I} = \frac{831 \times (4.41 + 2.50)\, 2.46}{0.6869}$$

$$\sigma_B = 20,600 \text{ psi}$$

Area of tube = $\pi \times 4.92 \times 0.015 = 0.232 \text{ in}^2$

$$\sigma_T = \frac{276.86}{0.232} = 1,190 \text{ psi}$$

$$\sigma = \sigma_B - \sigma_T = 20,600 - 1,190 = 19,410 \text{ psi}$$

$$\text{Safety factor} = \frac{31,800}{19,410} = 1.64$$

With 0.014 in. wall thickness check critical stress at cold end

$$\frac{6.61 \times 10^6 \, q_{cr} \times 0.011}{0.014} = 0.154$$

$$q_{cr} = \frac{0.154}{5.20 \times 10^6} = 29,600 \text{ psi}$$

at hot end

$$q_{cr} = 15,250 \times \frac{0.014}{0.011} = 19,400 \text{ psi}$$

at cold end

$$\sigma_B = \frac{Mc}{I} = \frac{831 \times (4.41 + 2.50)\, 2.46}{0.6414}$$

$$\sigma_B = 22,000 \text{ psi}$$

Area of tube = $\pi \times 4.92 \times 0.014 = 0.216 \text{ in}^2$

$$\sigma_T = \frac{P}{A} = \frac{276.86}{0.216} = 1,280 \text{ psi}$$

$$\sigma = \sigma_B - \sigma_T = 22,000 - 1,280 = 20,720 \text{ psi}$$

$$\text{Safety factor} = \frac{29,600}{20,720} = 1.43$$

With 0.015 in. wall thickness check actual stress at hot end

$$\sigma_B = \frac{Mc}{I} = \frac{831 \times 4.41 \times 2.46}{0.6869}$$

$$\sigma_B = 13,100 \text{ psi}$$

$$\sigma = \sigma_B - \sigma_T = 13,100 - 1,190 = 11,910 \text{ psi}$$

$$\text{safety factor} = \frac{20,800}{11,910} = 1.74$$

With 0.014 in. wall thickness check actual stress at hot end

$$\sigma_B = \frac{Mc}{I} \quad \frac{831 \times 4.41 \times 2.46}{0.6414}$$

$$\sigma_B = 14,100$$

$$\sigma = \sigma_B - \sigma_T = 14,100 - 1,280 = 12,820 \text{ psi}$$

$$\text{safety factor} = \frac{19,400}{12,820} = 1.51$$

Recommendation

The wall thickness of the tube should be 0.015 at the cold end and 0.014 at the hot end. Although the bending moment at the hot end is less than at the cold end, the modulus of elasticity is decreased at the hot end which cancels out the advantage of less moment.

APPENDIX C

CRITICAL STRESS CALCULATIONS 20-WATT CONCEPT
REF. 37-5001
(Twin 10-watt Concept)

Critical Stress Calculations

The method of analysis shown below assumes that the generator is mounted upright in its shipping container. The biological shield loads the inner case of the vacuum tube uniformly. The thin wall tube takes the load from the heavier wall of the vacuum tube as a shear load and moment at a point 1-15/16" from the end.

Biological shield weight = 390 lbs.

With 3G Shock Load $W\ell = 390 \times 3 = 1170$ lbs

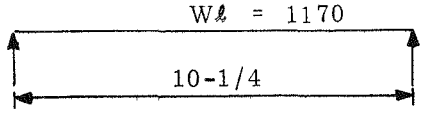

$$M \text{ at ends} = \frac{W\ell^2}{12} = \frac{1170 \times 10.25}{12} = 1000 \text{ in.-lbs.}$$

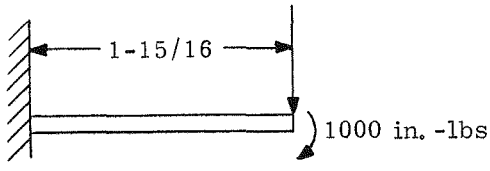

M Total = 585 x 1.93 + 1000 = 2130 in.-lbs.

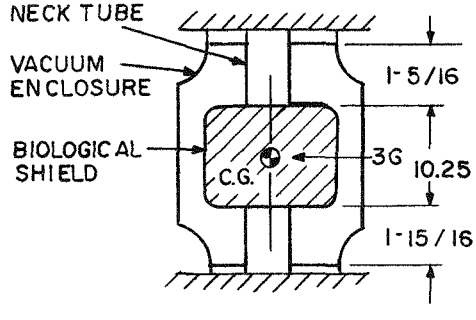

Check critical buckling stress (q_{cr}) in thin wall cylinder.

$$* \left(1 - \nu^2\right) q_{cr} \frac{R}{Eh} + \frac{(1 - \nu^2)}{(n^2 - 1)\left(1 + \frac{n^2 L^2}{\pi^2 R^2}\right)^2} +$$

$$\frac{h^2}{12 R^2}\left(n^2 - 1 + \frac{\left(2 n^2 - 1 - 2\right)}{1 + \frac{n^2 L^2}{\pi R^2}}\right)$$

in which

n = 2 Buckling Modes

L = 2.47 Neck Tube Length, in.

R = 2.46 Neck Tube Radius, in.

v = 0.29 Poisson's Ratio

E = 31.0×10^6 at 150° Modulus of Elasticity, psi

E = 21.2×10^6 at 1300° Modulus of Elasticity, psi

Try 0.009 in. wall thickness at cold end

$$\frac{(1 - 0.29^2)\, q_{cr}\, (2.46)}{31.0 \times 10^6 \times 0.009} = \frac{1 - 0.29^2}{\left(2^2 - 1\right)\left(1 + \frac{(2^2)(2.47^2)}{(3.14^2)(2.46^2)}\right)}$$

$$\frac{0.009^2}{(12) \times (2.46)^2}\left(2^2 - 1 + \frac{2 \times 2^2 - 1 - 0.29}{1 + \frac{(2^2)\ (2.47)^2}{(3.14)^2 (2.46)^2}}\right)$$

$8.10 \times 10^6\, q_{cr} = 0.154 + 0.0000129$

*Theory of Elastic Stability - Timoshenko, Page 450 - Equation 270

q_{cr} = 19,000 psi at 150°F

q_{cr} = 13,000 psi at 1300°F

$$\text{Actual stress} = \delta = \frac{Mc}{I}$$

$$I = \frac{\pi}{64}(do^4 - di^4) = \frac{\pi}{64}(\overline{4.900}^4 - \overline{4.882}^4)$$

$$I = 0.4137 \text{ in}^4$$

$$= \frac{2130 \times 2.461}{0.4137} = 12,650 \text{ psi (cold end)}$$

$$\text{safety factor} = \frac{19,000}{12,650} = 1.50$$

T_{ry} 0.007 at hot end

q_{cr} = 14,700 psi (hot end)

$$I = 0.3221 \text{ in}^4$$

$$= \frac{1000 \times 2.461}{0.3221} = 7,650 \text{ psi}$$

$$\text{safety factor} = \frac{14,700}{7650} = 1.92$$

Try 0.006 at hot end

$$q_{cr} = 12,600 \text{ psi}$$

$$I = 0.276 \text{ in}^4$$

$$= \frac{1000 \times 2.461}{0.276} = 8,920 \text{ psi}$$

$$\text{safety factor} = \frac{12,600}{8.920} = 1.41$$

Conclusion:

The wall thickness at the cold end should be 0.009 inch and at the hot end 0.007 inch.